The Behaviour of MHD Waves in a Structured Coronal Environment

Keith Bennett

Thesis submitted for the degree of Doctor of Philosophy
of the University of St. Andrews

August 31, 2000

Abstract

This thesis investigates the behaviour of wave motion within inhomogeneous plasmas and the effect of flow and transversal structuring on those waves.

We begin by outlining the basic techniques used in the analysis of waves under a variety of configurations and demonstrate how these can be applied to a specific set of models to provide us with an understanding of the fundamental characteristics of magnetoacoustic waves.

We move on to an investigation into the behaviour of waves within twisted magnetic flux tube configurations. We present a specific model of the twisted magnetic cylinder from which analytic methods may be used to obtain a dispersion relation. We use this equation to investigate the modes of the system and compare these results with those obtained in the limit where the tube is untwisted, pointing out new features introduced by the twisted component of the magnetic field.

Finally we study some of the effects introduced when the linear regime is relaxed and higher order terms are considered. A method for the analytical investigation of non-linear resonant interactions between wave modes is outlined and applied to a simple uniform slab configuration. We find that by a consideration of the most important non-linear terms we are able to gain an understanding of the processes involved in such interactions. A numerical study of the model is also considered and the results are shown to be in good agreement with analytical predictions.

Declaration

1. I, Keith Bennett, hereby certify that this thesis, which is approximately 20,000 words in length, has been written by me, that it is a record of work carried out by me and that it has not been submitted in any previous application for a higher degree.

   date 31 August 2000 signature of candidate

2. I was admitted as a research student in September 1996 and as a candidate for the degree of PhD in September 1997; the higher study for which this is a record was carried out in the University of St. Andrews between 1996 and 1999.

   date 31 August 2000 signature of candidate

3. I hereby certify that the candidate has fulfilled the conditions of the Resolution and Regulations appropriate to the degree of PhD in the University of St. Andrews and that the candidate is qualified to submit the thesis in application for that degree.

   date 31 August 2000 signature of supervisor

4. In submitting this thesis to the University of St. Andrews I understand that I am giving permission for it to be made available for use in accordance with the regulations of the University Library for the time being in force, subject to any copyright vested in the work not being affected thereby. I also understand that the title and abstract will be published and that a copy of the work may be made and supplied to any bona fide library or research worker.

   date 31 August 2000 signature of candidate

Acknowledgements

I would like to take this opportunity to offer my thanks to all those people without whom this thesis would never have made it to completion.

Many thanks to my supervisor Professor Bernard Roberts for all his support and encouragement. Thanks for putting up with many a missed deadline and not just giving up on me when it looked like I might never submit.

Thanks to all my friends and colleagues in the department who have pushed me on and assured me that I could do it even though I'm sure they didn't believe it themselves! I would especially like to thank the Friday night posse Tony, Aaron and Dan, for all their verbal abuse when it was needed (and when it wasn't). Many thanks also to Steve for his support and his inspired magnetic monopoles.

Thanks to my second family in Kettering, Sid, Charlotte, Jeconiah, Keir and Barnabas. Thanks for being there and providing normality when I needed it.

Finally, thanks to Mum and Dad for all their support. Thanks for all the parcels, visits and phone calls. Thanks for having faith in me and allowing me to make a complete mess of everything in any way I wanted.

"I love deadlines. I love the wooshing sound they make as they fly by."

— Douglas Adams

Contents

List of Figures

List of Tables

Chapter 1

Introduction

"I refuse to prove that I exist," says God, "for proof denies faith, and without faith I am nothing."

"But," says Man, "the Babel fish is a dead giveaway isn't is? It could not have evolved by chance. It proves you exist, and so therefore, by your own arguments, you don't. QED."

"Oh dear," says God, "I hadn't thought of that," and promptly vanishes in a puff of logic.

"Oh, that was easy," says Man, and for an encore goes on to prove that black is white and gets himself killed on the next zebra crossing.

— Douglas Adams, The Hitch Hiker's Guide to the Galaxy

1.1 Historical overview

Our Sun has long been the subject of fascination for mankind. It is the most prominent object in the sky and even at night its light is visible in the reflection from the Moon and other planets in the solar system. From the beginnings of mankind the Sun has been the focus of myth and legend. It has been worshipped by countless civilisations; and for good reason – it is the "bringer of life" for all creatures on Earth.

The first serious study into the true physical nature of the Sun would appear to have been carried out by the ancient Greeks (Wentzel, 1989, Phillips, 1992). Around the sixth century B.C., philosophers began to question the popular belief

in the Sun-god Helios and put forward alternative physical models. One of the earliest of these ideas on record is that of Anaximenes (585-528 B.C.) who proposed that the Sun might be a lighter than air, bright disc that was held up by the pressure of the atmosphere. The belief that the Sun was an ordinary physical object was reinforced by Thales of Miletus who was the first to predict a solar eclipse as early as the mid-sixth century B.C. Further insight into the nature of heavenly bodies was developed by the school set up by Pythagoras (*c.* 582-*c.* 507 B.C.) in 532 B.C. Pythagoras himself held the belief that the Sun, along with the Earth, Moon and other planets, were spherical objects. In the mid-fifth century B.C., an astronomer from Athens named Anaxagoras (500-428 B.C.) proposed that meteorites originated from the Sun and therefore the Sun must be composed of iron.

In the early third century B.C. an attempt was made by Aristarchus of Samos (310-230 B.C.) to estimate the distance of the Sun from the Earth by measuring the angle between the Sun and the Earth at half-moon. The inaccuracies of this measurement led to a value of about 19 times the distance between the Earth and the Moon - about one twentieth of the true value. Aristarchus also held the view that the Earth, along with all the other planets, revolved around the Sun. His view was not shared by others and was not seriously considered until the sixteenth century A.D. by Nicholas Copernicus (1473-1543). The grossly inaccurate estimate for the distance between the Sun and the Earth remained undisputed right up until the mid-seventeenth century when detailed observations of planets and their relative distances from the Sun began to make it clear that it was in error. A reasonable approximation was made by Giovanni Domenico Cassini (1625-1712) in 1672. A method for measuring the distance accurately, however, remained a dilemma for many years until the famous astronomer Edmund Halley (1656-1742) realised that accurate measurements could be made when Venus crossed the Sun's disc in front of our line of sight. He pointed out that since Venus is so close to the Earth, the time taken for it to traverse the Sun's disc would be observed differently from different locations on Earth. Actual measurements were a long time in coming, since the next transit of Venus was not to occur for another 53 years. Captain James Cook (1728-79) undertook the observations during his first voyage to New Zealand; due to the length of this journey and the advent of the Napoleonic wars at the turn of the century, the actual calculations were not performed until 1824, 108 years after Halley's suggestion! The distance between the Sun and the Earth was found to be 153,000,000 km on comparison of the measurements, differing from current measurements by only about 2%.

Reverence of the Sun led Aristotle (383-322 B.C.), in the early fourth century B.C., to expound the view that it was perfect and without blemish. Ironically his own pupil, Theophrastus (372-287 B.C.), is the first to have noticed sunspots on the solar surface. A large number of sunspots were observed and recorded in the middle east during the second and third centuries B.C. Many of these seem to be chance sightings, however, and are erratic and unreliable. The first methodical investigation into sunspots came with the invention of the telescope in the late sixteenth century. Galileo Galilei (1564-1642) made a detailed study of sunspots in 1610. After many careful observations he was able to deduce that the Sun rotated with a period of about a month and that its equator was slightly inclined with the plane of orbit of the Earth. He was also the first to notice that the spots were composed of a dark inner region, now known as the umbra, surrounded by a lighter ring, the penumbra, and that the spots were not evenly scattered over the Sun's surface but confined to two bands above and below the equator. A contemporary of Galileo's, Christoph Scheiner (1575-1650), spent 16 years observing sunspots and in 1630 published his findings in a book entitled "Rosa Ursina sive Sol".

Following the publication of Scheiner's books, sunspot observations continued fairly consistently by many astronomers in Europe, although there was a noticeable lull in sightings between 1645 and 1715, despite the intense interest in astronomy during this period. This was noticed by the German astronomer Friederich Wilhelm Gustav Spörer (1822-1895) who published a paper in which he concluded that the drop in sunspot numbers was due to an actual decrease in solar activity (Spörer, 1874). The paper went unnoticed until Edward Walter Maunder (1868-1947), an astronomer working in Greenwich, realised its significance in the 1920s and brought it to the attention of the solar community at large (Maunder, 1922). This period of inactivity, now known as the "Maunder minimum", is widely believed to be fact, with supporting evidence from other sources such as a corresponding drop in auroral sightings (Eddy, 1976).

The great tradition of solar physics in Scotland was put on a firm grounding by Glaswegian physicist Alexander Wilson (1714-1786) in 1769. He noticed that the Sun's surface appeared to be indented at the limb in the presence of sunspots, a phenomena often referred to as the "Wilson depression", and deduced that the spots must be funnel shaped. From this he was able to conclude that these were burrows made by creatures living beneath the surface of the Sun!

The next major advance in solar physics came in 1843 with the discovery of the 11 year sunspot cycle by the German chemist Heinrich Schwabe (1789-1875).

After 17 years spent making recordings of sunspots he began to notice that the numbers alternated between a maximum and a minimum over a period of about ten years, and he also pointed out that the spots appeared in small clusters of at least two rather than being evenly spread across the Sun. This observation was improved upon in 1848 by the Swiss astronomer Rudolf Wolf (1816-1893) who set up a small collaborative effort to record sunspot numbers, and also confirmed Schwabe's findings by scouring historical records to compile a list of recordings taken over the previous century and a half. A further major advancement in this field was made by the amateur astronomer Richard Christopher Carrington (1826-1875) in the nineteenth century. He made precise and frequent measurements of sunspots between 1853 and 1861, paying particular attention to the latitudes at which they occurred. He found that the Sun rotated faster at its equator than at higher latitudes and also that the sunspot groups drifted from high to low latitudes as the cycle progressed. The details of this sunspot drift were further worked upon by Spörer, after whom the theory has been named. The phenomena was beautifully illustrated by Maunder in 1902 who plotted sunspot latitude against time to produce the now famous "Butterfly diagram".

Of course, the most important discovery as far as magnetohydrodynamics (MHD) is concerned is that of the magnetic field. The observations of the solar corona during an eclipse revealed patterns very similar to those produced by iron filings under the influence of a bar magnet and this had led many physicists to conjecture that the structuring might be caused by such a field on the Sun. It had also been noted that the pattern appeared to coincide with large sunspot groupings. The idea that sunspots might contain regions of strong magnetic field was established by George Ellery Hale (1868-1938) in 1908. Hale, an astronomer from Chicago, had made huge advances in the observation of the Sun through his experiments with photographic methods, and in 1892 he built the first instrument, the spectroheliograph, for observing the Sun using the Fraunhofer emission lines. With this instrument he was able to observe the Sun in many different wavelengths as well as making detailed studies of faculae and prominences in the solar corona. He was able to observe new features on the surface of the Sun, including the mottled pattern formed by convection cells and filament channels. The clues pointing to the presence of the magnetism came from the splitting of emission lines in the presence of such a field. This had been discovered in the laboratory by Pieter Zeeman (1865-1943) and had first been observed in solar emission lines by Charles Augustus Young (1834-1908). Hale made careful observations of sunspot groupings using his spectrohelio-

graph from 1908 onwards and soon discovered the presence of line splitting in these regions. He was able to infer field strengths of several thousand gauss and also the bipolar nature of sunspot pairs. He continued his observations through to the beginning of the next solar cycle and discovered that the sunspots pairs reversed their polarity, implying a cycle of 22 rather than 11 years. It was soon found that much of the structuring in the Sun appeared to be related to strong magnetic fields, and it become apparent that changes in the Earth's magnetic field could also be connected with intense periods of activity on the Sun. A formulation of a number of these ideas, linking the Sun's plasma with its magnetic field, was presented by the Swedish physicist Hannes Alfvén (1908-1995) in 1942; the subject of magnetohydrodynamics was born (Alfvén, 1942).

There have been many other discoveries of great importance to the development of solar theory throughout history, such as the solar wind, prominences and flares, coronal holes, coronal mass ejections and the high temperature of the solar corona. A study of all these aspects, however, would fill an entire thesis in itself and so I leave the reader to browse the extensive body of literature on the subject, (e.g., Priest, 1982, Wentzel, 1989, Phillips, 1992).

1.2 Development of MHD theory

The equations of magnetohydrodynamics are an attempt to model the behaviour of a plasma under the influence of a magnetic field. The equations used to describe this model are chosen, in part, for their mathematical tractability and as such are restricted in their areas of applicability. The huge advancements made through the use of these simple equations, however, and the surprisingly good correspondence between theory and observation fully justifies their use. An overview of the governing equations and the assumptions that underlie them is outlined briefly below. More detailed discussions may be found in the books by Roberts (1967), Cowling (1976), Parker (1979), Priest (1982) and Sturrock (1994).

It is worth noting that the MHD equations may be derived from the simplification of a much more thorough analysis of particle motion using the Boltzmann equations. Possibly the most rigorous and complete treatment of this analysis may be found in the classic work by Braginskii (1965). We will write the equations derived from taking moments of the Boltzmann equation and then outline the assumptions commonly made in reducing these to the equations of ideal MHD.

To this end, we will begin by defining certain parameters used in our analysis. We will use L_0 to denote a typical length scale, t_0 a typical time scale and B_0 the magnitude of the magnetic field. We will also need to introduce the definitions for some of the plasmas characteristic properties. $V_i = (2k_B T_i/m_i)^{1/2}$ is the velocity corresponding to the ion thermal transit time L_0/V_i, where m_i and T_i are the ion mass and temperature, and can be deduced on consideration of the kinetic energy of the plasma. The ion gyration frequency $\Omega_i = eB_0/m_i$ (often referred to as the ion cyclotron frequency) and the corresponding ion gyro-radius $R_i = V_i/\Omega_i$ indicate the frequency and radius at which a typical ion particle rotates around the magnetic field.

The equations used for the electromagnetic description of the plasma are the well known *Maxwell equations*. These may be introduced from the outset, without simplification, as follows

Gauss's law for electricity:

$$\nabla \cdot \mathbf{E} = \frac{\rho^*}{\varepsilon_0}\,; \tag{1.1}$$

Faraday's law of induction:

$$\nabla \times \mathbf{E} = -\frac{\partial \mathbf{B}}{\partial t}\,; \tag{1.2}$$

Gauss's law for magnetism:

$$\nabla \cdot \mathbf{B} = 0\,; \tag{1.3}$$

and the *Maxwell-Ampére* law:

$$\nabla \times \mathbf{B} = \mu_0 \mathbf{j} + \frac{1}{c^2}\frac{\partial \mathbf{E}}{\partial t}\,. \tag{1.4}$$

The total charge density is $\rho^* = q_i n_i + q_e n_e$, where q is the charge on a particle and n is the number density; the subscripts i and e indicate ion and electron, respectively. The charge density ρ^* is usually extremely small since the condition for a singly charged plasma, $-q_i = q_e$, is almost always satisfied and the condition for charge neutrality, $n_i \approx n_e = n$, holds for most plasmas. For this reason the electric field, $\mathbf{E}$, is taken to be a secondary variable in MHD and is usually eliminated from the equations early on. Other variables introduced above are the magnetic field $\mathbf{B}$, time t, and current density $\mathbf{j}$; ε_0 and μ_0 are the permittivity and permeability of free space respectively (the values of which can be found in

Table 1.2, Section 1.3.2) and c is the speed of light in a vacuum ($c = (\mu_0\varepsilon_0)^{-1/2}$). Most phenomena on the Sun occur with a characteristic velocity which is much less than that of light and it is usually safe to neglect the second term on the right-hand side of the *Maxwell-Ampére* law (1.4).

The equations governing the fluid nature of the plasma are next introduced. We first make the assumption that the plasma continuum behaves as a single fluid and as such the motion of individual particles may be ignored. This is often referred to as a *macroscopic* model of particle motion and obviously introduces a restriction on the length scales that can be considered. The aim of this simplification is to enable us to use the well established equations governing the motion of a fluid. In order for these equations to be valid, however, we must also make the much more restrictive assumption that the plasma is collisionally dominated and the conditions for the plasma to be macroscopic are automatically satisfied.

A plasma can be described by a macroscopic model if there are enough interactions between particles to make the distribution function close to Maxwellian. This will occur if the time between collisions is much smaller than the typical timescales of interest in the problem. For MHD the typical timescale is the ion thermal transit time L_0/V_i. It is usually safe to assume that the kinetic energy involved in these collisions is approximately the same for both ions and electrons and therefore we may write $\tau_{ee} \sim (m_e/m_i)^{1/2}\tau_{ii}$, where $\tau_{ii,ee}$ are the ion-ion and electron-electron collision times. The condition for distribution of each species of particle to roughly Maxwellian is then

$$\text{Ions: } V_i\tau_{ii}/L_0 \ll 1\,, \tag{1.5}$$

$$\text{Electrons: } (m_e/m_i)^{1/2}V_i\tau_{ii}/L_0 \ll 1\,. \tag{1.6}$$

For a collisionally dominated description of the plasma we also must impose the restriction that the mean free path for each species of particle be much less than the macroscopic length scale. Such a condition is represented by the following inequalities.

$$V_i\tau_{ii}/L_0 \sim V_e\tau_{ee}/L_0 \ll 1\,, \tag{1.7}$$

This ensures that the collisions occur on a length scale that is negligible by macroscopic standards and can thus be ignored in the description of such a model. Since the mass of an ion is much larger than that of an electron, it is clear that inequality (1.7) is the most restrictive and it is the mean free path of

the ions that is of most importance here.

The first equation governing the fluid description of the plasma is *mass conservation*,

$$\frac{\mathrm{D}\rho}{\mathrm{D}t} + \rho\nabla\cdot\mathbf{v} = 0\,, \tag{1.8}$$

Here we have introduced the advective (or convective) derivative,

$$\frac{\mathrm{D}}{\mathrm{D}t} = \frac{\partial}{\partial t} + \mathbf{v}\cdot\nabla\,,$$

and we have used the single fluid approximation for $m_e \to 0$, from which we can write the plasma density $\rho = m_i n$ and the velocity $\mathbf{v} = \mathbf{v}_i$.

The next fluid equation to be obtained from the Boltzmann equation is the *equation of motion*,

$$\rho\frac{\mathrm{D}\mathbf{v}}{\mathrm{D}t} = -\nabla p + \mathbf{j}\times\mathbf{B} - \nabla\cdot(\mathbf{\Pi}_i + \mathbf{\Pi}_e)\,, \tag{1.9}$$

where we have used the pressure $p = p_i + p_e$ and the anisotropic component of the ion and electron pressure tensors $\mathbf{\Pi}_i, \mathbf{\Pi}_e$, which are usually referred to as stress tensors (see Braginskii, 1965). The stress tensors (see the Appendix at the end of this thesis) are somewhat complex and it is reasonable to neglect them under solar conditions. It can be shown that the leading order terms of these tensors give rise to viscous effects and that the ion term is larger than that of the electron by a factor $(m_i/m_e)^{1/2}$. As commented earlier, this term is large and so the electron tensor can be neglected.

If the plasma temperature is high and B_0 large, then the diagonal components of the stress tensor Π_{jj} dominate and have the form

$$\Pi_{jj} \sim \nu\left(2\nabla_{\|}\cdot\mathbf{v}_{\|} - \frac{2}{3}\nabla\cdot\mathbf{v}\right) \sim \nu\mathbf{v}_i/L_0\,, \tag{1.10}$$

$$\nu \sim nk_B T_i \tau_{ii}\,, \tag{1.11}$$

where ν is the kinematic viscosity coefficient and $\mathbf{v}_{\|}$ denotes the velocity component in the direction of the magnetic field. Armed with this information we can write down the ratio between the divergence of the stress tensor and the scalar

pressure gradient

$$\left|\frac{\nabla \cdot \mathbf{\Pi}_i}{\nabla p}\right| \sim \frac{V_i \tau_{ii}}{L_0} \ll 1\,; \tag{1.12}$$

so the effects of viscosity may be neglected if the plasma is collisionally dominated. We may thus write the *momentum* equation as

$$\rho \frac{\mathrm{D}\mathbf{v}}{\mathrm{D}t} = -\nabla p + \mathbf{j} \times \mathbf{B}\,. \tag{1.13}$$

The term distinguishing this equation from the one used to describe an ordinary fluid is the *Lorentz* force $\mathbf{j} \times \mathbf{B}$. It is this force that couples the fluid equations with the electromagnetic equations via *Ohm's* law. It should be noted that here we have neglected any additional external forces that may act on the plasma, including gravity.

After taking appropriate moments of the Boltzmann equation and rewriting the resultant two fluid equations in terms of single fluid variables (achieved by letting m_e, the electron mass, tend to zero) we obtain a general form for *Ohm's* law. In the version written below we have already neglected electron inertia and thus restrict our attention to time scales larger than the electron-ion collision time τ_{ei}. The general form for Ohm's law we obtain is

$$\mathbf{E} + \mathbf{v} \times \mathbf{B} = \frac{1}{ne}\left(\mathbf{j} \times \mathbf{B} - \nabla p_e - \nabla \cdot \mathbf{\Pi}_e\right) + \mathbf{j}/\sigma\,. \tag{1.14}$$

Here $\sigma = \tau_{ei} n e^2/m_e$ is the conductivity of the plasma. The stress tensor $\mathbf{\Pi}_e$ may be neglected for collisional plasmas by the same reasoning used above. The momentum equation indicates that the larger of the two terms $\mathbf{j} \times \mathbf{B}$ and ∇p_e must balance with the mass times acceleration term on the left hand side. Using this information we can make an order of magnitude comparison for either of the two terms with that of $\mathbf{v} \times \mathbf{B}$ in Ohm's law as follows

$$\left|\frac{\mathbf{j} \times \mathbf{B}/en}{\mathbf{v} \times \mathbf{B}}\right| \sim \frac{R_i}{L_0}\,; \tag{1.15}$$

hence we may neglect both the magnetic force term $\mathbf{j} \times \mathbf{B}$ and the electron pressure gradient ∇p_e if typical length scales L_0 are much greater than the ion gyroradius R_i, i.e. for $L_0 \gg R_i$. Finally, the resistive term $\mathbf{j}/\sigma$ can be neglected if it is much smaller than the $\mathbf{v} \times \mathbf{B}$ term, i.e. if

$$\left|\frac{\mathbf{j}/\sigma}{\mathbf{v} \times \mathbf{B}}\right| \sim \frac{(m_e/m_i)^{1/2}}{\omega \tau_{ii}} \left(\frac{R_i}{L_0}\right)^2 \ll 1\,, \tag{1.16}$$

We are then left with the reduced form for *Ohm's* Law,

$$\mathbf{E} + \mathbf{v} \times \mathbf{B} = 0\,. \tag{1.17}$$

The last and most complicated relation to be gained from the Boltzmann equation is the one determining the energy of the system. Most of the terms from this equation can be eliminated based on the assumptions already used. To combine the electron and ion components of the energy equations we must ensure that the time scale considered is greater than the time taken for changes in energy to be passed between species, the equilibration time τ_{eq}. This time is related to the ion-ion collision time by $\tau_{eq} \sim (m_i/m_e)^{1/2}\tau_{ii}$, and we obtain the condition

$$\left(\frac{m_i}{m_e}\right)^{1/2} \frac{V_i \tau_{ii}}{L_0} \ll 1\,, \tag{1.18}$$

which is more restrictive than condition (1.5) for collisionality. The single fluid *Energy* equation may now be written

$$\frac{\mathrm{D}}{\mathrm{D}t}\left\{\frac{p}{\rho^\gamma}\right\} = \frac{1}{3\rho^\gamma}\nabla_\parallel \cdot \left[(\kappa_\parallel + \kappa_\perp)\nabla_\parallel T\right]\,, \tag{1.19}$$

where $\kappa_\parallel$ and $\kappa_\perp$ are the parallel and perpendicular thermal conduction tensors and T is the temperature. The perpendicular thermal conduction tensor is much smaller than the parallel one and is dropped immediately. Transport theory may be used to show that the thermal conductivity tensor contributed by the electrons is greater than that of the ions by a factor $(m_i/m_e)^{1/2}$, and so the heat flux may be ignored provided

$$\left|\frac{\nabla_\parallel \cdot \left(\kappa_{\parallel e}\nabla_\parallel T\right)}{\partial p/\partial t}\right| \sim \left(\frac{m_i}{m_e}\right)^{1/2} \frac{V_i \tau_{ii}}{L_0} \ll 1\,. \tag{1.20}$$

This is the same restriction as given by the energy equilibration time. If condition (1.20) is satisfied then we are left with the adiabatic *energy* equation

$$\frac{\mathrm{D}}{\mathrm{D}t}\left\{\frac{p}{\rho^\gamma}\right\} = 0\,. \tag{1.21}$$

Finally, we use an equation of state to close the system. This is usually taken to be the *ideal gas* law

$$p = \frac{k_B}{m}\rho T\,. \tag{1.22}$$

Here ρ is the plasma density, p the plasma pressure, k_B is Boltzmann's constant, m is the mean atomic mass, and T is temperature.

There are more general descriptions of the plasma, commonly used by those studying the Earth's magnetosphere, in which the ions and electrons are considered as separate fluids giving rise to the *two fluid equations*. It is found in practise, however, that in solar applications it is reasonable to assume charge neutrality and hence the new information derived from this approach is slight.

Before putting figures to these equations brief comment about units is needed. We have adopted the S.I. (mks) system in which distance is measured in meters, weight in kilogrammes, time in seconds and magnetic field in Tesla. A discussion on units may be found in Boyd and Sanderson (1969).

1.3 Validity of solar MHD

In this section we summarise the assumptions that have gone into the derivation of equations (1.1)-(1.22). It is important to know exactly what these assumptions are so that we are aware of the shortcomings of any model we might wish to implement using the equations of ideal MHD. That is not to say that we cannot use MHD to describe plasmas whose parameters lie outside those for which MHD is strictly valid, only that we must be aware of the places in which errors might creep in. In order to gain some idea of the relative importance of the various assumptions made we will list each in turn, giving typical values to be found in the solar atmosphere. Before we can proceed, however, we must first give a brief overview of the general characteristics of the Sun and those regions by which it is commonly described.

1.3.1 The solar profile

On examination of the solar atmosphere it soon becomes clear that it is an extremely complex environment. Many of the basic plasma plasma properties, such as temperature, density and magnetic field strength vary significantly from one region to the next and consequently the theory of MHD is likely to be more valid in some areas than in others. The temperature profile of the Sun's atmosphere is highly stratified and roughly separates it into three regions, the photosphere, the chromosphere and the corona.

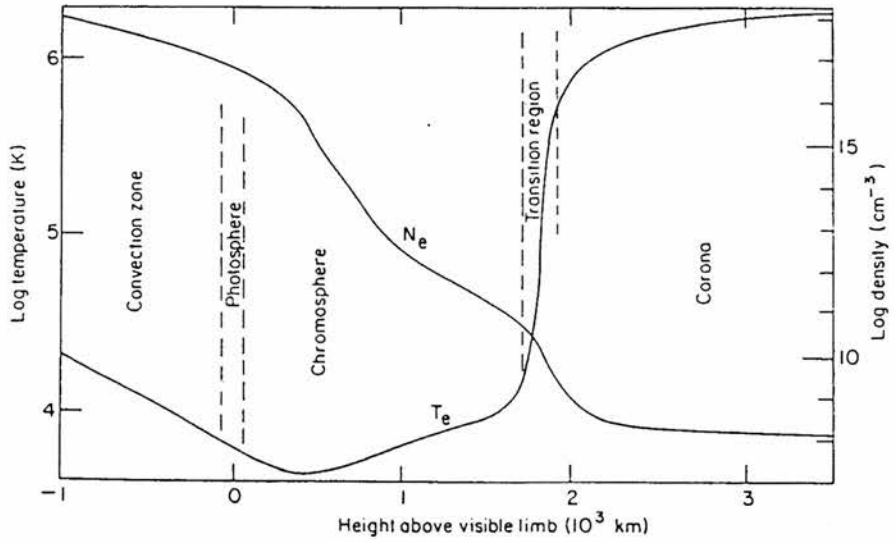

Figure 1.1: Profiles of the electron temperature T_e and electron density N_e for increasing height above the solar limb. Approximate ranges for the photosphere, chromosphere and corona are overlaid.

The photosphere is the "surface" of the Sun. It is a thin layer approximately 500 km deep from which most of the Sun's light is emitted. The photosphere is the region which separates the interior of the Sun from its atmosphere and many transitional features occur there. Clearly visible across the whole of the photosphere is the mottled pattern formed by *granulation cells*. These are approximately 1000 km in diameter and much like cobblestones in appearance. They are formed by convection cells just below the photosphere, in which hot gas rises to the surface in the centre of the cell, cools and falls back down at the edges, forming dark looking channels. It is from these channels that concentrated bundles of magnetic flux are thought to emerge, forming the loop like structures visible in the Sun's upper atmosphere. The temperature of photosphere is 5000 K, roughly 3.5 thousand times cooler than the Sun's core (at approximately 1.6×10^7 K). Above the photosphere, the temperature continues to fall until it reaches a minimum temperature of about 4300 K, the base of the chromosphere at a height of approximately 500 km above the photosphere.

The chromosphere derives its name from the Greek "chromo" meaning colour. It is deep red when seen in visible light, a consequence of the relatively low temperature of the Hydrogen plasma found there. This region is populated throughout with plasma jets referred to as *spicules*. Spicules emanate from supergranule boundaries and attain velocities of 20 to 30 $\mathrm{km\,s^{-1}}$. The temperature in the chromosphere does not continue to fall, as we might expect, but instead rises

steadily as we progress upwards from the base of the chromosphere until we reach the "transition region". Here the temperature rises sharply from approximately 3×10^4 K to 1×10^6 K over a distance of about 2500 km.

	Ion Number density n (m^{-3})	Ion Temperature T (K)	Magnetic field B (T)	Coulomb logarithm $\ln \Lambda$
Photosphere	10^{23}	6×10^3	–	~ 2.9
Lower chromosphere	10^{17}	4×10^3	–	~ 9.2
Upper chromosphere	10^{15}	3×10^4	–	~ 14.5
Corona	10^{13}	1×10^6	–	~ 19.8
Low loops	10^{16}	2×10^6	0.01	~ 17
Quiet loops	10^{15}	2×10^6	0.001	~ 18.2
Flare loops	10^{17}	2×10^6	0.05	~ 15.9

Table 1.1: Typical plasma properties of solar structures.

The region above the transition region is called the corona. It is this part of the solar atmosphere that can be seen during an eclipse. The large, cusp-like structures observed during such an event are evidence of the magnetic field's influence on the structuring of the Sun's upper atmosphere. When observed in more detail using telescopes and satellites, features such as *prominences* and *coronal loops* are detected (Tarbell and Hurlburt, 1998). Prominences are large, long-lived arches of cool plasma supported by the Sun's magnetic field. They are generally about 200 000 km long, 15 000 km high and 6000 km wide, lasting weeks or even months. Coronal loops are much more dynamic features with lifetimes ranging from 30 minutes to several days. They are commonly 100 000 km long and 5000 km wide, containing field strengths of about 100 G and plasma density enhancements of several times that of the surrounding plasma (Bray *et al.*, 1991). These properties suggest that coronal loops may be effective waveguides (e.g. Roberts *et al.*, 1984a), enabling energy to be transferred efficiently from the base of the corona and below, up to the outer corona. The temperature of the Sun's atmosphere continues its slow rise up through the corona, eventually reaching a maximum of about 2×10^6 K.

1.3.2 The collisionally dominated plasma assumption

As we have seen, the plasma properties of the Sun's atmosphere vary significantly from one region to the next and it is therefore necessary to consider the

effect of these variations on the validity of the governing equations. We begin by considering the assertion that the plasma must be collisionally dominated.

The mass of a proton	$m_i = 1.673 \times 10^{-27}\,\mathrm{kg}$
The mass of an electron	$m_e = 9.109 \times 10^{-31}\,\mathrm{kg}$
Electron charge	$e = 1.602 \times 10^{-19}\,\mathrm{coulomb}$
Electron volt	$1\ \mathrm{eV} = 1.602 \times 10^{-19}\,\mathrm{J} = 11\,605\,\mathrm{K}$
Boltzmann constant	$k_B = 1.381 \times 10^{-23}\,\mathrm{J\,deg^{-1}}$
Permeability of free space	$\mu_0 = 4\pi \times 10^{-7}\,\mathrm{henry\,m^{-1}} = 1.257 \times 10^{-6}\,\mathrm{henry\,m^{-1}}$
Permittivity of free space	$\varepsilon_0 = 8.854 \times 10^{-12}\,\mathrm{farad\,m^{-1}}$

Table 1.2: Global Plasma Properties

This was the assumption used to eliminate the viscosity from the momentum equation along with many of the terms from the energy equation. If this condition is satisfied then it may be reasonably assumed that the plasma evolves on a macroscopic level, thus justifying our use of the fluid equations. The condition that the plasma be collisionally dominated is

$$\frac{V_i \tau_{ii}}{L_0} = \frac{\tau_{ii}}{L_0}\left(\frac{k_B T}{m_i}\right)^{1/2} \ll 1\,. \tag{1.23}$$

where we have made use of the fact that the temperature of the ions and electrons are roughly the same and thus $T_i \approx T/2$, where T is the temperature of the plasma. Given the mass of a proton together with typical values for the temperature and number density of a given solar region or structure, we can then establish a minimum length scale above which the plasma is collisionally dominant. The lower chromosphere, for instance, has a typical temperature of about $T \approx 4 \times 10^3\,\mathrm{K}$ and number density of $n = 10^{17}\,\mathrm{m^{-3}}$. The ion-ion collision time can be found using the following formulae (Wesson, 1997)

$$\begin{aligned} \tau_{ii} &= \frac{12\pi^{3/2}\varepsilon_0^2 m_i^{1/2} k_B^{3/2} T_i^{3/2}}{1.1 n_i e^4 \ln\Lambda}\,, \\ &= 5.36 \times 10^6\,\frac{T^{3/2}}{n \ln\Lambda}\,, \end{aligned} \tag{1.24}$$

Here $\ln\Lambda$ is the Coulomb logarithm and may be found using the following for-

mula when temperatures are lower than 1.2×10^5 K

$$\begin{aligned} \ln \Lambda &= \frac{1}{2} \ln \left(\frac{144\pi^2 \varepsilon_0^3 k_B^3 T^3}{e^6 n} \right) , \\ &= 16.33 + \frac{1}{2} \ln \left(\frac{T^3}{n} \right) . \end{aligned} \tag{1.25}$$

For temperatures higher than this quantum mechanical effects are introduced and an alternative expression must be used,

$$\ln \Lambda = 20.97 + \frac{1}{2} \ln \left(\frac{T^2}{n} \right) . \tag{1.26}$$

Typical values found in solar plasmas are summarised in Table 1.1.

Substitution of density and temperature then gives us the minimum length scale that may be used in ideal MHD to satisfy the collisionally dominant condition. For example, in the lower chromosphere we obtain

$$\begin{aligned} L_0 &\gg 4.87 \times 10^8 \frac{T^2}{n \ln \Lambda} , \\ &= 8.47 \times 10^{-3} \, \mathrm{m} . \end{aligned} \tag{1.27}$$

A similar procedure can be followed, making use of the plasma properties listed in Table 1.1, to obtain the following lower bounds for L_0:

	Typical length scale L_0 (m)
Photosphere	6.04×10^{-8} m
Lower chromosphere	8.47×10^{-3} m
Upper chromosphere	30.18 m
Corona	2.46×10^6 m
Low loops	1.14×10^4 m
Quiet loops	1.07×10^5 m
Flare loops	1.22×10^3 m

The collisionality condition is easily satisfied for much of the Sun with the possible exception of the corona and quiet loop structures. The lack of validity in certain cases is compensated for by the Sun's magnetic field which is able to propagate information along its length and take the place of collisions.

1.3.3 The small ion gyro radius assumption

	ion-ion collision time τ_{ii} (s)	ion gyro radius r_i (m)	Thermal velocity V_i ($\mathrm{m\,s^{-1}}$)
Photosphere	8.59×10^{-12}	–	7.04×10^{3}
Lower chromosphere	1.47×10^{-6}	–	5.75×10^{3}
Upper chromosphere	1.92×10^{-3}	–	1.57×10^{4}
Corona	2.71×10^{1}	–	9.09×10^{4}
Low loops	8.89×10^{-2}	2.21×10^{-3}	1.28×10^{5}
Quiet loops	8.33×10^{-1}	2.21×10^{-2}	1.28×10^{5}
Flare loops	9.53×10^{-3}	4.43×10^{-4}	1.28×10^{5}

Table 1.3: Parameters indicating regions of validity for MHD.

The small ion gyro radius assumption was made so that we could neglect the pressure term from the right-hand side of Ohm's law. The ions in the plasma spiral around the magnetic field lines as they move and the radius of this spiral is the ion gyro radius R_i. It may be written as

$$R_i = \frac{(m_i k_B T_i)^{1/2}}{\sqrt{2}\, e B_0}. \tag{1.28}$$

As we can see, the quantity that this number takes is very much determined by the magnetic field of the plasma and so requires a little more thought. For most solar structures, however, the magnetic field is quite strong and so the ion gyro radius is usually much less than the length scales under consideration. A few typical values taken by the ion gyro radius are listed in Table 1.3.

1.4 Outline of thesis

In this chapter we have seen how the study of the Sun has progressed throughout history. The more our understanding has grown, the more we have become aware of the complexity and dynamics of this fascinating star. It is clear that the range of phenomena that demand thorough and detailed examination is vast and that in order to achieve any real understanding of the processes that occur it is necessary to restrict ones attention to small and much simplified models.

We have also examined the basic equations of MHD with which we will carry out our study. We have seen that these equations have their limitations and

that they certainly do not fully represent the processes involved in the dynamics of the Sun. They do, however, give a remarkably good approximation within their range of validity and are able to convey an excellent description of the physical processes involved whilst retaining a fairly high level of simplicity and mathematical tractability.

The focus of this thesis will be on the study of wave motion within inhomogeneous plasmas. As already mentioned, the scope for study is vast and to undertake a full, detailed analysis of the highly complex structures found on the Sun would be an extremely difficult task, yielding little that would further our understanding of the dynamics contained therein. Instead we will try to identify general cases in which our knowledge of wave motion is lacking and build up a picture of the behaviour of waves under these conditions by drawing on studies made of similar models.

In Chapter 2 we present an overview of the fundamental properties of waves in structured solar plasmas. We outline the basic techniques used in analysing the properties of waves within a given set of boundary conditions and show how these have been used to establish some of the fundamental characteristics of magnetoacoustic waves. These methods will be used throughout the remainder of the thesis in the study of specific models which aim to reflect some typical solar plasma configurations. We end this chapter with a review of recent wave observations and the characteristics of the waves found.

In Chapter 3 we investigate the behaviour of waves within a twisted magnetic flux tube. The flux tube is widely regarded as one of the fundamental building blocks in our understanding of the Sun. The immediately apparent features in any solar observation are the myriad of loops and arcades to be seen. These appear to be made up of many small tube like structures and closer analysis indicates that these are due to density or magnetic field enhancements. The magnetic cylinder is a good approximation to this phenomena, retaining most of the relevant structure whilst providing a simple mathematical framework from which we can gain insight and understanding. Much work has already been done in examining the characteristics of magnetoacoustic waves within such structures and a good understanding has been established. However, one area of study which has clearly been neglected is the effect that twist of the magnetic field will have on such a configuration. The main reason for the absence of such a study has been the mathematical complexity involved in such a calculation. No model has been found for which a fully analytical treatment can be performed. In this chapter we present a configuration under which an analytic methods may

be used to obtain a dispersion relation with which we are then able to investigate the modes of the system. We compare these results with those obtained in the limit where the tube is untwisted and point out new features that arise with the introduction of twist.

Chapter 4 deals with some of the effects introduced when the linear treatment is extended to take into account higher order terms. It is found that waves may interact with one another in a resonant manner within appropriate frequencies ranges and that this can enable the generation of higher harmonics to the original wave mode. A method for the analytical investigation of such phenomena is outlined and applied to the slab model commonly used in the linear treatment of a waveguide. We find that although the full non-linear equations are prohibitively complex, by a consideration of the most important features simplifications may be made which yield useful insight into the dynamics involved. We go on to investigate the model using numerical techniques in which the fully non-linear equations are solved. A comparison is made between the analytical predictions and the numerically calculated results and the merits of such a treatment are discussed.

In Chapter 5 we consider the effects of field aligned steady flows in a transversally structured, compressible plasma. A generalised dispersion relation is derived which governs the behaviour of waves in a sheared-field, Cartesian geometry. The chapter aims to provide a basic outline of the processes involved and considers the two simplest models commonly used in the investigation of magnetoacoustic waves; those of the single interface and the uniform slab. Comparisons are made with incompressible treatments of these models and new features are pointed out and explained.

Finally, in Chapter 6 conclusions are drawn on the results of the work undertaken and suggestions made for further study which may be undertaken to enhance our understanding of these models.

Chapter 2

MHD Waves

The idea was fantastically, wildly improbable. But like most fantastically, wildly improbable ideas it was at least as worthy of consideration as a more mundane one to which the facts had been strenuously bent to fit.

— Douglas Adams, The Long Dark Teatime of the Soul

2.1 Basic wave propagation

Magnetic waves provide a means of energy propagation via the Sun's magnetic field. This becomes particularly significant in the highly structured environment of the solar corona since the magnetic flux tube structures found in loops, arcades, spicules and the like, act as waveguides in which energy can be efficiently transferred from the footpoints at the photosphere up into the corona. The turbulent solar surface induces a large amount of energy into the corona by buffeting the footpoints of field lines and this is clearly a significant component in the heating of the corona.

The bulk of this thesis is devoted to a detailed analysis of the wave modes that occur in structured plasmas and the effect that these inhomogeneities have on the propagation of such waves. To gain a better understanding of the underlying physics of these waves, it is helpful to investigate the behaviour of one or two simple models before looking into more complex situations.

The first stage of most wave analysis is the linearisation of the MHD equations.

In this approach, we begin with an initial equilibrium configuration and then investigate the effect of a small perturbation about this equilibrium. If the perturbation is small enough then we need only consider the linear terms from the resultant equations.

To begin with we will write out the MHD equations in a slightly simplified form in which we combine equations (1.17), (1.4) and (1.8) with (1.2), (1.13) and (1.21), respectively, to give the following

$$\rho\frac{\mathrm{D}\mathbf{v}}{\mathrm{D}t} = -\nabla p + \frac{1}{\mu_0}(\nabla \times \mathbf{B}) \times \mathbf{B}\,, \tag{2.1}$$

$$\frac{\partial \mathbf{B}}{\partial t} = \nabla \times (\mathbf{v} \times \mathbf{B})\,, \tag{2.2}$$

$$\nabla \cdot \mathbf{B} = 0\,, \tag{2.3}$$

$$\frac{\mathrm{D}\rho}{\mathrm{D}t} = -\rho\nabla \cdot \mathbf{v}\,, \tag{2.4}$$

$$\frac{\mathrm{D}p}{\mathrm{D}t} = -\gamma p\nabla \cdot \mathbf{v}\,, \tag{2.5}$$

$$p = \frac{k_B}{m}\rho T\,. \tag{2.6}$$

The second term on the right-hand side of the momentum equation (2.1) is the Lorentz force and is often rewritten in the following form, using vector identities,

$$\mathbf{j} \times \mathbf{B} = \frac{1}{\mu_0}(\mathbf{B} \cdot \nabla)\,\mathbf{B} - \nabla\left(\frac{B^2}{2\mu_0}\right)\,. \tag{2.7}$$

When combined with the pressure gradient, the right-hand side of (2.1) becomes

$$-\nabla p + \mathbf{j} \times \mathbf{B} = \frac{1}{\mu_0}(\mathbf{B} \cdot \nabla)\,\mathbf{B} - \nabla\left(p + \frac{B^2}{2\mu_0}\right)\,. \tag{2.8}$$

It is clear from this that the quantity $(B^2/2\mu_0)$ has exactly the same effect as the pressure in the momentum equation and is hence known as the *magnetic pressure*. The plasma beta β is commonly used to refer to the ratio between gas and magnetic pressures

$$\beta = \frac{p}{(B^2/2\mu_0)}\,. \tag{2.9}$$

The $(\mathbf{B}\cdot\nabla)\,\mathbf{B}/\mu_0$ term in (2.8) acts in much the same way as the tension force in a taut wire. It is non-zero only when the field lines are curved and then acts in a direction perpendicular to the magnetic field in such a way as to straighten the field. For this reason it is often called the magnetic tension and it is one of the forces responsible for the generation of magnetic waves.

The equation deriving from Faraday's law may also be rewritten using vector products as follows

$$\frac{\mathrm{D}\mathbf{B}}{\mathrm{D}t} = \mathbf{B}\cdot\nabla\mathbf{v} - \mathbf{B}\nabla\cdot\mathbf{v}\,. \tag{2.10}$$

We must first find a stationary steady state about which we may perturb the field. To do this we take both the velocity and the time derivatives in the governing equations to be zero. Equilibrium quantities are denoted by a '0' subscript. The only equations which are not trivially satisfied are the momentum equation and the solenoidal constraint. From these, we gain an equilibrium condition that must always be satisfied by the model before any linearisation can be done:

$$\nabla\left(p_0 + \frac{B_0^2}{2\mu_0}\right) = \frac{1}{\mu_0}\left(\mathbf{B}_0\cdot\nabla\right)\mathbf{B}_0\,, \tag{2.11}$$

$$\nabla\cdot\mathbf{B}_0 = 0\,, \tag{2.12}$$

with equilibrium pressure p_0, plasma density ρ_0 and temperature T_0 related by

$$p_0 = \frac{k_B}{m}\rho_0 T_0\,. \tag{2.13}$$

The first of these requires that the forces due to tension and pressure are balanced in the steady state. In Cartesian geometry the solenoidal constraint (2.12) may be satisfied for a magnetic field $\mathbf{B}_0$ that is structured in the transversal coordinate x, i.e.,

$$\mathbf{B}_0 = B_0(x)\mathbf{e}_z\,. \tag{2.14}$$

Here $\mathbf{e}_z$ is the unit vector in the direction parallel to the unperturbed magnetic field $\mathbf{B}_0$. Once the magnetic field is specified, the remaining equilibrium conditions require that the pressure, density and temperature also vary only in a direction perpendicular to the magnetic field. Then (2.11) reduces to the follow-

ing

$$\frac{\partial}{\partial x}\left(p_0 + \frac{B_0^2}{2\mu_0}\right) = 0\,. \tag{2.15}$$

We now investigate the effect of a small perturbation about this equilibrium. We write all quantities as their steady state value plus a small perturbation:

$$\begin{aligned} \mathbf{B} &= \mathbf{B}_0(x) + \tilde{\mathbf{b}}\,, \qquad \rho = \rho_0(x) + \tilde{\rho}\,, \\ p &= p_0(x) + \tilde{p}\,, \qquad T = T_0(x) + \tilde{T}\,. \end{aligned} \tag{2.16}$$

When we substitute these into our governing equations, keeping only the first order terms, we arrive at the following

$$\rho_0 \frac{\partial \tilde{\mathbf{v}}}{\partial t} = -\nabla\left(\tilde{p} + \frac{1}{\mu_0} B_0 \tilde{b}_z\right) + \frac{B_0}{\mu_0}\frac{\partial \tilde{\mathbf{b}}}{\partial z} + \frac{1}{\mu_0}\tilde{b}_x \frac{\partial \mathbf{B}_0}{\partial x}\,, \tag{2.17}$$

$$\frac{\partial \tilde{\mathbf{b}}}{\partial t} = B_0 \frac{\partial \tilde{\mathbf{v}}}{\partial z} - \tilde{v}_x \frac{\partial \mathbf{B}_0}{\partial x} - \tilde{\Delta}\mathbf{B}_0\,, \tag{2.18}$$

$$\nabla \cdot \tilde{\mathbf{b}} = 0\,, \tag{2.19}$$

$$\frac{\partial \tilde{\rho}}{\partial t} = -\rho_0 \tilde{\Delta} - \tilde{v}_x \frac{\partial \rho_0}{\partial x}\,, \tag{2.20}$$

$$\frac{\partial \tilde{p}}{\partial t} = -\gamma p_0 \tilde{\Delta} - \tilde{v}_x \frac{\partial p_0}{\partial x}\,, \tag{2.21}$$

$$\tilde{p} = \frac{k_B}{m}\tilde{\rho} T\,. \tag{2.22}$$

In writing these we have defined $\tilde{\Delta} = \nabla \cdot \tilde{\mathbf{v}}$ which is a measure of the compressibility of the plasma. At this point it is useful to define a new quantity $p_T = \tilde{p} + \frac{1}{\mu_0} B_0 \tilde{b}_z$ representing the total pressure perturbation. We will also now drop the tildes for clarity.

Differentiating equation (2.17) with respect to time and eliminating $\mathbf{b}$ gives

$$\rho_0 \left(\frac{\partial^2}{\partial t^2} - c_{\mathrm{A}}^2 \frac{\partial^2}{\partial z^2}\right)\mathbf{v} = -\nabla \frac{\partial p_T}{\partial t} - \frac{B_0}{\mu_0}\mathbf{B}_0 \frac{\partial \Delta}{\partial z}\,. \tag{2.23}$$

Here we have introduced the Alfvén speed, c_{A}, which represents the character-

istic speed of propagation along the magnetic field. It is defined as follows

$$c_{\mathrm{A}} = \frac{B_0}{\sqrt{\mu_0 \rho_0}} . \tag{2.24}$$

The other characteristic speed, representing the fluid properties of the plasma, is the sound speed c_{S}. This is defined as follows

$$c_{\mathrm{S}} = \left(\frac{\gamma p_0}{\rho_0} \right)^{1/2} . \tag{2.25}$$

The adiabatic energy equation can be rewritten as

$$\frac{\partial p_T}{\partial t} = -\gamma p_0 \Delta - v_x \frac{\partial p_0}{\partial x} + \frac{B_0}{\mu_0} \frac{\partial b_z}{\partial t} . \tag{2.26}$$

Substituting the value for b_z from the induction equation (2.18) and making use of the equilibrium condition (2.15) this may be written as follows

$$\frac{\partial p_T}{\partial t} = -\rho_0 \left(c_{\mathrm{A}}^2 + c_{\mathrm{S}}^2 \right) \Delta + \rho_0 c_{\mathrm{A}}^2 v_x \frac{\partial v_z}{\partial x} . \tag{2.27}$$

Using the momentum equation (2.23) to eliminate v_z we can write the compressional term Δ in terms of the total perturbed pressure as follows

$$\frac{\partial^3 p_T}{\partial t^3} = -\rho_0 (c_{\mathrm{A}}^2 + c_{\mathrm{S}}^2) \left(\frac{\partial^2}{\partial t^2} - c_T^2 \frac{\partial^2}{\partial z^2} \right) \Delta , \tag{2.28}$$

where we have introduced the tube speed c_T. This speed is a result of the balance between magnetic and fluid forces and, as we shall see, it is a natural speed that often occurs in the wave motion of structured plasmas and it is defined as follows (see Roberts, 1981a),

$$c_T^2 = \frac{c_{\mathrm{S}}^2 c_{\mathrm{A}}^2}{c_{\mathrm{S}}^2 + c_{\mathrm{A}}^2} . \tag{2.29}$$

It is also convenient at this point to introduce the speed

$$c_{\mathrm{f}}^2 = c_{\mathrm{S}}^2 + c_{\mathrm{A}}^2 . \tag{2.30}$$

We may now eliminate Δ from the momentum equation (2.23). Writing out the components of the resultant expression gives

$$\rho_0 \left(\frac{\partial^2}{\partial t^2} - c_{\mathrm{A}}^2 \frac{\partial^2}{\partial z^2} \right) v_x = -\frac{\partial}{\partial x} \frac{\partial p_T}{\partial t} , \tag{2.31}$$

$$\rho_0 \left(\frac{\partial^2}{\partial t^2} - c_{\mathrm{A}}^2 \frac{\partial^2}{\partial z^2} \right) v_y = -\frac{\partial}{\partial y} \frac{\partial p_T}{\partial t} , \tag{2.32}$$

$$\rho_0 c_{\mathrm{f}}^2 \left(\frac{\partial^2}{\partial t^2} - c_T^2 \frac{\partial^2}{\partial z^2} \right) v_z = -c_{\mathrm{S}}^2 \frac{\partial}{\partial z} \frac{\partial p_T}{\partial t} . \tag{2.33}$$

where v_x, v_y and v_z are the velocity perturbations in the directions $\mathbf{e}_x$, $\mathbf{e}_y$ and $\mathbf{e}_z$ respectively.

Here we have three equations in four unknowns. The fourth equation required to close the system may be obtained by substituting the definition for the compressional term $\Delta = \nabla \cdot \mathbf{v}$ into equation (2.28),

$$\frac{\partial^3 p_T}{\partial t^3} = -\rho_0 c_{\mathrm{f}}^2 \left(\frac{\partial^2}{\partial t^2} - c_T^2 \frac{\partial^2}{\partial z^2} \right) \left(\frac{\partial v_x}{\partial x} + \frac{\partial v_y}{\partial y} + \frac{\partial v_z}{\partial z} \right) . \tag{2.34}$$

These may be reduced to the following two differential equations in terms of the two perturbation quantities p_T and v_x:

$$\rho_0 c_{\mathrm{f}}^2 \left(\frac{\partial^2}{\partial t^2} - c_{\mathrm{A}}^2 \frac{\partial^2}{\partial z^2} \right) \left(\frac{\partial^2}{\partial t^2} - c_T^2 \frac{\partial^2}{\partial z^2} \right) \frac{\partial v_x}{\partial x} = \left\{ c_{\mathrm{f}}^2 \frac{\partial^2}{\partial y^2} \left(\frac{\partial^2}{\partial t^2} - c_T^2 \frac{\partial^2}{\partial z^2} \right) - \left(\frac{\partial^2}{\partial t^2} - c_{\mathrm{A}}^2 \frac{\partial^2}{\partial z^2} \right) \left(\frac{\partial^2}{\partial t^2} - c_{\mathrm{S}}^2 \frac{\partial^2}{\partial z^2} \right) \right\} \frac{\partial p_T}{\partial t} , \tag{2.35}$$

$$\rho_0 \left(\frac{\partial^2}{\partial t^2} - c_{\mathrm{A}}^2 \frac{\partial^2}{\partial z^2} \right) v_x = -\frac{\partial}{\partial x} \frac{\partial p_T}{\partial t} . \tag{2.36}$$

We wish to investigate the waves in the system and so our next step is to perform a Fourier analysis. We assume that the perturbed quantities are oscillatory in time and spatially in the directions $\mathbf{e}_y$ and $\mathbf{e}_z$ and thus write p_T and v_x in the form

$$\psi = \hat{\psi}(x) \exp i(\omega t - k_y y - k_z z) , \tag{2.37}$$

where ω is the frequency and k_y and k_z are wavenumbers in the directions parallel and perpendicular to the field respectively. After a little algebra the resulting equations may be written as a single ordinary differential equation as follows (see Roberts, 1981a)

$$\frac{\mathrm{d}}{\mathrm{d}x} \left[\frac{\rho_0 (k_z^2 c_{\mathrm{A}}^2 - \omega^2)}{\mathrm{m}^2 + k_y^2} \frac{\mathrm{d}\hat{v}_x}{\mathrm{d}x} \right] - \rho_0 (k_z^2 c_{\mathrm{A}}^2 - \omega^2) \hat{v}_x = 0 , \tag{2.38}$$

where we have introduced the quantity m defined as

$$\mathrm{m}^2 = \frac{(k_z^2 c_\mathrm{A}^2 - \omega^2)(k_z^2 c_\mathrm{S}^2 - \omega^2)}{c_\mathrm{f}^2 (k_z^2 c_T^2 - \omega^2)} \,. \tag{2.39}$$

All other components of interest may now be written in terms of the perpendicular velocity perturbation

$$\hat{v}_y = -\frac{ik_y}{\left(\mathrm{m}^2 + k_y^2\right)} \frac{\mathrm{d}\hat{v}_x}{\mathrm{d}x} \,, \tag{2.40}$$

$$\hat{v}_z = -\frac{ic_\mathrm{S}^2 k_z (k_z^2 c_\mathrm{A}^2 - \omega^2)}{c_\mathrm{f}^2 (k_z^2 c_T^2 - \omega^2) \left(\mathrm{m}^2 + k_y^2\right)} \frac{\mathrm{d}\hat{v}_x}{\mathrm{d}x} \,, \tag{2.41}$$

$$\hat{b}_x = -\frac{k_z B_0}{\omega} \hat{v}_x \,, \tag{2.42}$$

$$\hat{b}_y = \frac{ik_z k_y B_0}{\omega(\mathrm{m}^2 + k_y^2)} \frac{\mathrm{d}\hat{v}_x}{\mathrm{d}x} \,, \tag{2.43}$$

$$\hat{b}_z = \frac{i}{\omega} \left\{ \frac{\mathrm{m}^2 B_0}{\mathrm{m}^2 + k_y^2} \frac{\mathrm{d}\hat{v}_x}{\mathrm{d}x} + \frac{\mathrm{d}B_0}{\mathrm{d}x} \hat{v}_x \right\} \,, \tag{2.44}$$

$$\hat{p}_T = \frac{i\rho_0 (k_z^2 c_\mathrm{A}^2 - \omega^2)}{\omega \left(\mathrm{m}^2 + k_y^2\right)} \frac{\mathrm{d}\hat{v}_x}{\mathrm{d}x} \,, \tag{2.45}$$

$$\hat{p} = -\frac{i}{\omega} \left\{ \frac{\rho_0 c_\mathrm{S}^2 \omega^2 (k_z^2 c_\mathrm{A}^2 - \omega^2)}{c_\mathrm{f}^2 (k_z^2 c_T^2 - \omega^2)(\mathrm{m}^2 + k_y^2)} \frac{\mathrm{d}\hat{v}_x}{\mathrm{d}x} + \frac{B_0}{\mu} \frac{\mathrm{d}B_0}{\mathrm{d}x} \hat{v}_x \right\} \,, \tag{2.46}$$

$$\hat{\rho} = -\frac{i}{\omega} \left\{ \frac{\rho_0 \omega^2 (k_z^2 c_\mathrm{A}^2 - \omega^2)}{c_\mathrm{f}^2 (k_z^2 c_T^2 - \omega^2)(\mathrm{m}^2 + k_y^2)} \frac{\mathrm{d}\hat{v}_x}{\mathrm{d}x} - \frac{\mathrm{d}\rho_0}{\mathrm{d}x} \hat{v}_x \right\} \,. \tag{2.47}$$

Equation (2.38) may be rewritten in the form

$$\frac{\partial}{\partial x} \left[\frac{\rho_0 c_\mathrm{f}^2 (\omega^2 - \omega_A(x)^2)(\omega^2 - \omega_T(x)^2)}{(\omega^2 - \omega_\mathrm{I}(x)^2)(\omega^2 - \omega_\mathrm{II}(x)^2)} \frac{\partial v_x}{\partial x} \right] + \rho_0 (\omega^2 - \omega_A(x)^2) v_x = 0 \,, \tag{2.48}$$

where the resonant frequencies are given by

$$\omega = \begin{cases} \pm\omega_T(x) = \pm k_z c_T(x) \,, \\ \pm\omega_A(x) = \pm k_z c_\mathrm{A}(x) \,, \end{cases} \tag{2.49}$$

and the cut-off frequencies are given by

$$\omega = \begin{cases} \pm\omega_{\mathrm{I}}(x) = \pm\left\{\frac{1}{2}\kappa^2\left(c_{\mathrm{A}}^2 + c_{\mathrm{S}}^2\right) - \frac{1}{2}\sqrt{\kappa^4\left(c_{\mathrm{A}}^2 + c_{\mathrm{S}}^2\right)^2 - 4\kappa^2 k_z^2 c_{\mathrm{A}}^2 c_{\mathrm{S}}^2}\right\}^{1/2}, & \text{(slow)} \\ \pm\omega_{\mathrm{II}}(x) = \pm\left\{\frac{1}{2}\kappa^2\left(c_{\mathrm{A}}^2 + c_{\mathrm{S}}^2\right) + \frac{1}{2}\sqrt{\kappa^4\left(c_{\mathrm{A}}^2 + c_{\mathrm{S}}^2\right)^2 - 4\kappa^2 k_z^2 c_{\mathrm{A}}^2 c_{\mathrm{S}}^2}\right\}^{1/2}. & \text{(fast)} \end{cases} \tag{2.50}$$

If both the equilibrium density, ρ_0, and magnetic field, B_0, are uniform in space, Equation (2.38) may be rewritten as follows

$$\rho_0(k_z^2 c_{\mathrm{A}}^2 - \omega^2)\left\{\frac{\mathrm{d}^2\hat{v}_x}{\mathrm{d}x^2} - (\mathrm{m}^2 + k_y^2)\hat{v}_x\right\} = 0\,. \tag{2.51}$$

From this representation it is plain that one of the admissible solutions can be written as

$$\omega = \pm k_z c_{\mathrm{A}}\,. \tag{2.52}$$

This solution is the Alfvén wave. The phase speed, c_{ph}, and group velocity, $\mathbf{c}_{\mathrm{g}}$, are

$$c_{\mathrm{ph}} = \frac{\omega}{\kappa} = \pm c_{\mathrm{A}}\cos\theta\,, \tag{2.53}$$

$$\mathbf{c}_{\mathrm{g}} = \frac{\mathrm{d}\omega}{\mathrm{d}\mathbf{k}} = \pm c_{\mathrm{A}}\mathbf{e}_z\,. \tag{2.54}$$

From equations (2.45) and (2.40) we see that $\hat{p}_T$ and $\hat{v}_z$ are both zero when (2.52) is satisfied. With these conditions, the Alfvén wave solution can easily be seen from equations (2.33)-(2.32). The Alfvén wave is driven by tension forces alone, unlike the sound wave which owes its existence to pressure forces. Combining this with the fact that the velocity perturbations only occur in a direction perpendicular to magnetic field lines, we see that Alfvén waves behave in much the same way as those formed by plucking a taut string. Referring to the equation for the total perturbed pressure (2.26) we see that the compressional term $\nabla\cdot\mathbf{v}$ must also be zero. This implies that the Alfvén wave does not compress the plasma as it propagates.

2.2 Waves in an homogeneous environment

The case in which there is no structuring may be investigated by Fourier analysing in all three spatial directions, writing all quantities in the form

$$\psi = \hat{\psi} \exp i(\omega t - k_x x - k_y y - k_z z)\,, \tag{2.55}$$

where $\hat{\psi}$ is a constant. The two ordinary differential equations (2.35) and (2.36) then imply the following dispersion relation

$$\left\{\omega^4 - \kappa^2 \left(c_{\rm A}^2 + c_{\rm S}^2\right)\omega^2 + \kappa^2 k_z^2 c_{\rm S}^2 c_{\rm A}^2\right\} v_x = 0\,, \tag{2.56}$$

where $\kappa^2 = k_x^2 + k_y^2 + k_z^2$ is the magnitude of the wavenumber squared. Note that we have omitted the Alfvén wave solution from this dispersion relation. This quadratic equation admits two wave solutions which are referred to as the fast and slow magnetoacoustic wave modes. The notation $\omega_{\rm f}$ and $\omega_{\rm s}$ is sometimes used to represent these modes whose solution may be written as

$$\omega_{\rm f,s} = \left\{\frac{1}{2}\kappa^2\left(c_{\rm A}^2 + c_{\rm S}^2\right) \pm \frac{1}{2}\sqrt{\kappa^4\left(c_{\rm A}^2 + c_{\rm S}^2\right)^2 - 4\kappa^2 k_z^2 c_{\rm A}^2 c_{\rm S}^2}\right\}^{1/2}. \tag{2.57}$$

They are a hybrid of the Alfvén and sound waves.

If there is no magnetic field ($c_{\rm A} = 0$) then Equation (2.56) reduces to

$$\omega^4\left(\omega^2 - \kappa^2 c_{\rm S}^2\right) v_x = 0\,, \tag{2.58}$$

and we obtain the dispersion relation for the sound wave, $\omega = \pm\kappa c_{\rm S}$. This wave propagates equally in all directions with phase speed

$$c_{\rm ph} = \frac{\omega}{\kappa} = \pm c_{\rm S}\,,$$

and group velocity

$$\mathbf{c}_{\rm g} = \frac{{\rm d}\omega}{{\rm d}\mathbf{k}} = \pm\frac{c_{\rm S}}{\kappa}\mathbf{k}\,.$$

This means that the group velocity has a magnitude of $c_{\rm S}$ in the direction of propagation. Examining the momentum equation (2.23) we see that the pressure gradient is the force driving this wave.

When a magnetic field is present, a new set of pressure and tension forces are introduced resulting in new waves. The first thing to note is that from Equa-

tion (2.19) we obtain the condition $\mathbf{k} \cdot \mathbf{b} = 0$ for the homogeneous case. This means that the perturbation in the magnetic field is always perpendicular to the direction of propagation.

We begin by considering the two limiting cases of incompressibility and zero beta plasma. The incompressible case is found by taking $\nabla \cdot \mathbf{v} = 0$ in the governing equations. This is equivalent to considering the case in which the sound speed becomes infinitely large and corresponds to the removal of the sound speed from the system. Clearly, any remaining wave motion owes its existence to the magnetic field alone. If we let $c_S^2 \to \infty$ in (2.56) we obtain

$$\kappa^2 \left(k_z^2 c_A^2 - \omega^2\right) v_x = 0 \,. \tag{2.59}$$

Considering only the non-trivial solution, we obtain the dispersion relation for the incompressible slow wave in an homogeneous plasma,

$$\omega = \pm k_z c_A \,, \tag{2.60}$$

which gives a phase speed of

$$c_{ph} = \pm c_A \cos\theta \,.$$

Since $k_z = \kappa \cos\theta$ where θ is the angle between the magnetic field and the direction of propagation of the wave. The group velocity is given by

$$\mathbf{c}_g = \pm c_A \mathbf{e}_z \,.$$

This wave is sometimes called the shear Alfvén wave, although in reality it has nothing to do with the Alfvén wave at all but is just the slow wave in the incompressible limit. However, the misleading description is understandable since this wave exhibits very similar behaviour to that of the Alfvén wave. The behaviour of the wave can best be seen using a polar plot (Figure 2.1) which shows how the phase speed changes with the direction of propagation of the wave. The polar plot for the Alfvén wave is identical.

In the opposite extreme, we take the limit of a zero beta plasma. This is often named the cold plasma approximation since it is equivalent to setting the temperature equal to zero in the ideal gas law (2.22). The sound speed becomes zero and equation (2.56) reduces to

$$\omega^2 \left(\omega^2 - \kappa^2 c_A^2\right) v_x = 0 \,. \tag{2.61}$$

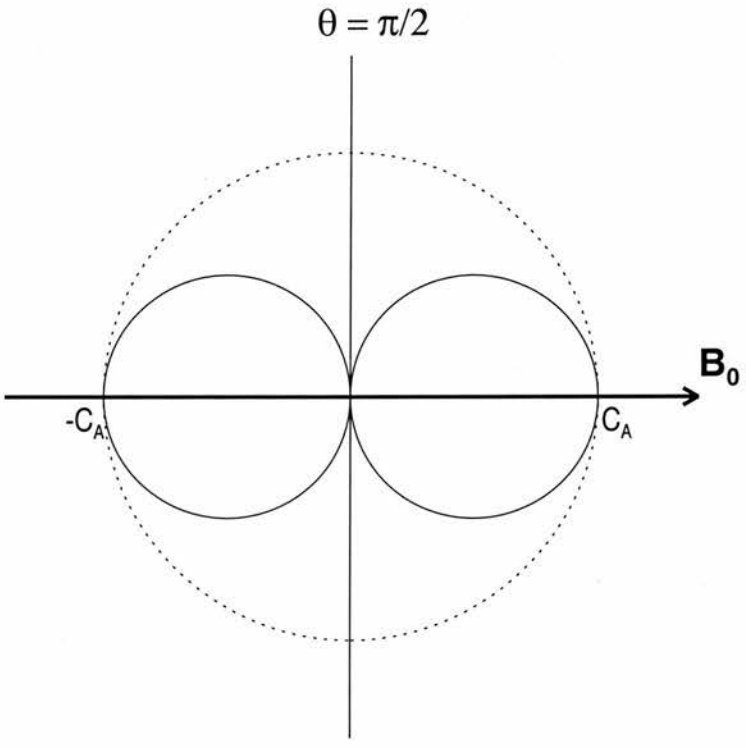

Figure 2.1: Polar plots of the phase velocity for the incompressible slow wave and the zero beta fast wave. The arrow indicates the direction of the magnetic field and theta is the angle of inclination to this field. The slow wave is given by the solid curve and the fast wave is given by the dashed curve. The polar plot of the Alfvén wave is identical to that of the incompressible slow wave shown.

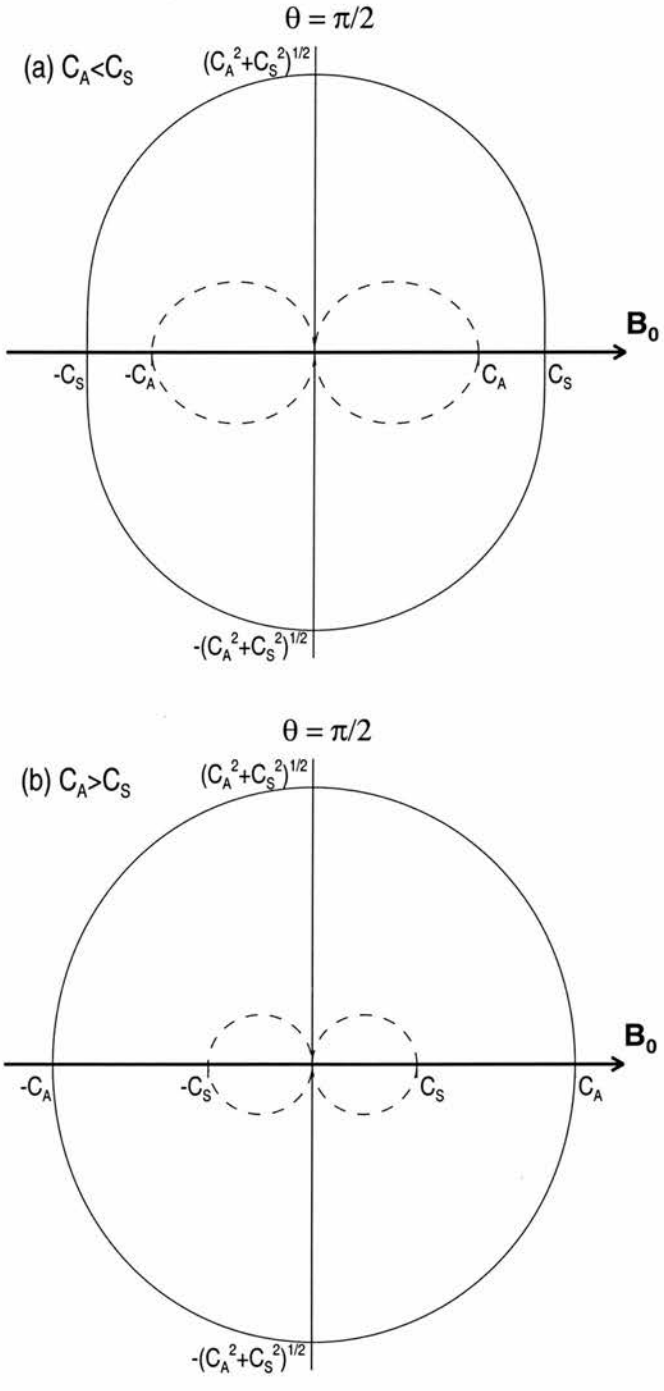

Figure 2.2: Polar plots of the phase speed of magnetoacoustic modes in an homogeneous plasma. Figure (a) illustrates the case for which $c_A < c_S$, specifically the value $c_S = 1.4\,c_A$ is used here. Figure (b) shows the opposite scenario in which we have used $c_S = 0.4\,c_A$.

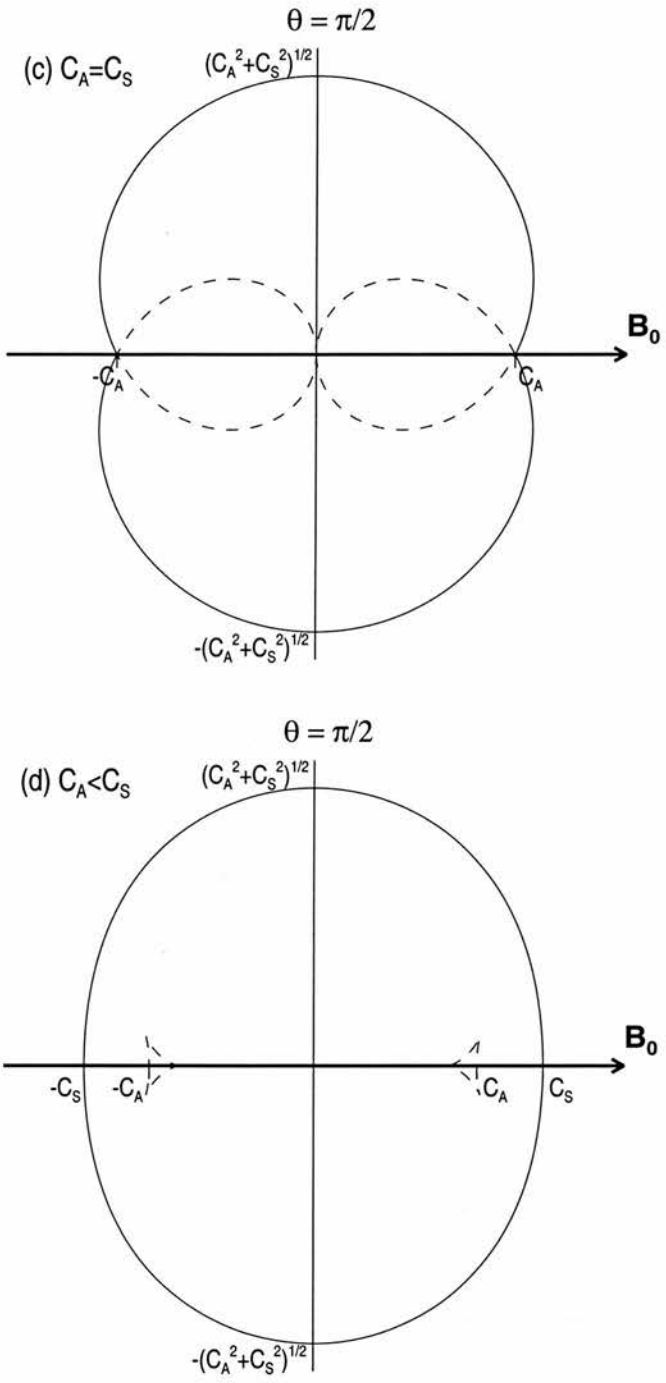

Figure 2.3: Polar plots of the group velocity of magnetoacoustic modes in an homogeneous plasma. Figures (a) and (b) correspond with the values for sound and Alfvén speeds given in Figure 2.2.

The solution $\omega^2 = 0$ corresponds to the slow wave and the remaining solution is the fast wave with phase speed and group velocity given by

$$c_{\rm ph} = \pm c_{\rm A}\,, \qquad \mathbf{c}_{\rm g} = \pm c_{\rm A}\frac{\mathbf{k}}{\kappa}\,. \tag{2.62}$$

This is the same as the sound wave solution shown earlier with the sound speed replaced by the Alfvén speed. It propagates with equal speed in all directions and its group velocity has amplitude $c_{\rm A}$ in the direction of propagation. In this limit the fast wave is driven purely by magnetic pressure. The polar plot for this wave is shown in Figure 2.1.

In general, the slow wave has a phase speed in the range $0 \leq c_{\rm ph} \leq \min(c_{\rm A}, c_{\rm S})$. It has a maximum speed when propagating along the magnetic field and is unable to propagate in a direction perpendicular to it. The fast wave has a phase speed in the range $\max(c_{\rm A}, c_{\rm S}) \leq c_{\rm ph} \leq \sqrt{c_{\rm A}^2 + c_{\rm S}^2}$. This wave achieves its maximum speed when propagating in a direction perpendicular to the magnetic field. Polar plots for the two wave modes are given in Figure 2.2, showing the cases in which the Alfvén speed is either less than or greater than the sound speed. The corresponding group velocities are shown in Figure 2.3.

2.3 Waves in a stratified environment

We have seen how waves behave in an homogeneous environment, we now turn to the case in which there is some structure to either the equilibrium magnetic field or the equilibrium density. This structuring introduces new features into the behaviour of the waves and it is necessary to introduce some terminology to describe it. As soon as any interface is introduced into the plasma, such that the properties of the plasma differ on either side of the interface, a type of wave known as the *surface* wave appears. This type of wave "clings" to the interface, that is it has its maximum amplitude at the interface wall and decays exponentially away from it (see Parker, 1964, 1974a, Wentzel, 1979). In contrast, when more than one interface exists in the plasma configuration *body* modes are supported. These occur within the cavity formed between two boundaries and, unlike the surface wave, they do not decay away from the boundary but oscillate throughout the cavity. Terminology has also arisen to distinguish between modes based on their symmetry about the centre of the cavity on which they act. When the perturbations are symmetric about the centre of the cavity, the term *sausage* mode is used and when the disturbance is asymmetric the

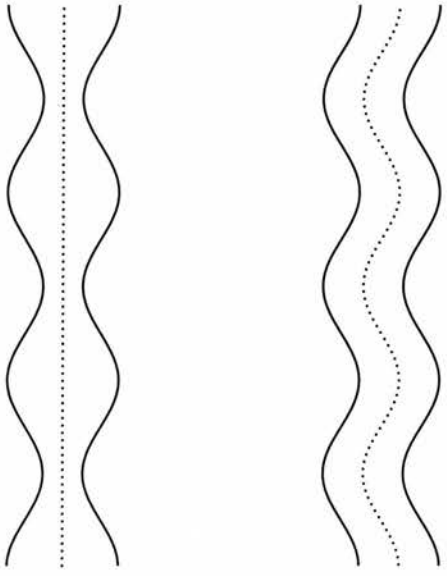

Figure 2.4: Behaviour of the sausage and kink modes. The wave on the left oscillates symmetrically and is known as the sausage wave. The wave on the right oscillates asymmetrically and is known as the kink wave.

term *kink* mode is employed. These two types of wave mode are illustrated in Figure 2.4.

The next step in the study of waves in a structured environment is usually taken by the introduction of inhomogeneities to the Cartesian model outlined in the previous section. However, the specific model we examine here is that of the magnetic flux tube since we will be investigating the twisted magnetic flux tube in the next chapter. The two models often introduce very similar features into the behaviour of the waves and we will make comparisons where appropriate.

In the flux tube model, the magnetic field is directed along the z-axis and has infinite extent. All equilibrium quantities are structured in the radial direction as follows

$$\mathbf{B}_0 = B_0(r)\mathbf{e}_z\,, \qquad p_0 = p_0(r)\,, \qquad \rho_0 = \rho_0(r)\,. \tag{2.63}$$

Following the method used in the previous section we assume a perturbation of the form $f(r)e^{i(\omega t - m\theta - k_z z)}$ obtain the following ordinary differential equations for p_T and v_r

$$\rho_0(r)\left({k_z}^2 c_{\mathrm{A}}^2(r) - \omega^2\right) v_r = -i\omega \frac{\mathrm{d}p_T}{\mathrm{d}r}\,, \tag{2.64}$$

$$\rho_0(r)\left(k_z{}^2c_{\mathrm{A}}^2(r)-\omega^2\right)\frac{1}{r}\frac{\mathrm{d}(rv_r)}{\mathrm{d}r}=-i\omega\left(m_0^2(r)+\frac{m^2}{r^2}\right)\frac{\mathrm{d}p_T}{\mathrm{d}r}\,, \tag{2.65}$$

where we have defined $m_0(r)$ as follows

$$m_0^2(r)=\frac{\left(k_z{}^2c_{\mathrm{A}}^2(r)-\omega^2\right)\left(k_z{}^2c_{\mathrm{S}}^2(r)-\omega^2\right)}{c_{\mathrm{f}}^2(r)\left(k_z{}^2c_T^2(r)-\omega^2\right)}\,. \tag{2.66}$$

For the flux tube it turns out to be easier to solve in terms of the total pressure perturbation rather than the normal component of the velocity perturbation. Combining the two ordinary differential equations above yields the following second order differential equation in terms of the total pressure perturbation

$$\rho_0(r)\left(k_z{}^2c_{\mathrm{A}}^2(r)-\omega^2\right)\frac{1}{r}\frac{\mathrm{d}}{\mathrm{d}r}\left\{\frac{r}{\rho_0(r)\left(k_z{}^2c_{\mathrm{A}}^2(r)-\omega^2\right)}\frac{\mathrm{d}p_T}{\mathrm{d}r}\right\}=\left(m_0^2(r)+\frac{m^2}{r^2}\right)p_T\,. \tag{2.67}$$

For the magnetic tube model we specify regions inside and outside a tube of radius $r=a$ and suppose that the equilibrium quantities are constant everywhere else. We will subscript these quantities with i and e to distinguish between the the regions inside and outside the tube respectively as follows

$$\begin{aligned}&\mathbf{B}_{\mathrm{i}}\,,\ p_{\mathrm{i}}\ \text{and}\ \rho_{\mathrm{i}}\ \text{where}\ r\leq a\,,\\ &\mathbf{B}_{\mathrm{e}}\,,\ p_{\mathrm{e}}\ \text{and}\ \rho_{\mathrm{e}}\ \text{where}\ r>a\,.\end{aligned} \tag{2.68}$$

This type of configuration is illustrated in Figure 2.5. The second order differential equation for p_T can then be written for the two separate regions

$$\frac{\mathrm{d}^2p_T}{\mathrm{d}r^2}+\frac{1}{r}\frac{\mathrm{d}p_T}{\mathrm{d}r}-\left(m_{\mathrm{i,e}}^2+\frac{m^2}{r^2}\right)p_T=0\,. \tag{2.69}$$

Here we have used m_{i} and m_{e} to represent the values of m_0 inside and outside the tube respectively. Note that the Alfvén wave decouples from the system due to the uniform media and has been removed from this equation by cancellation leaving only the fast and slow magnetoacoustic modes. Equation (2.69) takes the same form as the modified Bessel equation and we can immediately write the solution

$$p_T=\begin{cases}C_{\mathrm{i,e}}I_n(m_{\mathrm{i,e}}r)+D_{\mathrm{i,e}}K_n(m_{\mathrm{i,e}}r)\,, & m_{\mathrm{i,e}}^2>0\,,\\ E_{\mathrm{i,e}}J_n(n_{\mathrm{i,e}}r)+F_{\mathrm{i,e}}Y_n(n_{\mathrm{i,e}}r)\,, & n_{\mathrm{i,e}}^2=-m_{\mathrm{i,e}}^2>0\,,\end{cases} \tag{2.70}$$

where $C_{\mathrm{i,e}}, D_{\mathrm{i,e}}, E_{\mathrm{i,e}}$ and $F_{\mathrm{i,e}}$ are constants, J_n and Y_n are the first and second

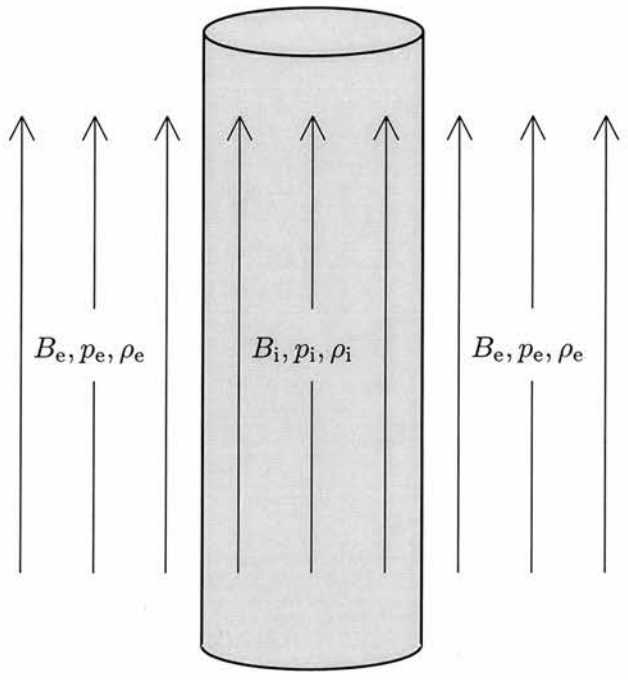

Figure 2.5: Magnetic flux tube model.

ordinary Bessel functions and I_n and K_n are the first and second modified Bessel functions (see Abramowitz and Stegun, 1967). The ordinary Bessel functions represent outgoing wave solutions (see Cally, 1986) and so will not be considered for the external region. We also require that the solution remains bounded at an infinite distance from the tube in the radial direction, a condition which only the second modified Bessel function K_n is able to satisfy. We, therefore, set C_e, E_e and F_e equal to zero. We also require that the solution be finite at the centre of the tube, leading us to set D_i and F_i to zero. We are now left with the solutions

$$p_T = \begin{cases} C_i I_n(m_i r)\,, & m_i^2 > 0\,, \\ E_i J_n(n_i r)\,, & n_i^2 = -m_i^2 > 0\,, \end{cases} \tag{2.71}$$

for the interior of the tube and

$$p_T = D_e K_n(m_e r)\,, \tag{2.72}$$

outside the tube. We match these two solutions at the tube boundary $r = a$ using the conditions that both the radial velocity component v_r and total pressure be continuous. A detailed discussion about the reasoning behind these matching conditions is given in the next chapter (Section 3.3.3). Applying these boundary

conditions yields the dispersion relations

$$\rho_{\rm i}({k_z}^2 c_{\rm Ai}^2 - \omega^2) m_{\rm e} \frac{K_n'(m_{\rm e}a)}{K_n(m_{\rm e}a)} = \rho_{\rm e}({k_z}^2 c_{\rm Ae}^2 - \omega^2) m_{\rm i} \frac{I_n'(m_{\rm i}a)}{I_n(m_{\rm i}a)}\,, \tag{2.73}$$

for surface waves where $m_{\rm i}^2 > 0$ and

$$\rho_{\rm i}({k_z}^2 c_{\rm Ai}^2 - \omega^2) m_{\rm e} \frac{K_n'(m_{\rm e}a)}{K_n(m_{\rm e}a)} = \rho_{\rm e}({k_z}^2 c_{\rm Ae}^2 - \omega^2) n_{\rm i} \frac{J_n'(n_{\rm i}a)}{J_n(n_{\rm i}a)}\,, \tag{2.74}$$

for body waves where $m_{\rm i}^2 < 0$ (Edwin and Roberts, 1983). The dash here denotes the derivative of a Bessel function (e.g. $I_m'(m_{\rm i}a) \equiv (d/dx)I_m(x)$ evaluated at $x = m_{\rm i}a$, etc.).

When the n subscript to the Bessel functions are zero, the mode is symmetric (i.e., a sausage mode) and when it is equal to one it is asymmetric (a kink mode). Higher values of n give rise to mode with a more complex radial symmetry and are known as *fluting* modes.

Another frequently used model is that of the magnetic slab. This is a very similar model to that of the tube, with magnetic field of infinite extent directed along the z-axis and equilibrium quantities separated into to regions in which they are constant. However, in the slab geometry the Cartesian coordinate system is used and the structuring occurs in the x direction rather than the r direction. This simplifies the mathematics somewhat but the geometry is not always a realistic representation of solar structures. In particular, there is no means of realistically modelling the complexity introduced by twisting the magnetic field, which forms the topic of the next chapter. Despite its simplicity, the results obtained by this model bear striking similarities to that of the magnetic tube and we will draw comparisons between the two models in the discussion that follows. The dispersion relation for the slab model is

$$\rho_{\rm e}({k_z}^2 c_{\rm Ae}^2 - \omega^2) m_{\rm i} \left\{ \begin{matrix} \tanh \\ \coth \end{matrix} \right\} m_{\rm i}a + \rho_{\rm i}({k_z}^2 c_{\rm Ai}^2 - \omega^2) m_{\rm e} = 0\,. \tag{2.75}$$

Detailed discussions of this model have been made in Roberts (1981b), Edwin and Roberts (1982), Spruit (1982).

Returning now to the magnetic tube, in the incompressible limit, $m_{\rm i}$ and $m_{\rm e}$ both become $|k_z|$ so the only supported wave is the slow surface mode. Simplifying

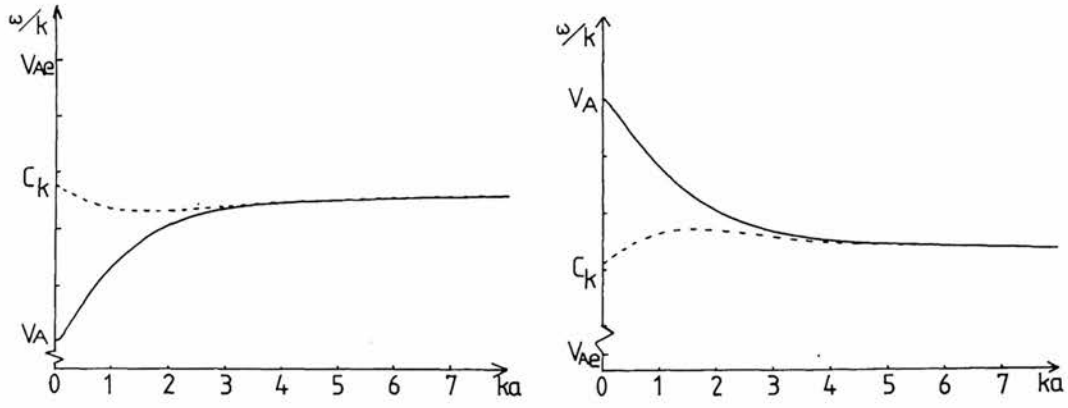

Figure 2.6: The dispersion relation for the slow surface wave in an incompressible medium. The left figure illustrates the case in which the Alfvén speed for the external medium is greater than that of the medium inside the tube. The figure on the right shows the opposite regime. The sausage mode is represented by a solid line whilst the kink mode is given by the dotted line.

equation (2.73), this mode can be written

$$\omega^2 = \frac{{k_z}^2 \left(c_{\mathrm{Ae}}^2 - \frac{\rho_{\mathrm{i}}}{\rho_{\mathrm{e}}} c_{\mathrm{Ai}}^2 \phi_n \right)}{\left(1 - \frac{\rho_{\mathrm{i}}}{\rho_{\mathrm{e}}} \phi_n \right)}, \tag{2.76}$$

where $\phi_n = I_n(a|k_z|)K_n'(a|k_z|)/(I_n'(a|k_z|)K_n(a|k_z|))$. A detailed discussion of this result can be found in Uberoi and Somasunddaram (1979). This wave mode is illustrated in Figure 2.6 where we plot the phase speed ω/k_z against the dimensionless wavenumber $k_z a$. We see that for large values of $k_z a$ both the kink and sausage modes tend towards the kink speed which is defined as

$$c_{\mathrm{k}} = \left(\frac{\rho_{\mathrm{i}} c_{\mathrm{Ai}}^2 + \rho_{\mathrm{e}} c_{\mathrm{Ae}}^2}{\rho_{\mathrm{i}} + \rho_{\mathrm{e}}} \right)^{1/2}. \tag{2.77}$$

This is the same as the result obtained in the case of an infinite slab model for which the medium is structured in the x-direction alone. However, for a narrow tube ($k_z a \to 0$) the behaviour of the kink mode is different. In the slab model the wave mode tends towards the Alfvén speed of the external medium but in the tube model it tends towards the kink speed. Parker (1979) suggests that this behaviour can be explained on physical grounds, since the kink mode displaces less of the surrounding plasma for a tube than it does for a slab. It is this significant feature of the kink mode in a magnetic tube which gives rise to the naming of the kink speed which was first identified by Kruskal and Schwarzschild (1954)

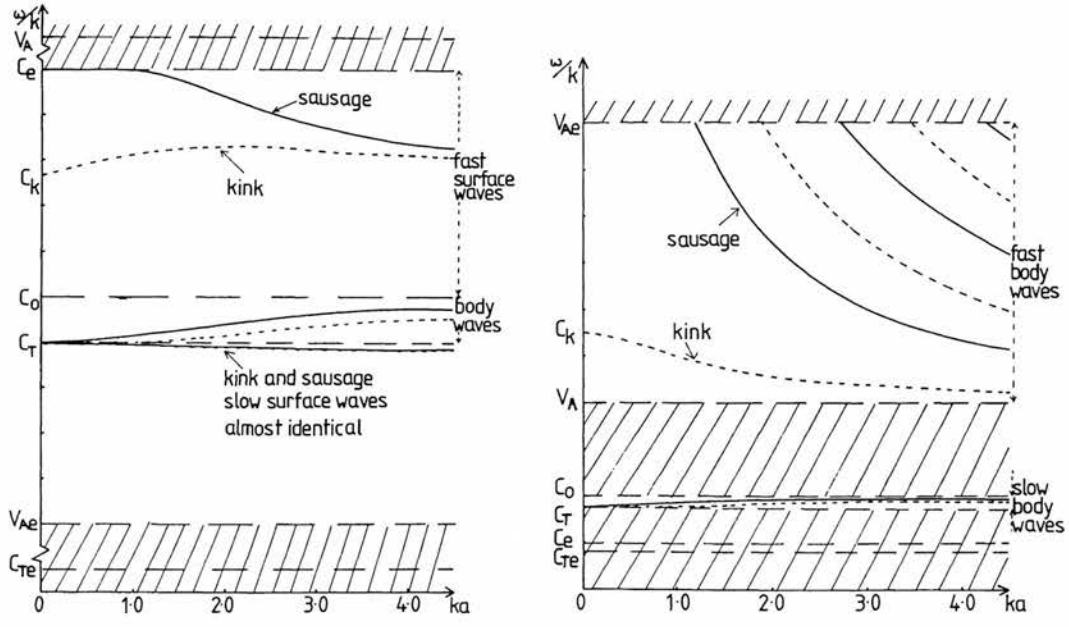

Figure 2.7: Phase speeds for wave modes of the compressible magnetic flux tube. The diagram on the left illustrates a the modes present under typical photospheric conditions. The actual parameters used are $c_{\mathrm{Ai}} = 2c_{\mathrm{Si}}$, $c_{\mathrm{Se}} = 1.5c_{\mathrm{Si}}$ and $c_{\mathrm{Ae}} = 0.5c_{\mathrm{Si}}$. The diagram on the right illustrates a typical coronal case. The parameters used for this are $c_{\mathrm{Ai}} = 2c_{\mathrm{Si}}$, $c_{\mathrm{Se}} = 0.5c_{\mathrm{Si}}$ and $c_{\mathrm{Ae}} = 5c_{\mathrm{Si}}$.

in their study of a single magnetic interface. The two dimensionless wavenumber extremes can easily be verified by taking the appropriate limits in the Bessel functions.

Figure 2.7 illustrates the general compressible results for both photospheric and coronal conditions. In the photosphere the magnetic field inside the tube is typically much stronger than that of the external region. The high magnetic pressure within the tube is balanced by a higher gas pressure in the surrounding environment and therefore the tube typically has a lower sound speed than that of the external medium. We see that two surface modes can occur, a slow mode with phase speed close to the tube speed and approaching it in the limit of zero dimensionless wavenumber, and a fast wave. The fast kink mode tends towards the kink speed in the slender tube limit. This again is different from the slab model in which the mode tends towards the tube speed. The slow kink mode also differs in this limit, with speed becoming the external Alfvén speed in the slab model. Due to the oscillatory nature of the ordinary Bessel equation, there are infinite number of body mode solutions although only two are shown in the diagram for simplicity.

In the corona, the plasma environment is dominated by the magnetic field and the Alfvén speed is thus much higher than the sound speed. Magnetic structures such as coronal arcades and loops are generally at a higher temperature than their surrounding environment and therefore the sound speed is increased within them. The Alfvén speed must therefore be lower than that of the surrounding plasma to maintain pressure balance. From Figure 2.7 we see that there are no longer any surface modes present. This is an important point as it implies that most of the observable oscillations in the corona are channelled along magnetic flux tubes which act as wave guides.

Chapter 3

Waves in Twisted Magnetic Flux Tubes

... was rather startled to discover that he had managed to create the long sought after golden Infinite Improbability generator out of thin air. It startled him even more when just after he was awarded the Galactic Institute's Prize for Extreme Cleverness he got lynched by a rampaging mob of respectable physicists who had finally realized that the one thing they really couldn't stand was a smartass.

— Douglas Adams, The Hitch Hiker's Guide to the Galaxy

3.1 Introduction

With the wealth of observational data from recent space missions such as Yohkoh, SoHO and TRACE, we are made increasingly aware of the complex nature of the Sun and the importance of its highly structured and stratified atmosphere in shaping the processes observed. As the resolution and cadence of observations improve we find that understanding the magnetic structure is essential to our understanding of the Sun. The magnetic field has many important properties which mould the way the Sun behaves: it brings with it new forces, the tension and pressure forces. An important concept in the study of magnetic fields is the magnetic flux tube. The Sun exhibits a wide range of shapes, sizes and strengths of magnetic flux tubes. From the small intense tubes found in the supergranular network, through sunspots and arches, to huge features such as

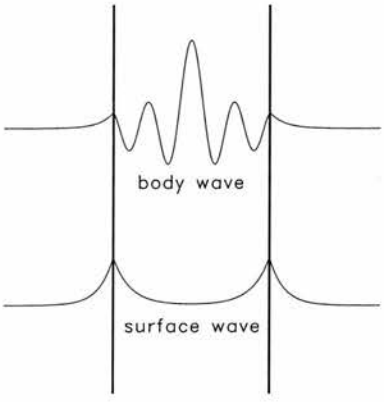

Figure 3.1: The contrasting behaviour of the body wave and the surface wave, as exhibited by the perturbations.

coronal loops and prominences (Bray *et al.*, 1991).

An important aspect in the propagation of energy on the Sun is waves. As described in Chapter 2, oscillations of many types have been observed on the Sun and much work has been done in trying to understand the processes by which they are created. Of particular interest here are the investigations of waves in magnetically structured media by Roberts (1981a,b) and Edwin and Roberts (1982, 1983). They looked at the nature of wave propagation in structures such as the magnetic interface, the magnetic slab and the flux tube. Due to the complexity of the problem, however, their discussion did not include the influence of magnetic twist. This chapter will consider the influence of magnetic twist on the modes of a magnetic flux tube.

An important distinction in the classification of waves has been that between the surface and body waves (Roberts, 1981a,b). The surface wave decays away from any boundary between different plasma properties. By contrast, body waves oscillate uniformly throughout the medium. In either case, the wave is confined to the magnetic structure (Figure 3.1). When a region of plasma is surrounded by regions of differently structured plasmas, waves become trapped within a cavity (Allan and Wright, 1998). One of the notable facts about waves in an incompressible medium which has a straight magnetic field embedded is the absence of body waves, though there are Alfvén waves that may propagate along field lines. However, in the presence of a *twisted* magnetic field it turns out that body waves may arise even for an incompressible medium. We demonstrate this in the present chapter (see also Bennett *et al.*, 1999).

The study of tubes involving a twist in the magnetic field is important. A flux

tube that begins with straight field lines may have twist introduced by granular motions in the photosphere (Brown *et al.*, 2001) and below or by vortex motions local to the flux tube. Erupting prominences commonly give the appearance of having twisted field lines. In any case, it is inconceivable that every flux tube on the Sun is *entirely* twist-free. As we shall see, the introduction of even a small amount of twist has a noticeable effect on the spectrum of waves the tube may support. Twisted tubes have been investigated by Dungey and Loughhead (1954), Goedbloed (1971a,b,c), Goedbloed and Hagenbeuk (1972), Parker (1974b), Bogdan (1984) and Goossens *et al.* (1995) but these discussions have generally concentrated on either the stability aspects or the general classification of the MHD spectra of a twisted tube. By contrast, a detailed study of the specific modes of oscillation of a twisted tube has not been carried out. We begin such a study here, examining a *uniformly twisted* tube embedded in an *incompressible* medium. Under these assumptions, it proves possible to obtain an explicit dispersion relation (see also Dungey and Loughhead, 1954) and to examine in detail the modes that it reveals together with a study of the associated motions.

The assumption of incompressibility is convenient for analytical purposes, but has restrictive implications for any general conclusions about the fully compressible problem. In the more general case it can be shown that three distinct subspectra exist, containing the slow, Alfvén and fast waves. Within each of these subspectra, discrete eigenfrequencies may be found. In addition, the slow and Alfvén singularities, ω_T and ω_A, give rise to continuous spectra. In the compressible case, the fast subspectrum is removed from the system since it corresponds to eigenfrequencies of greater magnitude than that of the sound frequency which becomes infinite in this limit. The other effect caused by the incompressible assumption is the merging of the slow continuum with that of the Alfvén wave (the slow wave tube speed becoming the Alfvén speed in an incompressible medium); see Goedbloed and Hagenbeuk (1972) and Section 2. This collapse in the spectra of the general compressible problem leaves a discrete spectrum of Sturmian modes below the slow continuum (and accumulating at the minimum of the continuum) and a discrete spectrum of anti-Sturmian modes above the slow continuum (and accumulating at the maximum of the continuum); Goedbloed and Hagenbeuk (see 1972). In our treatment here we present the discrete modes in detail for the special case of a uniformly twisted tube. For a uniformly twisted tube the Alfvén frequency is reduced to a constant and the continuum to a single point.

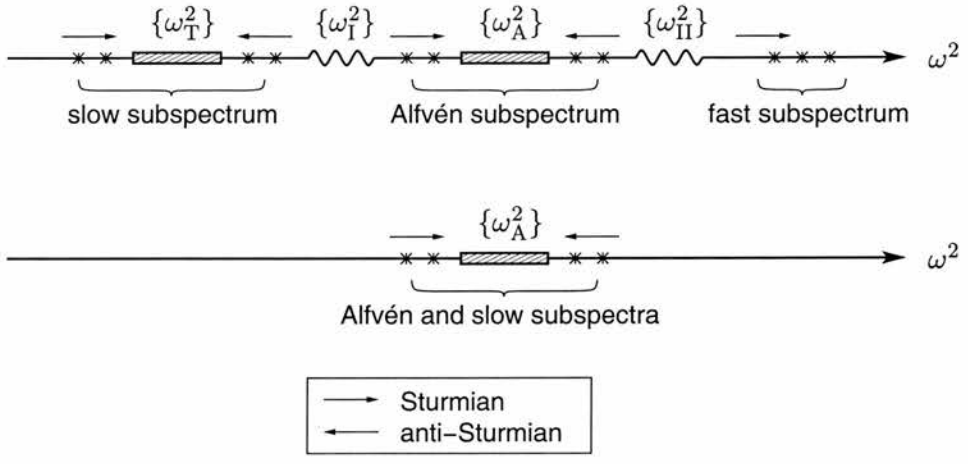

Figure 3.2: The eigenfrequencies of a twisted flux tube. Continuous spectra are marked with shaded regions, occurring for the Alfvén and slow waves. The first diagram illustrates the compressible case in which the two continua are clearly defined and the regions ω_I and ω_{II} separate the range of frequencies containing discrete spectra. The second figure shows the incompressible case in which the slow subspectrum has merged with the Alfvén subspectrum and the fast subspectrum has been shifted to ∞.

Altogether, our assumptions of uniform twist and incompressibility reduce the complexity of the general spectra of a twisted flux tube but have the virtue of allowing a specific analytic study of the discrete modes.

3.2 Derivation of the dispersion relation

One of the main reasons that a detailed description of wave modes in a twisted magnetic flux tube has not previously been carried out is the difficulty in obtaining an analytical dispersion relation. A dispersion relation provides us with information on all the wave modes permitted for a given configuration and is a necessary pre-requisite to a detailed analytical study of wave modes in a system. As can be seen from the derivation of the dispersion relation for the straight field case (given in Chapter 2.1) any magnetic structuring in the model introduces considerable complexity into the governing equations and a solution cannot always be found. The introduction of twist brings with it further complexity since it has an inherent structure related to the particular profile chosen. Twisting the field also has the effect of bending field lines, causing magnetic tension forces to be introduced into the problem. These factors, along with the difficulties involved in working with polar coordinates, make the formulation of the dispersion

relation for this system a much more involved task. It is therefore convenient to consider the reduction of the MHD equations for the general case of a twisted magnetic field.

We begin with the following set of ideal MHD equations. The momentum balance is written in the form

$$\rho\frac{\mathrm{D}\mathbf{v}}{\mathrm{D}t} = -\nabla\left(p + \frac{B^2}{2\mu_0}\right) + \frac{1}{\mu_0}(\mathbf{B}\cdot\nabla)\,\mathbf{B}\,, \tag{3.1}$$

where $\mathbf{v}$ is the flow, $\mathbf{B}$ is the magnetic field (of magnitude $B = |\mathbf{B}|$), and p and ρ are the plasma pressure and density. The field evolves according to the ideal induction equation,

$$\frac{\partial\mathbf{B}}{\partial t} = \nabla\times(\mathbf{v}\times\mathbf{B})\,, \tag{3.2}$$

with $\mathbf{B}$ satisfying the solenoidal initial condition

$$\nabla\cdot\mathbf{B} = 0\,. \tag{3.3}$$

The pressure p and density ρ satisfy

$$\frac{\partial p}{\partial t} = -\gamma p\nabla\cdot\mathbf{v} - \mathbf{v}\cdot\nabla p\,, \tag{3.4}$$

$$\frac{\partial \rho}{\partial t} = -\rho\nabla\cdot\mathbf{v} - \mathbf{v}\cdot\nabla\rho\,. \tag{3.5}$$

The temperature of the plasma is considered to be a secondary variable in our study and so the ideal gas law has not been included in this set of governing equations. It is a straightforward task to obtain the temperature from the calculated values for density and pressure, should it be required.

3.2.1 Equilibrium

To model the disturbances we rewrite the field and pressure as the equilibrium value plus a small perturbation. In Equations (3.1) to (3.5) we replace p, ρ and $\mathbf{B}$ by

$$\tilde{p} = p_0 + p\,, \qquad \tilde{\rho} = \rho_0 + \rho\,, \qquad \tilde{\mathbf{B}} = \mathbf{B} + \mathbf{b}\,. \tag{3.6}$$

In equilibrium (i.e. when perturbations $\mathbf{b}, \mathbf{v}, p, \rho = 0$), Equation (3.1) becomes

$$0 = -\nabla\left(p_0 + \frac{B^2}{2\mu_0}\right) + \frac{1}{\mu_0}(\mathbf{B}\cdot\nabla)\mathbf{B}\,. \tag{3.7}$$

In a cylindrical coordinate system (r, θ, z), the equilibrium pressure $p_0(r)$ and magnetic field $\mathbf{B} = (0, B_\theta(r), B_z(r))$ is assumed to vary purely with radius r, so the magnetostatic pressure balance becomes

$$\frac{\mathrm{d}}{\mathrm{d}r}\left(p_0 + \frac{B^2}{2\mu_0}\right) = -\frac{B_\theta^2}{\mu_0 r}\,, \tag{3.8}$$

where $B = (B_\theta^2 + B_z^2)^{1/2}$ is the strength of the equilibrium field ($B = |\mathbf{B}|$). This equation provides a constraint to be satisfied by the total pressure gradient in the radial direction. It plays an important role in restricting the forms that the magnetic field profile may take. In practise it implies that the radial profile for the equilibrium pressure is prescribed by the choice of magnetic field or vice-versa. This equation corresponds with the equilibrium condition (2.15) given in the previous chapter. The B_θ term on the right-hand side of (3.8) is a result of the tension force exerted by the magnetic field when it is bent.

3.2.2 Obtaining the ordinary differential equations

It is convenient to introduce two new variables: the total pressure perturbation $p_T = p + \mathbf{B}\cdot\mathbf{b}/\mu_0$ and the Lagrangian position perturbation vector $\boldsymbol{\xi}$.

We take $\mathbf{r}$ to be the position vector of a fluid element and $\mathbf{r}_0$ its position vector in the equilibrium state; then $\mathbf{r} = \mathbf{r}_0 + \boldsymbol{\xi}$, with the velocity $\mathbf{v}$ of the fluid element being defined to be

$$\mathbf{v} = \frac{\mathrm{d}\mathbf{r}}{\mathrm{d}t}\,. \tag{3.9}$$

Thus, for small (linear order) perturbations about a static equilibrium,

$$\mathbf{v} = \frac{\partial\boldsymbol{\xi}}{\partial t}\,. \tag{3.10}$$

For the sake of simplicity, we make the assumption that disturbances are incompressible ($\nabla\cdot\mathbf{v} = 0$), so

$$\nabla\cdot\boldsymbol{\xi} = 0\,. \tag{3.11}$$

Since the equilibrium field $\mathbf{B}$, density ρ_0 and pressure p_0 are not functions of time, we may write down the linearised form of Equations (3.1) to (3.4), in the form

$$\rho_0 \frac{\partial^2 \boldsymbol{\xi}}{\partial t^2} = -\nabla p_T + \frac{1}{\mu_0} (\mathbf{B} \cdot \nabla) \mathbf{b} + \frac{1}{\mu_0} (\mathbf{b} \cdot \nabla) \mathbf{B}, \tag{3.12}$$

$$\mathbf{b} = (\mathbf{B} \cdot \nabla) \boldsymbol{\xi} - (\boldsymbol{\xi} \cdot \nabla) \mathbf{B}, \tag{3.13}$$

with

$$p_T = p + \frac{1}{\mu_0} \mathbf{B} \cdot \mathbf{b}. \tag{3.14}$$

Equations (3.12) and (3.13) combine to give

$$\rho_0 \frac{\partial^2 \boldsymbol{\xi}}{\partial t^2} = -\nabla p_T + \frac{1}{\mu_0} (\mathbf{B} \cdot \nabla)^2 \boldsymbol{\xi} - \frac{1}{\mu_0} (\mathbf{B} \cdot \nabla) (\boldsymbol{\xi} \cdot \nabla) \mathbf{B} + \frac{1}{\mu_0} \{[(\mathbf{B} \cdot \nabla) \boldsymbol{\xi}] \cdot \nabla\} \mathbf{B} - \frac{1}{\mu_0} \{[(\boldsymbol{\xi} \cdot \nabla) \mathbf{B}] \cdot \nabla\} \mathbf{B}. \tag{3.15}$$

Equation (3.15) can now be written in component form,

$$\mathcal{D} \xi_r = \frac{\partial p_T}{\partial r} + \frac{2B_\theta}{\mu_0 r} (\mathbf{B} \cdot \nabla) \xi_\theta - \frac{2B_\theta}{\mu_0} \frac{\mathrm{d}}{\mathrm{d}r} \left(\frac{B_\theta}{r} \right) \xi_r, \tag{3.16}$$

$$\mathcal{D} \xi_\theta = \frac{1}{r} \frac{\partial p_T}{\partial \theta} - \frac{2B_\theta}{\mu_0 r} (\mathbf{B} \cdot \nabla) \xi_r, \tag{3.17}$$

$$\mathcal{D} \xi_z = \frac{\partial p_T}{\partial z}, \tag{3.18}$$

with

$$\frac{\partial}{\partial r} (r \xi_r) + \frac{\partial \xi_\theta}{\partial \theta} + r \frac{\partial \xi_z}{\partial z} = 0. \tag{3.19}$$

Here the operator $\mathcal{D}$ is

$$\mathcal{D} = \rho_0 \left(\frac{1}{\mu_0 \rho_0} (\mathbf{B} \cdot \nabla)^2 - \frac{\partial^2}{\partial t^2} \right). \tag{3.20}$$

At this stage it is convenient to study the Fourier components of the system.

Each variable $\alpha(r,\theta,z,t)$ takes the form

$$\alpha \rightarrow \alpha(r)e^{i(m\theta+k_z z-\omega t)}\,, \tag{3.21}$$

where $m(=0,\pm1,\pm2,\ldots)$ is the azimuthal order of the mode, k_z is its longitudinal wavenumber, and ω is its frequency. Equations (3.16)-(3.19) become

$$D\xi_r = \frac{\mathrm{d}p_T}{\mathrm{d}r} + i\frac{2f_B B_\theta}{\mu_0 r}\xi_\theta - \frac{2B_\theta}{\mu_0}\frac{\mathrm{d}}{\mathrm{d}r}\left(\frac{B_\theta}{r}\right)\xi_r\,, \tag{3.22}$$

$$D\xi_\theta = i\frac{m}{r}p_T - i\frac{2f_B B_\theta}{\mu_0 r}\xi_r\,, \tag{3.23}$$

$$D\xi_z = ik_z p_T\,, \tag{3.24}$$

where

$$f_B = \frac{m}{r}B_\theta + k_z B_z\,, \tag{3.25}$$

and

$$D = \rho_0(\omega^2 - \omega_\mathrm{A}^2)\,. \tag{3.26}$$

This system of equations may be reduced to two first order ordinary differential equations for ξ_r and p_T:

$$D\frac{\mathrm{d}}{\mathrm{d}r}(r\xi_r) = C_1 r\xi_r - C_2 r p_T\,, \tag{3.27}$$

$$D\frac{\mathrm{d}}{\mathrm{d}r}(p_T) = C_3\xi_r - C_1 p_T\,. \tag{3.28}$$

Here

$$C_1 = -\frac{2mf_B B_\theta}{\mu_0 r^2}\,, \tag{3.29}$$

$$C_2 = -\left(\frac{m^2}{r^2} + {k_z}^2\right)\,, \tag{3.30}$$

$$C_3 = D^2 + D\frac{2B_\theta}{\mu_0}\frac{\mathrm{d}}{\mathrm{d}r}\left(\frac{B_\theta}{r}\right) - \frac{4B_\theta^2}{\mu_0 r^2}\rho_0\omega_A^2\,, \tag{3.31}$$

where we have defined the local Alfvén frequency $\omega_A(r)$ as

$$\omega_A = \frac{f_B}{(\mu_0\rho_0)^{1/2}} = \frac{1}{(\mu_0\rho_0)^{1/2}}\left(\frac{m}{r}B_\theta + k_z B_z\right) . \tag{3.32}$$

Equations (3.27) and (3.28) are of the same form as would be obtained by taking the incompressible limit ($\gamma \to \infty$) in the Hain-Lüst equations (Hain and Lüst, 1958, Goedbloed and Hagenbeuk, 1972, Appert *et al.*, 1974, Goossens, 1991).

The variable ξ_r can be eliminated from equations (3.27) and (3.28) to give to a second order ordinary differential equation in terms of p_T alone:

$$\frac{\mathrm{d}^2 p_T}{\mathrm{d}r^2} + \left\{\frac{C_3}{rD}\frac{\mathrm{d}}{\mathrm{d}r}\left(\frac{rD}{C_3}\right)\right\}\frac{\mathrm{d}p_T}{\mathrm{d}r} + \left\{\frac{C_3}{rD}\frac{\mathrm{d}}{\mathrm{d}r}\left(\frac{rC_1}{C_3}\right) + \frac{1}{D^2}(C_2C_3 - C_1^2)\right\}p_T = 0 . \tag{3.33}$$

3.3 The model

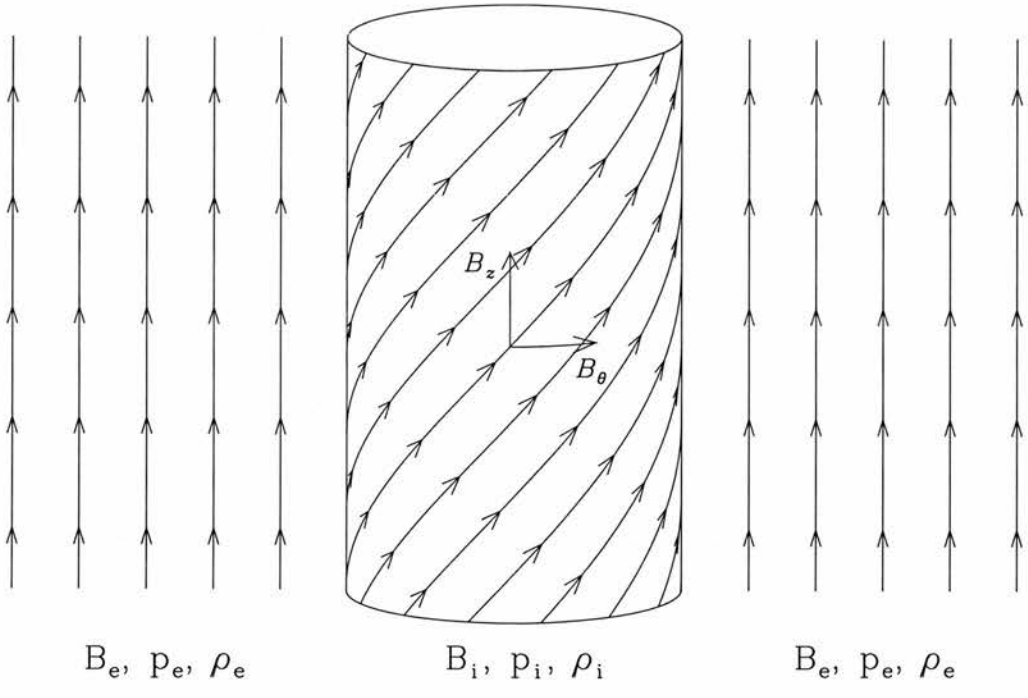

Figure 3.3: A twisted magnetic flux tube surrounded by a uniform magnetic field $\mathbf{B}_e$.

3.3.1 Uniform twist

As discussed in Chapter 3.2, the introduction of twist into the system brings with it an inherent radial structure relating to the particular type of twist profile considered. This generally makes the equations much more difficult to work with and also introduces singularities through the continual variation of the Alfvén speed. These difficulties can be overcome by a careful choice of the profile used. Of particular interest is the *uniform twist* profile (Figure 3.3). This, when considered for a fluid of constant density, is the only profile for which the Alfvén frequency ω_A is constant, removing any possible Alfvén singularity from the system. In the uniform twist profile the twisted component of the magnetic field increases linearly in the radial direction, counteracting the r^{-1} decrease in field that is a natural effect of the polar geometry.

We take the equilibrium field to be of the form $\mathbf{B} = (0, A_i r, B_0)$, so that $B_\theta = A_i r$ and $B_z = B_0$, for constants A_i and B_0. Then the coefficients C_1, C_2 and C_3 become

$$C_1 = -\frac{2mf_B A_i}{\mu_0 r}, \tag{3.34}$$

$$C_2 = -\left(\frac{m^2}{r^2} + {k_z}^2\right), \tag{3.35}$$

$$C_3 = D^2 - \frac{4A_i^2}{\mu_0}\rho_0\omega_A^2, \tag{3.36}$$

with

$$\omega_A^2 = \frac{f_B^2}{\mu_0\rho_0}, \quad f_B = \mathbf{k}\cdot\mathbf{B} = mA_i + k_z B_0. \tag{3.37}$$

Since A_i, ω_A and f_B are constants, Equation (3.33) reduces to

$$\frac{\mathrm{d}^2 p_T}{\mathrm{d}r^2} + \frac{1}{r}\frac{\mathrm{d}p_T}{\mathrm{d}r} - \left(\frac{m^2}{r^2} + m_0^2\right)p_T = 0, \tag{3.38}$$

where

$$m_0^2 = {k_z}^2\left(1 - \frac{4A_i^2\omega_A^2}{\mu_0\rho_0(\omega^2 - \omega_A^2)^2}\right). \tag{3.39}$$

Equation (3.38) is a form of the modified Bessel's equation. This equation is valid for all frequencies except $\omega = \omega_A$. When this frequency is considered, the equations become degenerate and it is necessary to derive a new relation

from the governing set of MHD equations. This degenerate case arises since the operator $\mathcal{D}$ used in writing Equations (3.16) to (3.18) becomes zero. The governing set of equations then reduce to the following

$$\frac{\partial p_T}{\partial r} = -i\frac{2A_\mathrm{i}}{\mu_0}\left(mA_\mathrm{i} + k_z B_0\right)\xi_\theta\,, \tag{3.40}$$

$$-imp_T = i\frac{2A_\mathrm{i}}{\mu_0}\left(mA_\mathrm{i} + k_z B_0\right) r\xi_r\,, \tag{3.41}$$

$$-ik_z p_T = 0\,, \tag{3.42}$$

with

$$\frac{\partial}{\partial r}\left(r\xi_r\right) - im\xi_\theta - ik_z r\xi_z = 0\,. \tag{3.43}$$

From these equations it can clearly be seen that only two solutions exist for which the total pressure perturbation is zero. One solution is found for the straight flux tube in which A_i is zero. In this case we need only satisfy the incompressible condition (3.43) and an infinite number of possible solutions exist. Since the total pressure perturbation is zero and the solution is incompressible, these correspond to Alfvén waves. Another solution is found by setting the wavenumbers k_z, m and the radial perturbation equal to zero. This is the torsional Alfvén wave solution. If we specify that the total pressure perturbation is non-zero, equation (3.42) implies that k_z must be zero. Equations (3.40) and (3.41) can then be combined and the system is reduced to the following two equations

$$im\frac{2A_\mathrm{i}^2}{\mu_0}\left\{\frac{\partial}{\partial r}\left(r\xi_r\right) - im\xi_\theta\right\} = 0\,, \tag{3.44}$$

$$\frac{\partial}{\partial r}\left(r\xi_r\right) - im\xi_\theta = 0\,. \tag{3.45}$$

Clearly these are linearly dependant and so an infinite number of solutions exist. These correspond to incompressible slow waves.

3.3.2 Solutions

Inside the tube

Inside the twisted flux tube, where $\mathbf{B} = \mathbf{B}_\mathrm{i} = (0, A_\mathrm{i} r, B_\mathrm{i})$, $r < a$, we have

$$\frac{\mathrm{d}^2 p_{T\mathrm{i}}}{\mathrm{d}r^2} + \frac{1}{r}\frac{\mathrm{d}p_{T\mathrm{i}}}{\mathrm{d}r} - \left(\frac{m^2}{r^2} + m_\mathrm{i}^2\right) p_{T\mathrm{i}} = 0\,, \quad r < a\,, \tag{3.46}$$

where

$$m_\mathrm{i}^2 = {k_z}^2 \left(1 - \frac{4A_\mathrm{i}^2\omega_\mathrm{Ai}^2}{\mu_0\rho_\mathrm{i}(\omega^2 - \omega_\mathrm{Ai}^2)^2}\right)\,.$$

We will consider the case when ω^2 and ${k_z}^2$ are real. Writing $x = m_\mathrm{i} r$, so that $d/dr = m_\mathrm{i} d/dx$, Equation (3.46) becomes

$$\frac{\mathrm{d}^2 p_{T\mathrm{i}}}{\mathrm{d}x^2} + \frac{1}{x}\frac{\mathrm{d}p_{T\mathrm{i}}}{\mathrm{d}x} - \left(1 + \frac{m^2}{x^2}\right) p_{T\mathrm{i}} = 0\,, \tag{3.47}$$

with solutions $p_{T\mathrm{i}} \sim I_m(m_\mathrm{i} r), K_m(m_\mathrm{i} r)$ in terms of the modified Bessel functions I_m and K_m (see Abramowitz and Stegun, 1967). We require that $p_{T\mathrm{i}}$ is finite at $r = 0$ and so we must have

$$p_{T\mathrm{i}}(r) = \alpha_\mathrm{i} I_n(m_\mathrm{i} r)\,, \quad r < a\,, \tag{3.48}$$

where α_i is an arbitrary constant. This is in fact the general solution, but for the case when m_i^2 is negative it is convenient to write

$$n_\mathrm{i}^2 = -m_\mathrm{i}^2 > 0\,, \tag{3.49}$$

so that solutions of Equation (3.46) are $p_{T\mathrm{i}} \sim J_m(n_\mathrm{i} r), Y_m(n_\mathrm{i} r)$. The condition that $p_{T\mathrm{i}}$ be finite at $r = 0$ gives the solution

$$p_{T\mathrm{i}} = \beta_\mathrm{i} J_m(n_\mathrm{i} r)\,, \quad r < a\,, \tag{3.50}$$

where β_i is an arbitrary constant.

Outside the tube

Outside the tube, in $r > a$, we suppose that the magnetic field is uniform and take $\mathbf{B} = \mathbf{B}_e = (0, 0, B_e)$. Then, in the absence of twist, the expression for m_e^2 reduces to $m_e^2 = {k_z}^2$ and so Equation (3.47) has solutions $p_{Te} \sim I_m(|k_z|r), K_m(|k_z|r)$.

We require that p_{Te} is bounded as $r \to \infty$. Therefore we must have

$$p_{Te} = \alpha_e K_m(|k_z|r), \quad r > a, \tag{3.51}$$

where α_e is an arbitrary constant.

When either ω or k_z are complex, there is the possibility of leaky waves (Cally, 1986) a discussion of which is beyond the scope of our present study.

3.3.3 Boundary conditions

It is necessary to determine how the waves propagate from the inner region of the tube to the outer region. Some care must be taken here, since the boundary is not fixed at $r = a$ but is perturbed by the waves moving across it. This fact is often glossed over when dealing with straight field-line configurations, since it has no effect on the resulting equations. Once twist is introduced, however, the magnetic tension force brings extra terms to the problem which are more sensitive to the exact position at which the matching conditions are derived.

There are two approaches that can be taken when finding conditions for matching two separate plasma regions across the boundary; one is based on physical grounds and the other from an entirely mathematical viewpoint. We outline both approaches here, beginning with the more commonly used method based on heuristic arguments.

In this approach it is argued that the normal component of the perturbed boundary ξ_r must remain continuous across the tube boundary $r = a$. This has to be true in a collisionally dominated plasma, one of the basic assumptions made when formulating the equations of MHD. We also require that the total pressure $(\tilde{p} + \tilde{B}^2/2\mu_0)$ is conserved across the *perturbed boundary* $(r = a + \xi_r)$.

The total magnetic pressure is defined to be the sum of the gas pressure $\tilde{p}$ and the magnetic pressure $\tilde{B}^2/2\mu_0$, so our first step is to write the pressure and the

magnetic field in the form of an equilibrium value plus a small perturbation

$$\tilde{p} = p_0 + p\,, \qquad \tilde{\mathbf{B}} = \mathbf{B}_0 + \mathbf{b}\,. \tag{3.52}$$

Expanding $\tilde{p}$ and $\tilde{B}^2/2\mu_0$ in Taylor series about $r = a$ gives (to first order)

$$\tilde{p}(a+\xi_r) = p_0|_a + p|_a + \xi_r \frac{\mathrm{d}p_0}{\mathrm{d}r}\bigg|_a + \dots \tag{3.53}$$

$$\frac{\tilde{B}^2}{2\mu_0}(a+\xi_r) = \frac{B_0^2}{2\mu_0}\bigg|_a + \frac{\mathbf{B}_0\cdot\mathbf{b}}{\mu_0}\bigg|_a + \xi_r \frac{\mathrm{d}}{\mathrm{d}r}\left(\frac{B_0^2}{2\mu_0}\right)\bigg|_a + \dots \tag{3.54}$$

Adding these together we obtain the total magnetic pressure of the system expanded in a Taylor series about the boundary $r = a$

$$\left[\tilde{p} + \frac{\tilde{B}^2}{2\mu_0}\right](a+\xi_r) = \left(p_0 + \frac{B_0^2}{2\mu_0}\right)\bigg|_a + p_T|_a + \xi_r \frac{\mathrm{d}}{\mathrm{d}r}\left(p_0 + \frac{B_0^2}{2\mu_0}\right)\bigg|_a + \dots \tag{3.55}$$

The leading order terms may be eliminated by considering the continuity of total pressure when the system is in equilibrium

$$\left[p_0 + \frac{B_0^2}{2\mu_0}\right]^{inner} = \left[p_0 + \frac{B_0^2}{2\mu_0}\right]^{outer}. \tag{3.56}$$

On eliminating the equilibrium pressure from (3.55), we finally obtain the two boundary conditions

$$[\xi_r]^{inner} = [\xi_r]^{outer}\,, \tag{3.57}$$

$$\left[p_T - \frac{B_\theta^2}{\mu_0 a}\xi_r\right]^{inner} = \left[p_T - \frac{B_\theta^2}{\mu_0 a}\xi_r\right]^{outer}. \tag{3.58}$$

Alternative approach

In a slightly more rigorous treatment, the two boundary conditions may also be obtained by considering the form of the equations (3.27) and (3.28). In order for these to be mathematically correct, the terms which are differentiated must be functions of a type which is consistent with those terms not involving a derivative. For example, if we take the derivative of a step function we know that the other terms in the equation must involve Dirac-delta functions to balance the result. Armed with this knowledge, we are able to obtain parameters to be conserved across the boundary without the use of physical arguments. The

advantage of such an approach is that it does not rely on our understanding of the physics governing the situation, which may be flawed.

In this method we begin by gathering together any terms involving derivatives and combine them to give an equation of the form

$$\frac{\mathrm{d}}{\mathrm{d}r}(\ldots) = (\ldots)\,. \tag{3.59}$$

The term to be differentiated may then be thought of as a new variable, the characteristics of which must be consistent with those of the functions on the right-hand side. Once these conditions have been established we can then integrate such an equation over a thin layer crossing the tube boundary, resulting in an expression of the form

$$[\ldots]_{a-\epsilon}^{a+\epsilon} = \int_{a-\epsilon}^{a+\epsilon} (\ldots) dr\,. \tag{3.60}$$

There are three cases to consider in this equation. The first two cases are those in which the integrand consists of continuous functions or step functions. Under these conditions we know that the integral must tend to zero as $\epsilon \to 0$ and therefore the quantity $[\ldots]$ on the left-hand side must be continuous across the boundary. The third possibility is that the integrand consists of delta functions. In this case the integral will evaluate to a constant as $\epsilon \to 0$ and we obtain a "jump condition" to be satisfied across the boundary.

Our governing equations are the Hain-Lüst equations (3.27) and (3.28). On substitution of full expressions for the coefficients D, C_1, C_2 and C_3, we obtain

$$\rho_0(\omega^2 - \omega_{\mathrm{A}}^2)\frac{\mathrm{d}(r\xi_r)}{\mathrm{d}r} = -\frac{2mf_B B_\theta}{\mu_0 r}\xi_r + \left(\frac{m^2}{r^2} + {k_z}^2\right) r p_T\,, \tag{3.61}$$

$$\begin{aligned}\rho_0(\omega^2 - \omega_{\mathrm{A}}^2)\frac{\mathrm{d}p_T}{\mathrm{d}r} = \{&\rho_0^2(\omega^2 - \omega_{\mathrm{A}}^2)^2 \\ &+\rho_0(\omega^2 - \omega_{\mathrm{A}}^2)\frac{2B_\theta}{\mu_0}\frac{\mathrm{d}}{\mathrm{d}r}\left(\frac{B_\theta}{r}\right) - \rho_0\omega_{\mathrm{A}}^2\frac{4B_\theta^2}{\mu_0 r^2}\Big\}\xi_r + \frac{2mf_B B_\theta}{\mu_0 r^2}p_T\,.\end{aligned} \tag{3.62}$$

We begin by rewriting Equation (3.61) so that it is in the same form as (3.59). On dividing through by $r\rho_0(\omega^2 - \omega_{\mathrm{A}}^2)$ and expanding the derivative of $(r\xi_r)$ we arrive at the following

$$\frac{\mathrm{d}}{\mathrm{d}r}(\xi_r) = -\left[\frac{2mf_B B_\theta}{\rho_0(\omega^2 - \omega_{\mathrm{A}}^2)\mu_0 r^2} + \frac{1}{r}\right]\xi_r + \frac{m^2 + {k_z}^2 r^2}{r^2\rho_0(\omega^2 - \omega_{\mathrm{A}}^2)}\,p_T\,. \tag{3.63}$$

Turning now to the second of the governing equations (3.62), dividing by $\rho_0(\omega^2 - \omega_A^2)$ and moving the derivative term from the right-hand side to the left gives

$$\frac{\mathrm{d}}{\mathrm{d}r}(p_T) - \frac{2B_\theta}{\mu_0}\frac{\mathrm{d}}{\mathrm{d}r}\left(\frac{B_\theta}{r}\right)\xi_r = \frac{2mf_B B_\theta}{\rho_0(\omega^2-\omega_A^2)\mu_0 r^2}\,p_T + \left[\rho_0(\omega^2-\omega_A^2) - \frac{\omega_A^2}{(\omega^2-\omega_A^2)}\frac{4B_\theta^2}{\mu_0 r^2}\right]\xi_r\,. \quad (3.64)$$

A small amount of algebra is required to write the left-hand side of this expression in the correct form. This can be accomplished by noting that the second term can be derived using the following expression

$$\frac{\mathrm{d}}{\mathrm{d}r}\left[\frac{1}{\mu_0}\left(\frac{B_\theta}{r}\right)^2 r\xi_r\right] = \frac{2}{\mu_0}\frac{B_\theta}{r}\frac{\mathrm{d}}{\mathrm{d}r}\left(\frac{B_\theta}{r}\right)(r\xi_r) + \frac{1}{\mu_0}\left(\frac{B_\theta}{r}\right)^2\frac{\mathrm{d}}{\mathrm{d}r}(r\xi_r)\,. \quad (3.65)$$

Using this in (3.64) yields

$$\frac{\mathrm{d}}{\mathrm{d}r}(p_T) - \frac{\mathrm{d}}{\mathrm{d}r}\left[\frac{B_\theta^2}{\mu_0 r}\xi_r\right] + \frac{B_\theta^2}{\mu_0 r^2}\left[\xi_r + r\frac{\mathrm{d}\xi_r}{\mathrm{d}r}\right] = \frac{2mf_B B_\theta}{\rho_0(\omega^2-\omega_A^2)\mu_0 r^2}\,p_T + \left[\rho_0(\omega^2-\omega_A^2) - \frac{\omega_A^2}{(\omega^2-\omega_A^2)}\frac{4B_\theta^2}{\mu_0 r^2}\right]\xi_r\,. \quad (3.66)$$

Combining the first two derivatives on the left-hand side and using the previously obtained expression to eliminate the remaining derivative term we finally arrive at an equation of the required form

$$\frac{\mathrm{d}}{\mathrm{d}r}\left[p_T - \frac{B_\theta^2}{\mu_0 r}\xi_r\right] = \left[\frac{2mf_B}{\rho_0(\omega^2-\omega_A^2)}\frac{B_\theta}{\mu_0 r^2} - \frac{m^2+{k_z}^2r^2}{\rho_0(\omega^2-\omega_A^2)}\frac{B_\theta^2}{\mu_0 r^3}\right]p_T + \left[\rho_0(\omega^2-\omega_A^2) + \frac{2mf_B}{\rho_0(\omega^2-\omega_A^2)}\frac{B_\theta^3}{\mu_0^2 r^3} - \frac{\omega_A^2}{(\omega^2-\omega_A^2)}\frac{4B_\theta^2}{\mu_0 r^2}\right]\xi_r\,. \quad (3.67)$$

For the purpose of clarity, it is convenient at this point to introduce a new variable representing the term on the right-hand side of this equation,

$$\alpha = p_T - \frac{B_\theta^2}{\mu_0 r}\xi_r\,. \quad (3.68)$$

Rewriting both of the equations in terms of this new variable we now have the

two governing equations for this system written in the form of Equation (3.59),

$$\frac{\mathrm{d}}{\mathrm{d}r}(\xi_r) = \left[\frac{\left(m^2 + {k_z}^2 r^2\right) B_\theta^2}{\rho_0(\omega^2 - \omega_\mathrm{A}^2)\mu_0 r^3} - \frac{2m f_B B_\theta}{\rho_0(\omega^2 - \omega_\mathrm{A}^2)\mu_0 r^2} - \frac{1}{r}\right]\xi_r + \frac{m^2 + {k_z}^2 r^2}{\rho_0(\omega^2 - \omega_\mathrm{A}^2) r^2}\alpha\,, \quad (3.69)$$

$$\frac{\mathrm{d}}{\mathrm{d}r}(\alpha) = \left[\rho_0(\omega^2 - \omega_\mathrm{A}^2) + \frac{4m f_B B_\theta^3}{\rho_0(\omega^2 - \omega_\mathrm{A}^2)\mu_0^2 r^3} - \frac{4\omega_\mathrm{A}^2 B_\theta^2}{(\omega^2 - \omega_\mathrm{A}^2)\mu_0 r^2} - \frac{\left(m^2 + {k_z}^2 r^2\right) B_\theta^4}{\rho_0(\omega^2 - \omega_\mathrm{A}^2)\mu_0^2 r^4}\right]\xi_r + \left[\frac{2m f_B B_\theta}{\rho_0(\omega^2 - \omega_\mathrm{A}^2)\mu_0 r^2} - \frac{\left(m^2 + {k_z}^2 r^2\right) B_\theta^2}{\rho_0(\omega^2 - \omega_\mathrm{A}^2)\mu_0 r^3}\right]\alpha\,. \quad (3.70)$$

All that now remains is to determine the nature of the variables ξ_r and α, yielding either variables to be conserved or jump conditions. In the model under consideration the variables B_θ, B_z and ρ_0 behave as step functions across the boundary $r = a$. From this we see that all coefficients on the right-hand side of the two equations above are step functions. For the equations to be mathematically consistent, therefore, we require that the variables ξ_r and α are continuous functions with a discontinuous gradient at the tube boundary. We conclude that the quantities ξ_r and $p_T - (B_\theta^2/\mu_0 r)\xi_r$ are conserved as we cross the boundary at $r = a$; the same conditions found in the previous section.

It should be noted that the use of step functions across the boundary leads us to ignore a potential problem with this matching condition. If, instead of changing discontinuously between the two profiles, we introduce a small layer in which B_θ, B_z and ρ_0 change smoothly from $A_\mathrm{i} a$, B_i and ρ_i on one side to 0, B_e and ρ_e on the other, we find that a singularity has been introduced for frequencies lying in the range $\min(\omega_\mathrm{Ae}, \omega_\mathrm{Ai}) < \omega < \max(\omega_\mathrm{Ae}, \omega_\mathrm{Ai})$. In such circumstances a continuous spectrum of eigenmodes is introduced which may be investigated either by a consideration of the initial value problem or by using a series expansion around the singular point to obtain jump conditions across the singularity. The analytical treatment of this problem is extremely complex and a solution is unlikely to be forthcoming for the model under current consideration. The problem has been tackled for many other models, however, and it has been found that two possible cases arise. When a continuum is found, each field line has its own Alfvén mode solution. In this scenario, an initially uniform wave packet will travel at different speeds for each field line and small length scales develop such that eventually the ideal MHD assumptions are no longer valid. This process is known as phase mixing and it demonstrates one of the possible methods by which wave energy may be used to heat the solar plasma. A second possible

range of solutions within the continuum are those of quasi-modes. It can be shown that on the principle Riemann sheet, solutions of the linear wave system only occur for purely real or purely imaginary frequencies. However, in the continuum the singularities represent branch cuts in the complex plane. From these we may consider solutions on other Riemann sheets which may provide discrete solutions with complex eigenfrequency. These wave modes remain the same as those found by the normal mode analysis but become damped within the continuous spectra (Goedbloed, 1983), a process known as resonant absorption. The time scale for this damping depends upon the separation between the two Alfvén speeds, the thickness of the transition layer and the frequency of the mode concerned. Rather than become involved in a numerical treatment of this initial value problem, the regions in which continuous spectra occur have been highlighted in the diagrams that follow. The normal modes in these regions remain coherent oscillations of the system, but decay in time.

3.3.4 The dispersion relation

Regardless of the method used, we now have two quantities which must remain continuous across the boundary, enabling us to match the solutions from each side. Using Equation (3.28) and the first boundary condition (Equation (3.57)), we may write the following relationship between solutions from either side of the tube boundary,

$$\frac{1}{C_{3\mathrm{i}}}\left\{D_{\mathrm{i}}\left.\frac{\mathrm{d}p_{T\mathrm{i}}}{\mathrm{d}r}\right|_a + C_{1\mathrm{i}}\,p_{T\mathrm{i}}|_a\right\} = \frac{1}{C_{3\mathrm{e}}}\left\{D_{\mathrm{e}}\left.\frac{\mathrm{d}p_{T\mathrm{e}}}{\mathrm{d}r}\right|_a + C_{1\mathrm{e}}\,p_{T\mathrm{e}}|_a\right\}, \tag{3.71}$$

where the coefficients D, C_1 and C_3 correspond to those given in Section (3.2.2) with subscripts i and e used to denote the internal and external regions, respectively. Explicitly, these are:

$$D_{\mathrm{i}} = \rho_{\mathrm{i}}(\omega^2 - \omega_{\mathrm{Ai}}^2)\,, \qquad D_{\mathrm{e}} = \rho_{\mathrm{e}}(\omega^2 - \omega_{\mathrm{Ae}}^2)\,, \tag{3.72}$$

$$C_{1\mathrm{i}} = -\frac{2mf_B A_{\mathrm{i}}}{\mu_0 r}\,, \qquad C_{1\mathrm{e}} = 0\,, \tag{3.73}$$

$$C_{3\mathrm{i}} = D_{\mathrm{i}}^2 - \frac{4A_{\mathrm{i}}^2}{\mu_0}\rho_{\mathrm{i}}\omega_{\mathrm{Ai}}^2\,, \qquad C_{3\mathrm{e}} = D_{\mathrm{e}}^2\,. \tag{3.74}$$

The lack of twist in the external magnetic field implies a null value for the coefficient C_{1e}, enabling us to simplify the right-hand side of Equation (3.71)

$$\frac{1}{C_{3i}}\left\{D_i \left.\frac{dp_{Ti}}{dr}\right|_a + C_{1i}\, p_{Ti}|_a\right\} = \left.\frac{1}{D_e}\frac{dp_{Te}}{dr}\right|_a . \tag{3.75}$$

A second identity is formulated on application of the remaining boundary condition (3.58). Writing this out explicitly for the given model gives

$$p_{Ti}|_a - \frac{A_i^2 a}{\mu_0}[\xi_r]^{inner} = p_{Te}|_a . \tag{3.76}$$

In the left-hand side of this expression r is replaced with a since it is evaluated at the tube boundary. The quantity representing ξ_r evaluated at the inner tube boundary may be exchanged with its counterpart specified on the outer boundary since it is continuous. Upon performing this change and substituting expressions for ξ_r and p_T obtained by the rearrangement of Equations (3.27) and (3.28) we obtain

$$p_{Ti}|_a = \frac{A_i^2 a}{\mu_0}\frac{1}{D_e}\left.\frac{dp_{Te}}{dr}\right|_a + p_{Te}|_a . \tag{3.77}$$

Now dividing (3.75) by (3.77) gives

$$\frac{D_i\left[\dfrac{r}{p_{Ti}}\dfrac{dp_{Ti}}{dr}\right]_a + aC_{1i}}{C_{3i}} = \frac{\left[\dfrac{r}{p_{Te}}\dfrac{dp_{Te}}{dr}\right]_a}{D_e + \dfrac{A_i^2}{\mu_0}\left[\dfrac{r}{p_{Te}}\dfrac{dp_{Te}}{dr}\right]_a} . \tag{3.78}$$

Finally, substituting in the values for the coefficients D_i, C_{1i}, C_{3i} and D_e and the expression (3.77) for p_T we obtain

$$\frac{(\omega^2-\omega_{Ai}^2)\dfrac{m_i a I_m'(m_i a)}{I_m(m_i a)} - 2m\omega_{Ai}\dfrac{A_i}{\sqrt{\mu_0\rho_i}}}{(\omega^2-\omega_{Ai}^2)^2 - 4\omega_{Ai}^2\dfrac{A_i^2}{\mu_0\rho_i}} = \frac{\dfrac{|k_z|aK_m'(|k_z|a)}{K_m(|k_z|a)}}{\dfrac{\rho_e}{\rho_i}(\omega^2-\omega_{Ae}^2) + \dfrac{A_i^2}{\mu_0\rho_i}\dfrac{|k_z|aK_m'(|k_z|a)}{K_m(|k_z|a)}} , \tag{3.79}$$

where the dash denotes the derivative of a Bessel function (e.g. $I_m'(m_i a) \equiv (d/dx)I_m(x)$ evaluated at $x = m_i a$, etc.). We have defined the following quantities:

$$\omega_{Ai} = \frac{1}{\sqrt{\mu_0\rho_i}}(mA_i + k_z B_i) , \tag{3.80}$$

$$\omega_{\mathrm{Ae}} = \frac{B_{\mathrm{e}}}{\sqrt{\mu_0 \rho_{\mathrm{e}}}}, \tag{3.81}$$

$$m_{\mathrm{i}}^2 = {k_z}^2 \left(1 - \frac{4A_{\mathrm{i}}^2 \omega_{\mathrm{Ai}}^2}{\mu_0 \rho_{\mathrm{i}} (\omega^2 - \omega_{\mathrm{Ai}}^2)^2}\right). \tag{3.82}$$

Equation (3.79) is the dispersion relation for waves in an incompressible magnetic flux tube with uniform twist embedded within an untwisted magnetic environment. A dispersion relation of this form was first obtained by Dungey and Loughhead (1954) for the case of no external magnetic field. However, there is a sign error in their dispersion relation (equivalent to a negative rather than a positive sign on the right-hand side denominator of equation 3.79). This appears to be a typographical error and does not affect the remainder of their paper, concerned with a discussion of stability; they do not discuss the wave modes.

In the limit of no twist, when $B_\theta = 0$, the dispersion relation (3.79) reduces to

$$\rho_{\mathrm{i}}(\omega^2 - \omega_{\mathrm{Ai}}^2)\frac{K_m'(|k_z|a)}{K_m(|k_z|a)} = \rho_{\mathrm{e}}(\omega^2 - \omega_{\mathrm{Ae}}^2)\frac{I_m'(|k_z|a)}{I_m(|k_z|a)}. \tag{3.83}$$

A dispersion relation of this form was obtained previously by Edwin and Roberts (1983) who found that surface waves only were able to propagate. We illustrate this case in Figure 3.4 for the sausage mode $m = 0$ and later, in Figure 3.11, for the kink mode $m = 1$.

3.4 Results

For the diagrams that follow, it is convenient to introduce the following speeds: $c_{\mathrm{Ae}}(= B_{\mathrm{e}}/(\mu_0\rho_{\mathrm{e}})^{1/2})$ is the Alfvén speed outside the tube, $c_{\mathrm{A}z}(= B_{\mathrm{i}}/(\mu_0\rho_{\mathrm{i}})^{1/2})$ is the Alfvén speed obtained by using the longitudinal component of the magnetic field inside the tube, and $c_{\mathrm{A}\theta}(= B_\theta(a)/(\mu_0\rho_{\mathrm{i}})^{1/2})$ is the Alfvén speed determined by the azimuthal component of the field (taking the value of B_θ on the tube boundary). In addition, we introduce the total Alfvén speed c_{Ai} and the kink mode speed c_{k} through

$$c_{\mathrm{Ai}} = \left(c_{\mathrm{A}\theta}^2 + c_{\mathrm{A}z}^2\right)^{1/2}, \quad c_{\mathrm{k}} = \left(\frac{\rho_{\mathrm{i}} c_{\mathrm{Ai}}^2 + \rho_{\mathrm{e}} c_{\mathrm{Ae}}^2}{\rho_{\mathrm{i}} + \rho_{\mathrm{e}}}\right)^{1/2}. \tag{3.84}$$

Each of our figures is for the case of equal plasma densities and for an external

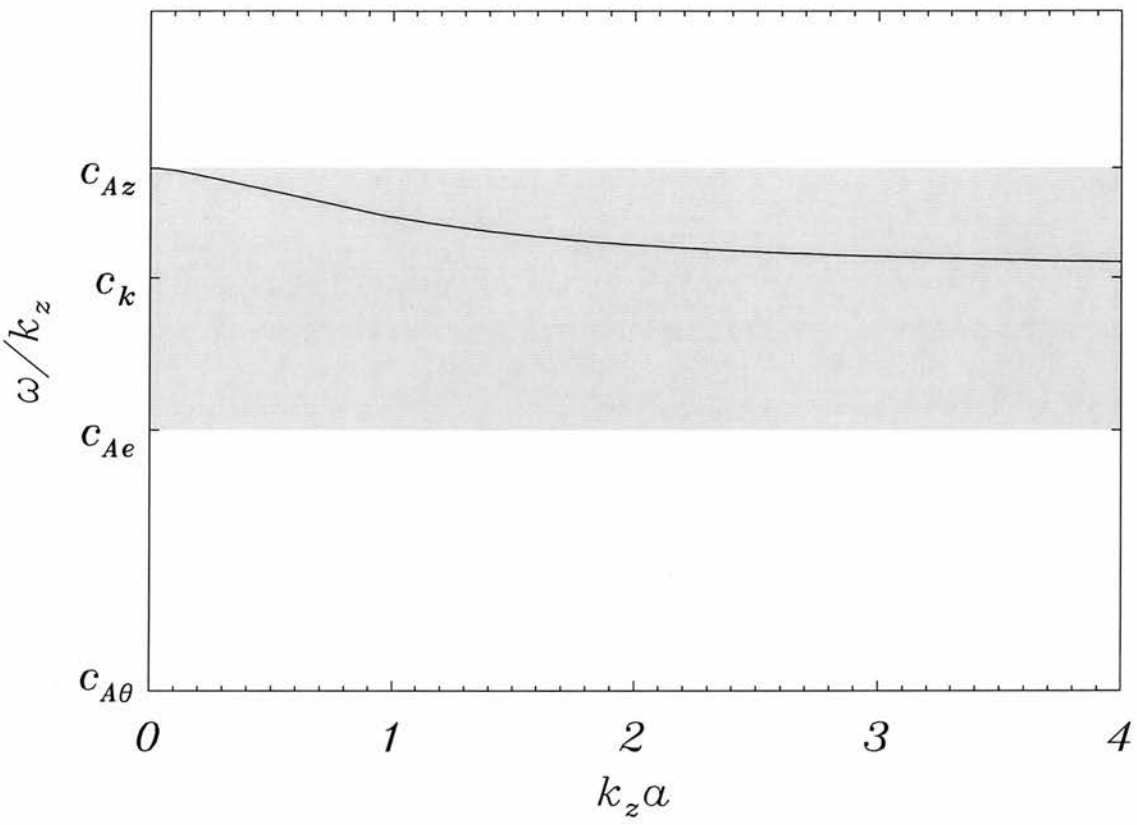

Figure 3.4: Phase velocity of the $m = 0$ mode in an untwisted flux tube ($B_\theta = 0$), with field strength B twice the field strength of the environment ($B = 2B_e$). The shaded region corresponds to the slow continuum.

field B_e one half the field strength $B = (A^2a^2 + B_i^2)^{1/2}$ on the inner boundary:

$$\rho_e = \rho_i \quad \text{and} \quad B_e = \frac{1}{2}\left(B_\theta^2(a) + B_z^2(a)\right)^{1/2} = \frac{1}{2}\left(A^2a^2 + B_i^2\right)^{1/2} .$$

In the absence of twist (see Figure 3.4), there are no body waves in a flux tube in an incompressible medium. However, soon as twist is introduced body waves appear. The body wave has a very different behaviour to the surface wave; the amplitude of the surface wave decays exponentially from the tube boundary to the centre of the tube, where the body wave's amplitude is oscillatory throughout the interior of the tube (see Figure 3.1).

The shaded region in these figures indicate the frequency range for which the modes are damped due to resonant absorption as discussed earlier in this chapter (see Section 3.3.3). The damping becomes more pronounced as the frequency moves further into the region. In Figure 3.4, for example, the mode is damped at

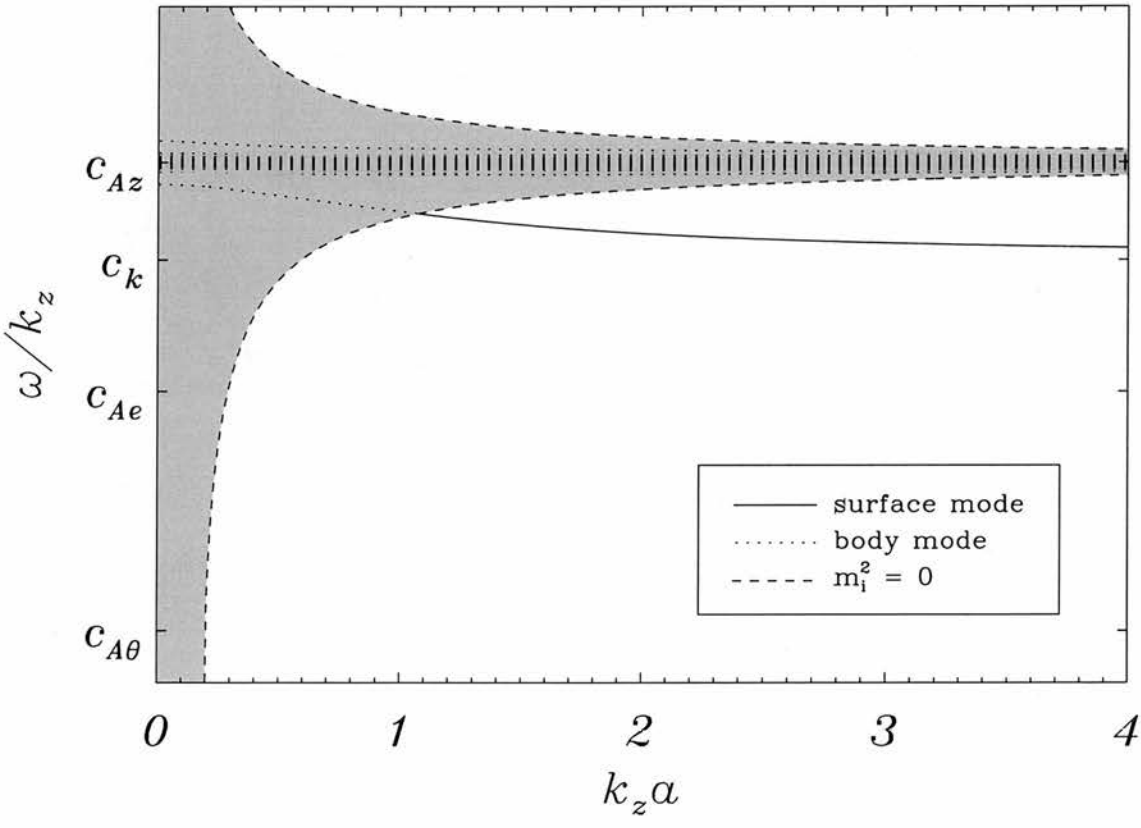

Figure 3.5: Phase velocity of the $m = 0$ modes in a twisted tube with external magnetic field $B_e = 0.5B$, $\rho_e = \rho_i$ and magnetic twist $B_\theta(a) = 0.1B_i$. Note the change of character, from body to surface wave, at $k_z a = 1.03$. The region $0.96c_{Az} < \omega/k_z < 1.04c_{Az}$ contains an infinite number of body wave harmonics. Also shown is the envelope separating regions of body and surface waves.

a much faster rate for short wavelengths than it is for long ones, with the mode becoming undamped as the wavelength tends to infinity.

As twist is increased, the body modes become more distinct and cover a wider range of phase speeds. The band of body modes moves with the Alfvén phase velocity which for the $m = 0$ mode occurs at $c_{\mathrm{A}z}$. Figure 3.6 displays the phase speed for the sausage mode corresponding to $m = 0$ with a small amount of magnetic twist.

The nature of the waves depends on the quantity m_{i}^2. If we plot the curves $m_{\mathrm{i}}^2 = 0$ we may distinguish between regions where body ($m_{\mathrm{i}}^2 < 0$) or surface ($m_{\mathrm{i}}^2 > 0$) waves occur (Figure 3.5). Typically, long wavelength modes display the characteristics of body waves. This can be seen from Figure 3.5 where the distribution of the body waves becomes restricted as $k_z a$ increases, reducing to the single phase speed $c_{\mathrm{A}z}$ in the limit $k_z a \to \infty$. A study of the eigenfunctions corresponding to these solutions shows that the modes are Sturmian for the harmonics lying below the Alfvén speed $c_{\mathrm{A}z}$, so each new harmonic contains an increasing number of radial nodes. The harmonics lying above the Alfvén speed $c_{\mathrm{A}z}$ are anti-Sturmian, so each new harmonic here displays a decreasing number of radial nodes.

A significant new feature of the waves is the behaviour of the fundamental mode. This mode changes in character, from body to surface mode, at finite $k_z a$. The feature can be understood by considering the spatial characteristics of the wave in the region of interest. A plot of the eigenfunction, ξ_r, of the mode shows that as we cross over the point at which it changes its behaviour, the only difference is that in the body mode region the wave increases up to the tube boundary in a convergent manner, whilst in the surface region it increases exponentially; see Figures 3.9 and 3.10. For completeness a plot of p_T has been made although this is perhaps not a sensible quantity to consider when studying the behaviour of waves near the boundary since it is discontinuous there. The fact that the mode behaves like a body mode for long wavelengths may be seen from the first figure in which a node occurs at $r = 0.95a$. When the frequency is such that the mode can neither be said to be body or surface mode in nature, Figure 3.10(c), the pressure perturbation is a constant throughout the tube and the radial displacement ξ_r is linear in r. Studies of the other harmonics reveal that they also display a dual nature, acting like body waves for long wavelengths but displaying surface-like attributes for small wavelengths.

Hybrid waves of the form arising in twisted flux tubes have been noted in other

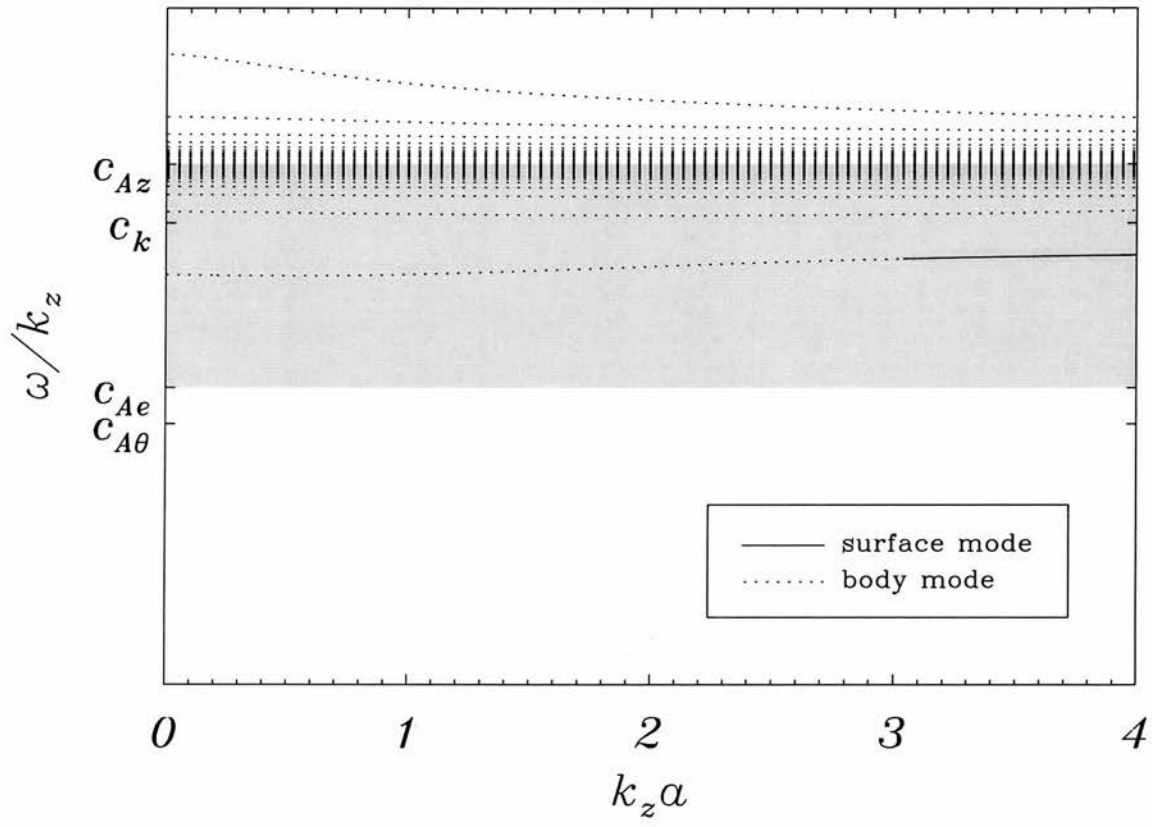

Figure 3.6: Phase velocity of the $m = 0$ modes in a twisted tube with external magnetic field $B_e = 0.5B$, $\rho_e = \rho_i$ and magnetic twist $B_\theta(a) = 0.5B_i$. Wave modes occuring within the shaded region correspond to quasi-mode solutions in the slow continuum. The hybrid mode changes from body to surface at $k_z a = 3.00$. Harmonics of body waves lie in $0.79c_{Az} < \omega/k_z < 1.21c_{Az}$.

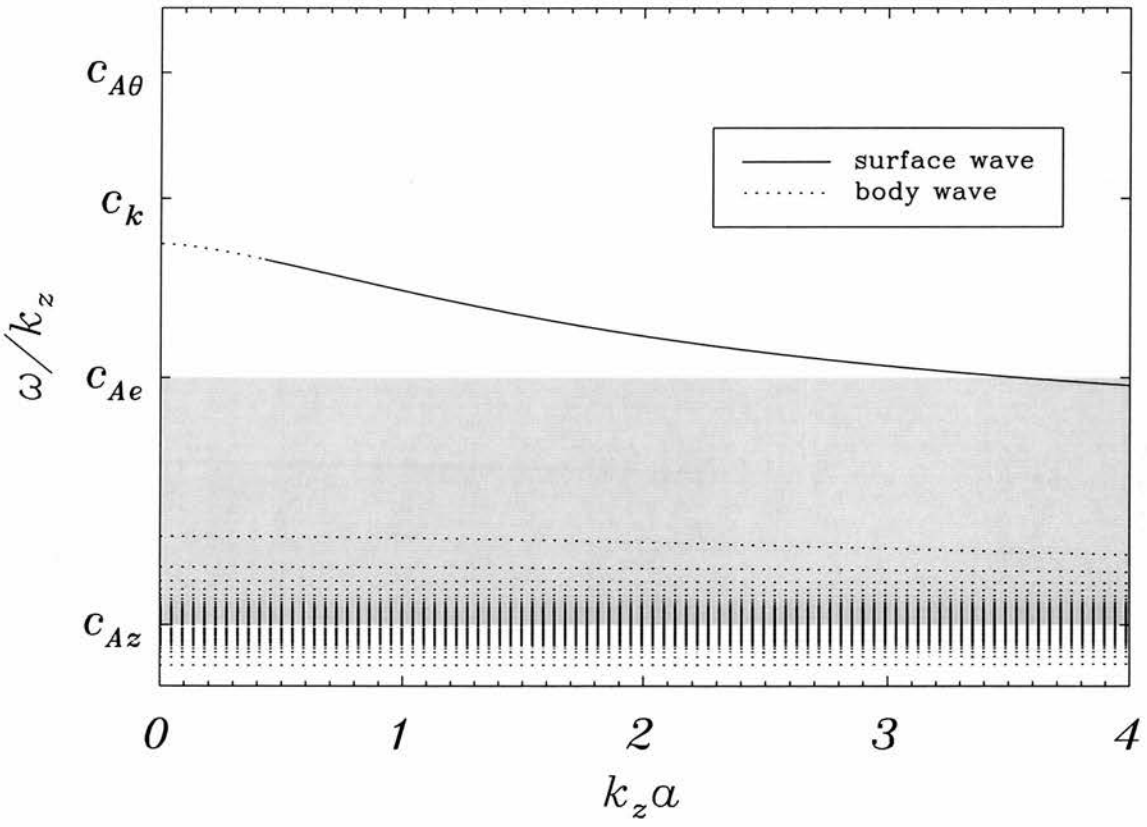

Figure 3.7: Phase velocity of the $m = 0$ modes when $B_e/B_i = 0.5$ and $B_\theta/B_z = 10$.

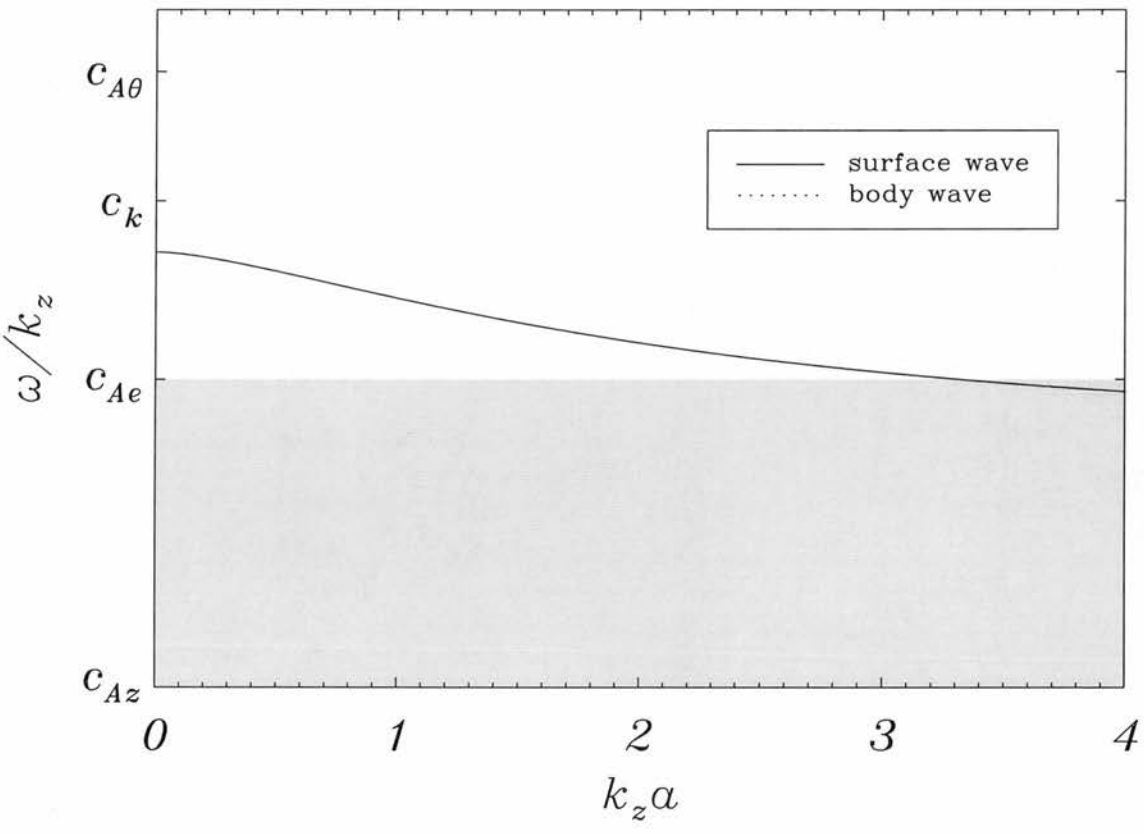

Figure 3.8: Phase velocity of the $m = 0$ mode when $B_e/B_i = 0.5$ and $B_\theta/B_z \to \infty$.

areas of magnetohydrodynamics; Smith *et al.* (1997) describes such behaviour in certain magnetoacoustic waves in current sheets. A change in character in the behaviour of motions is common in stratified media; p-modes, for example, are oscillatory within their cavity but evanescent outside it. However, for p-modes the change in character occurs with depth and so is a function of position in space, whereas here the change in character is a function of wavenumber, making the feature distinctive.

Figures 3.7 and 3.8 illustrate the behaviour of the modes as the twist becomes large. In Figure 3.7 we see that the fundamental mode has switched from the outermost Sturmian mode to its anti-Sturmian counterpart. This mode picks up the dual nature displayed by the previous fundamental mode, displaying more of a surface mode characteristic as the twist is increased. The band of modes surrounding the Alfvén speed $c_{\mathrm{A}z}$ becomes narrower and disappears altogether as the tube becomes infinitely twisted.

We turn now to a consideration of the kink mode, $m = 1$. Figure 3.11 illustrates the mode which occurs when the field is untwisted. This agrees with the results found by Edwin and Roberts (1983) for a magnetic cylinder in an incompressible plasma. Figure 3.12(a) displays the phase speed ω/k_z of the kink mode as twist is introduced with $B_\theta(a) = 0.1B_{\mathrm{i}}$. It is interesting to note that the phase velocity of the body waves tends to infinity as $k_z a \to 0$, so that waves of arbitrarily long wavelength propagate with arbitrarily large phase speed. It is of interest also to consider the group velocity. The group velocity $\partial\omega/\partial k_z$ along the tube is appropriate here, and this remains bounded; (Figure 3.12(b)). The velocity has been calculated numerically by approximating the value as

$$\left.\frac{\partial\omega}{\partial k_z}\right|_1 \approx \frac{\omega_2 - \omega_0}{k_{z2} - k_{z0}} = \frac{(\omega/k_z)_2(k_z a)_2 - (\omega/k_z)_0(k_z a)_0}{(k_z a)_2 - (k_z a)_0}\,.$$

There is also an occurrence of a maximum in the group velocity for the surface wave. A similar feature may be seen in the work of Roberts *et al.* (1984a), relating to a minimum in group velocity, or in the work of Wright (1994) that exhibited a group velocity maximum. In any case, a distinctive wave signature for impulsively excited disturbances is expected.

Figure 3.13 illustrates the behaviour of the kink modes when the magnetic environment has a stronger field than that of the tube. Note that the fundamental mode tends to infinity for long wavelengths, rather than approaching the kink speed as before. An entirely different mode approaches the kink speed in the

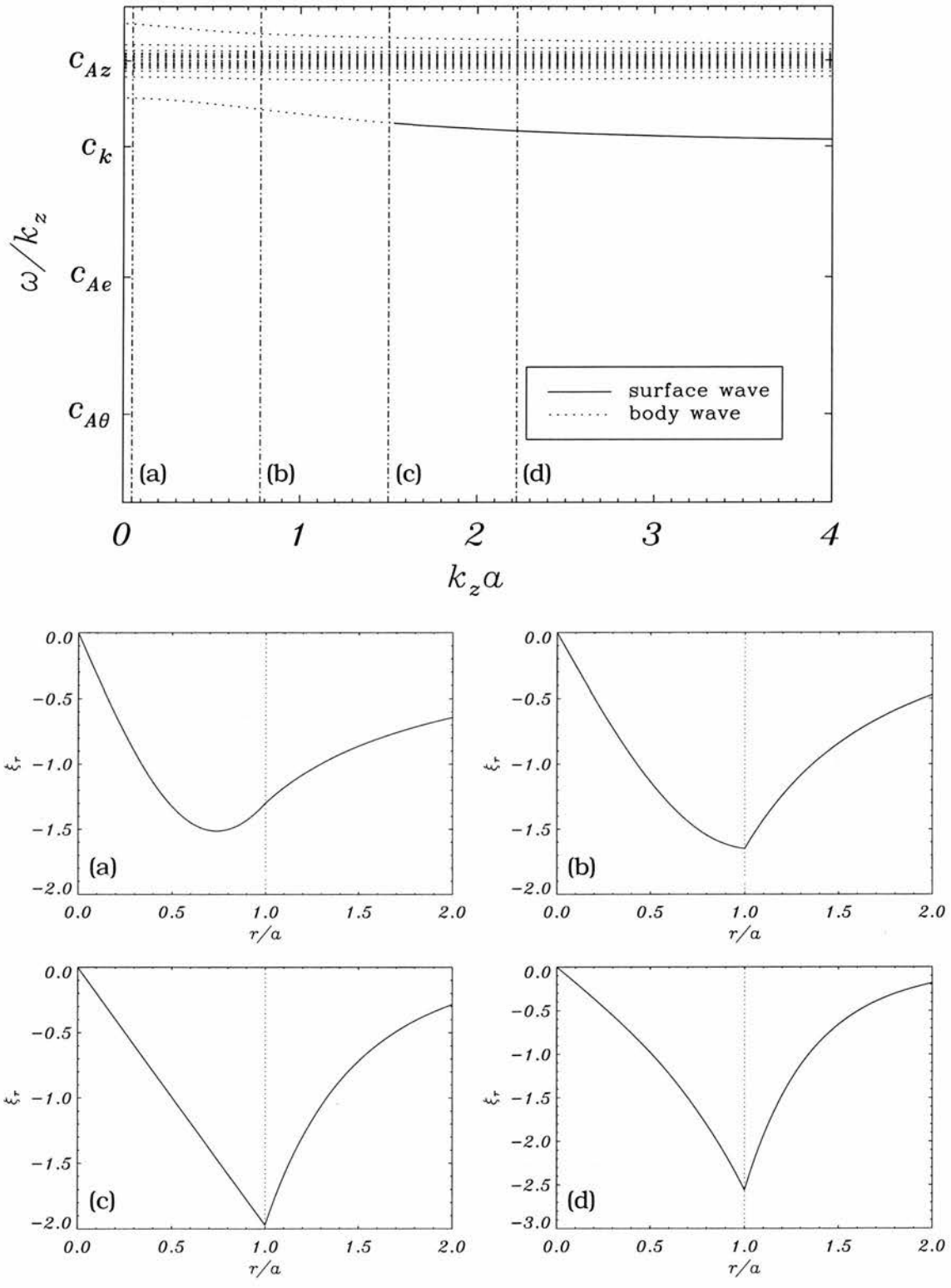

Figure 3.9: Eigenfunctions for ξ_r of the fundamental sausage mode as it changes in character from body to surface mode. Figures (a)–(d) correspond to the wavenumbers given in the top figure with the values: (a) $k_z a = 0.05$, (b) $k_z a = 0.775$, (c) $k_z a = 1.5$, and (d) $k_z a = 2.225$. Here we have taken the tube parameters to be $B_e = 0.5B$, $B_\theta = 0.1B_0$ and $\rho_e = \rho_0$.

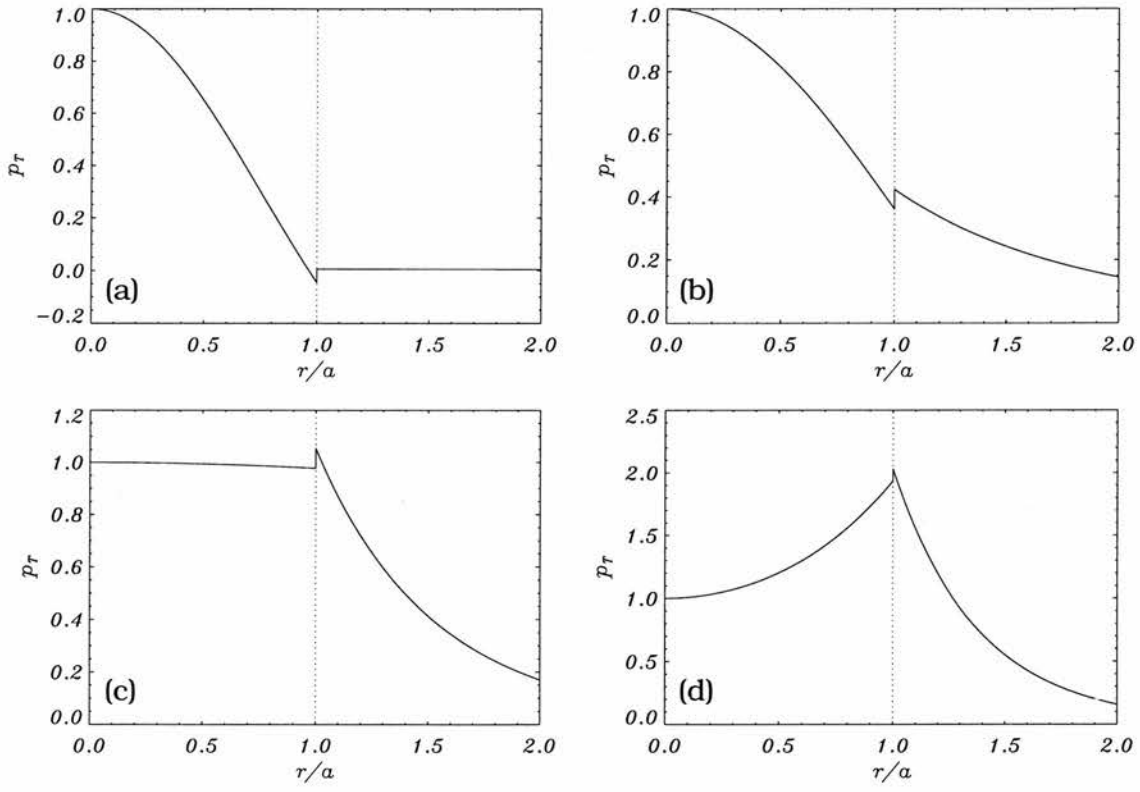

Figure 3.10: Eigenfunctions for p_T as it crosses the point at which it changes in character from body to surface mode. Figures (a)–(d) illustrate eigenfunctions for the corresponding wavenumbers in Figure 3.9. The jump in p_T at $r = a$ appears as a consequence of the jump in the equilibrium twist across $r = a$.

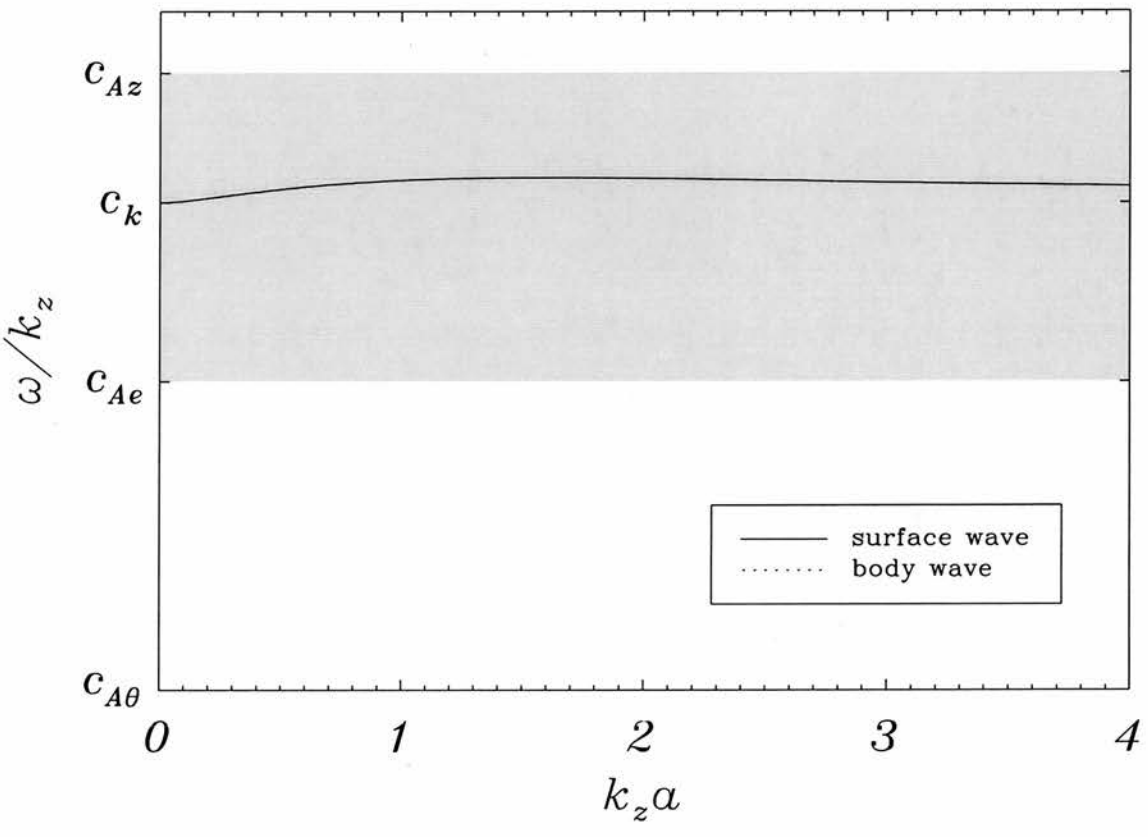

Figure 3.11: Phase velocity of the $m = 1$ mode when $B_e/B_i = 0.5$ and the field has no twist ($B_\theta = 0$). This is the kink mode as found by Edwin and Roberts (1983) for the untwisted magnetic cylinder. It corresponds to the quasi-mode identified by Goedbloed (1975).

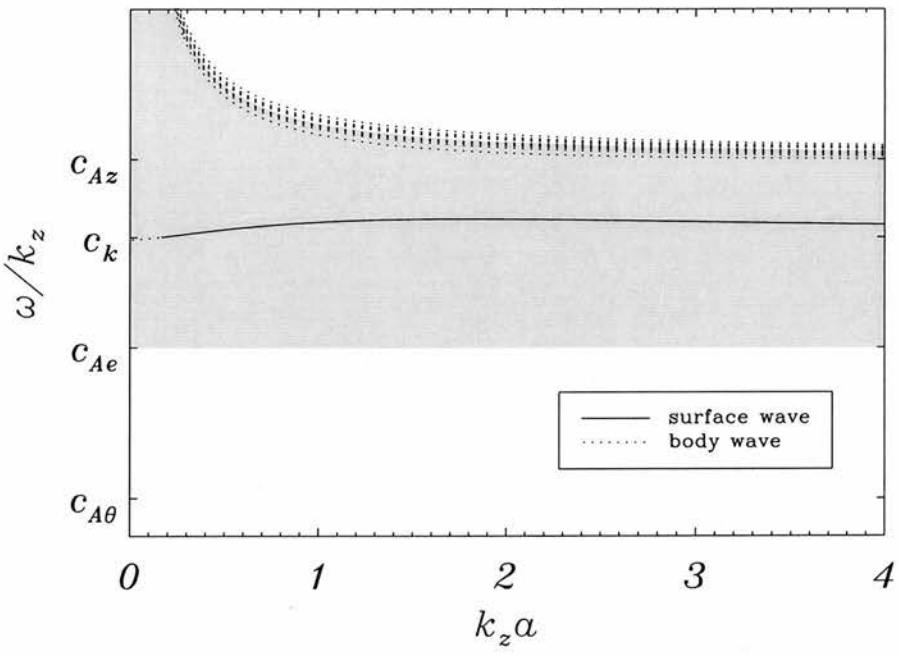

(a)

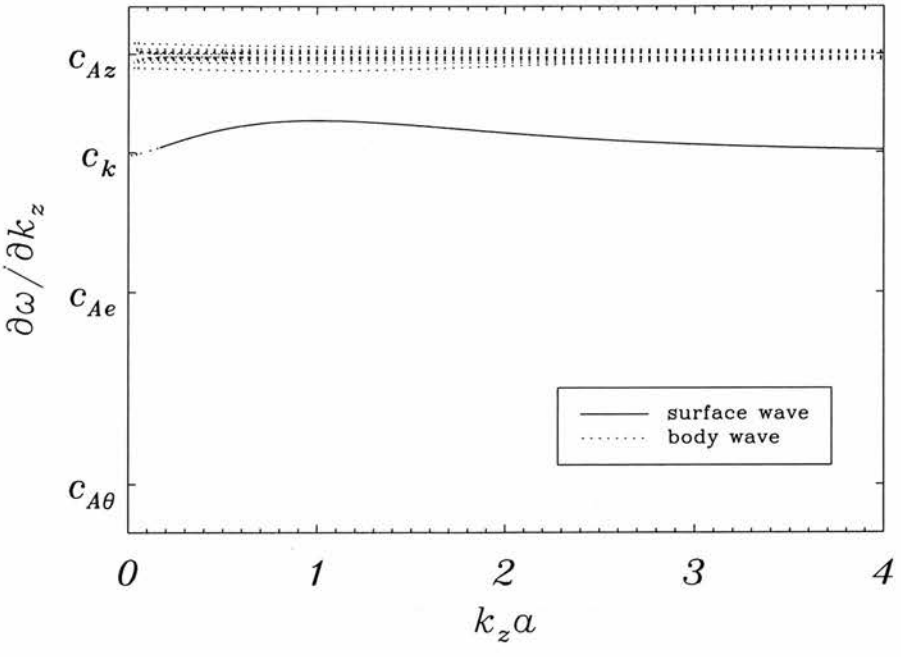

(b)

Figure 3.12: The phase and group velocities for the $m = 1$ modes when $B_e = 0.5B$ and $B_\theta(a) = 0.1B_i$. (a) Phase velocity. Note the band of modes above the Alfvén speed c_{Az} which have $\omega/k_z \to \infty$ as $k_z a \to 0$. (b) Group velocity. The group velocity follows much the same kind of pattern as the phase speeds for the $m = 0$ case. Note the occurrence of a maximum in the group velocity.

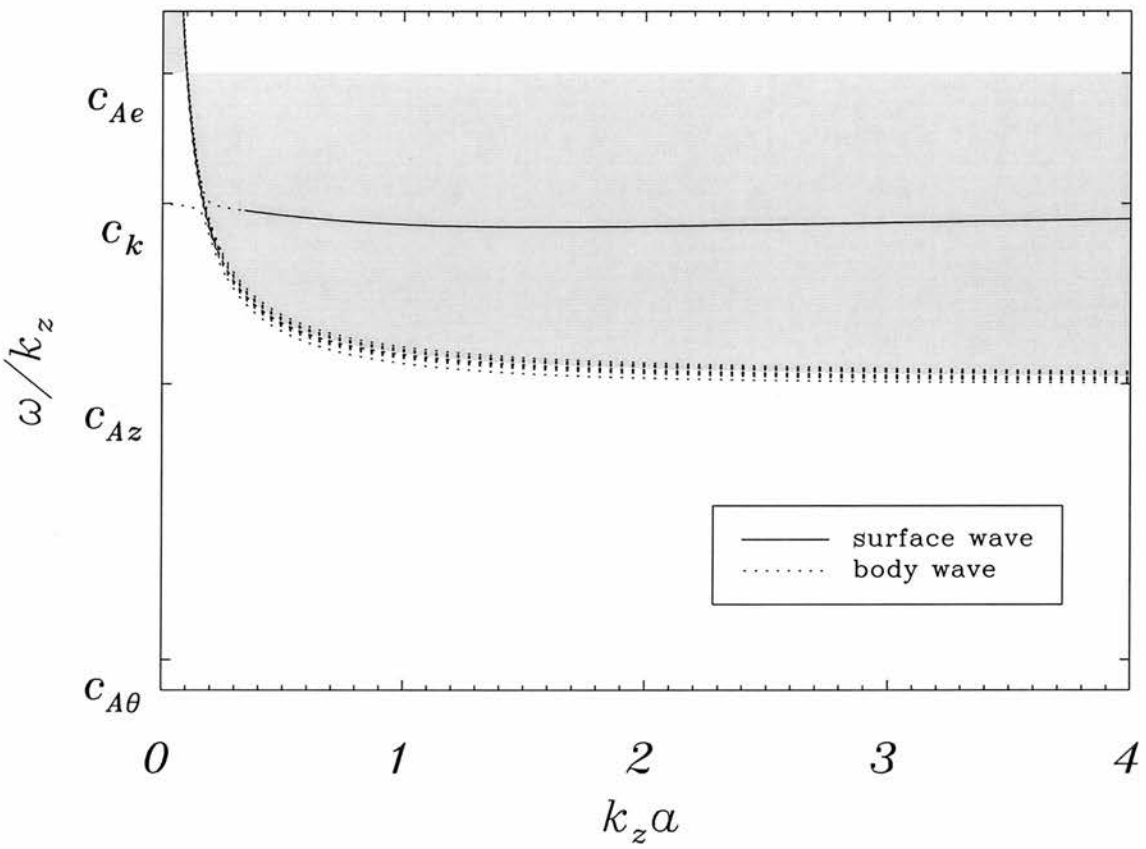

Figure 3.13: Phase velocity of the $m = 1$ modes when $B_e/B_i = 2$ and $B_\theta/B_z = 0.1$. Note the unusual behaviour of the fundamental mode for long wavelengths.

limit of infinite wavelength.

3.5 Expansions

The next step is to consider the behaviour of the twisted tube dispersion relation (3.79) in the extremes of small and large $k_z a$. We begin by rewriting the dispersion relation in terms of speeds as opposed to frequencies,

$$\frac{\left(c_{\rm ph}{}^2 - v_{\rm Ai}^2\right)\mathcal{J}_m - 2mv_{\rm Ai}\dfrac{c_{\rm A\theta}}{k_z a}}{\left(c_{\rm ph}{}^2 - v_{\rm Ai}^2\right)^2 - 4v_{\rm Ai}^2\dfrac{c_{\rm A\theta}^2}{(k_z a)^2}} = \frac{\mathcal{K}_m}{\frac{\rho_e}{\rho_i}\left(c_{\rm ph}{}^2 - c_{\rm Ae}^2\right) + \dfrac{c_{\rm A\theta}^2}{(k_z a)^2}\mathcal{K}_m}. \tag{3.85}$$

We have written

$$\mathcal{K}_m = \frac{k_z a K_m'(k_z a)}{K_m(k_z a)}, \qquad \mathcal{J}_m = \frac{x J_m'(x)}{J_m(x)},$$

where

$$x^2 = n_{\rm i}^2 a^2 = \frac{4 v_{\rm Ai}^2 c_{\rm A\theta}^2}{\left({c_{\rm ph}}^2 - v_{\rm Ai}^2\right)^2} - (k_z a)^2, \tag{3.86}$$

and $c_{\rm ph} = \omega/k_z$ is the phase speed of the wave; note that $v_{\rm Ai} = \omega_{\rm Ai}/k_z = (m/k_z a)c_{\rm A\theta} + c_{\rm Az}$, and we have taken $k_z > 0$.

To describe analytically the behaviour of the various waves for large and small $k_z a$, we restrict attention to the sausage ($m = 0$) modes. Modes with $m \geq 1$ are more difficult to describe in the limit of small $k_z a$ and will not be discussed here.

3.5.1 Sausage mode: Small values of $k_z a$

When $m = 0$, $v_{\rm Ai} = c_{\rm Az}$ and (3.79) may be written in the form

$$({c_{\rm ph}}^2 - c_{\rm Az}^2)\mathcal{J}_0 \left\{ \frac{\frac{\rho_{\rm e}}{\rho_{\rm i}}(k_z a)^2}{\mathcal{K}_0} \left({c_{\rm ph}}^2 - c_{\rm Ae}^2\right) + c_{\rm A\theta}^2 \right\} = (k_z a)^2({c_{\rm ph}}^2 - c_{\rm Az}^2)^2 - 4c_{\rm Az}^2 c_{\rm A\theta}^2 . \tag{3.87}$$

Then, as $k_z a \to 0$, Equation (3.87) yields

$$({c_{\rm ph}}^2 - c_{\rm Az}^2)\left[-\frac{x J_1(x)}{J_0(x)}\right] \approx -4c_{\rm Az}^2,$$

$$x \approx \pm \frac{2c_{\rm Az}c_\theta}{({c_{\rm ph}}^2 - c_{\rm Az}^2)},$$

$$\pm({c_{\rm ph}}^2 - c_{\rm Az}^2)\frac{2c_{\rm Az}c_\theta}{({c_{\rm ph}}^2 - c_{\rm Az}^2)}\frac{J_1(x)}{J_0(x)} \approx 4c_{\rm Az}^2,$$

giving

$$2\frac{J_0(x)}{J_1(x)} \approx \pm \frac{c_{\rm A\theta}}{c_{\rm Az}}. \tag{3.88}$$

Equation (3.88) provides a transcendental relation determining x. From (3.86) we have

$$\left(x^2 + (k_z a)^2\right)({c_{\rm ph}}^2 - c_{\rm Az}^2)^2 = 4c_{\rm Az}^4 (c_{\rm A\theta}/c_{\rm Az})^2, \tag{3.89}$$

$$c_{\rm ph} = c_{Az}\left(1 \pm \frac{2c_{A\theta}/c_{Az}}{(x^2+(k_z a)^2)^{1/2}}\right)^{1/2}.$$

From (3.88) we see that if $c_{A\theta}/2c_{Az} \ll 1$ then x corresponds to the zeros of $J_0(x)$ (i.e.. $x \approx j_{0,s}$, where $s = 1, 2, 3, \ldots$ denotes the sth positive zero of $J_0(x)$). Similarly, if $c_{A\theta}/2c_{Az} \gg 1$ then $x \approx j_{1,s}$, the zeros of $J_1(x)$ (see Abramowitz and Stegun, 1967).

For high harmonic numbers s, $x \gg 1$, (3.88) may be approximated by

$$2\frac{\cos(x-\pi/4)}{\cos(x-3\pi/4)} = \pm\frac{c_{A\theta}}{c_{Az}},$$

yielding

$$x = \arctan\left(\frac{c_{A\theta}/c_{Az} \pm 2}{c_{A\theta}/c_{Az} \mp 2}\right) + N\pi, \tag{3.90}$$

where $N = 0, 1, 2, \ldots$. These approximate relationships determine $c_{\rm ph}$ for the $m = 0$ modes.

The approximation is compared with the full numerical solution in Figure 3.14. This is the long wave approximation corresponding to Figure 3.5. The approximation gives an extremely good estimate for wavenumbers less than $k_z a = 0.1$. The two outermost modes of the band diverge from their values for smaller wavelengths, the fundamental mode in particular deviating far from the large wavenumber expansion. The rest of the modes in the band, however, give remarkably good predictions right out to the point at which the expansion can no longer be considered valid. This provides an excellent method for estimating the frequencies of the transcendental band of modes without requiring the solution of the full dispersion relation. It also confirms the band to be a real phenomena of the problem and not merely a numerical artifact of the method taken in solving the dispersion relation.

3.5.2 Sausage mode: Large values of $k_z a$

When $k_z a$ is large, x^2 is negative and we must replace the ordinary Bessel function J_0 in the dispersion relation (3.85) by its counterpart, the modified Bessel

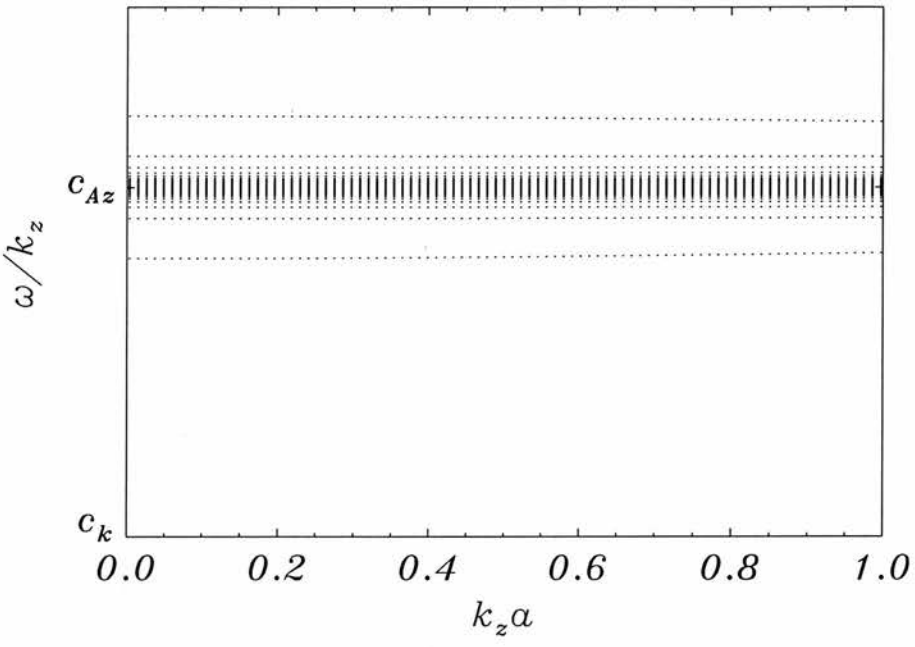

(a) Analytical

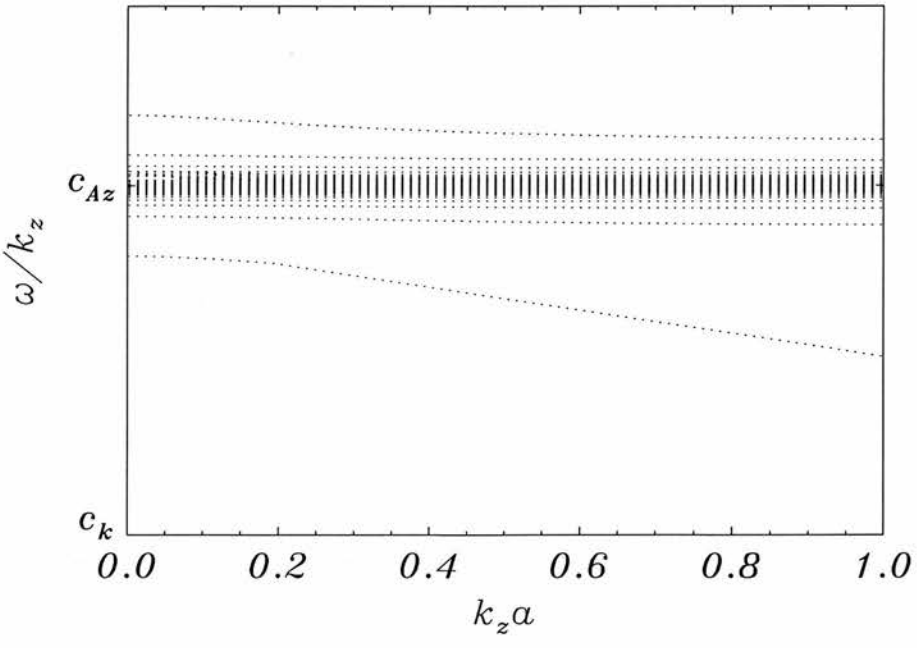

(b) Numerical

Figure 3.14: Phase velocity of the $m = 0$ modes when $B_e/B_i = 0.5$ and $B_\theta/B_z = 0.1$.

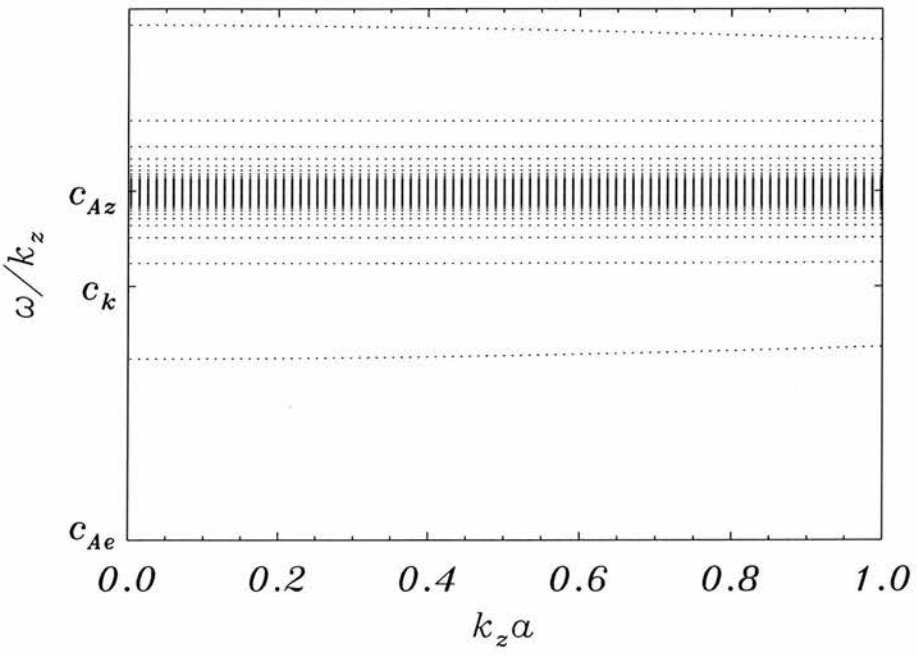

(a) Analytical

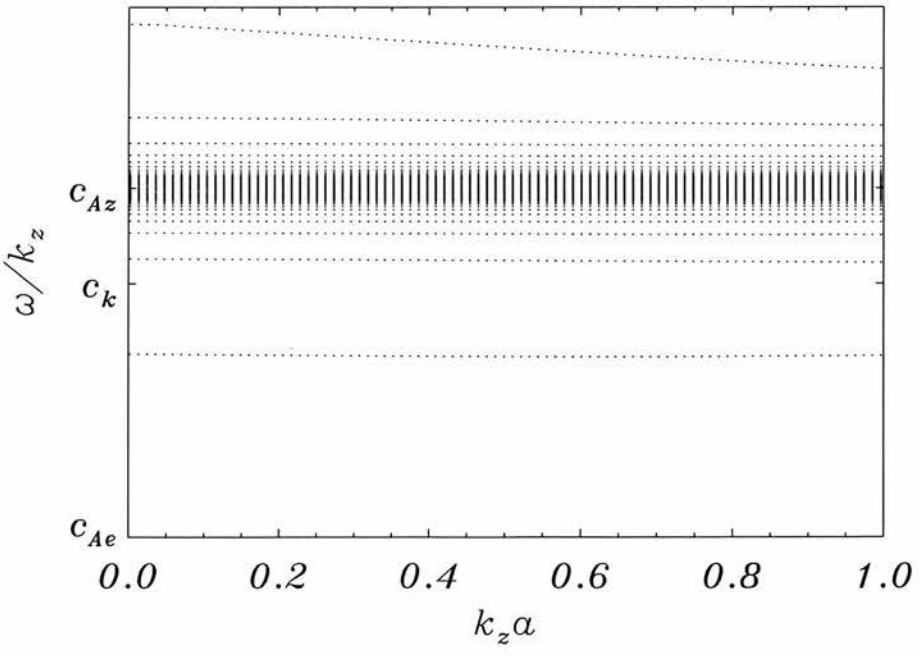

(b) Numerical

Figure 3.15: Phase velocity of the $m = 0$ modes when $B_e = 0.5B$, $\rho_e = \rho_i$ and $B_\theta(a) = 0.5B_i$, determined (a) numerically, from the full dispersion relation, and (b) analytically from the approximate dispersion relation.

function I_0. For large x and y, we write:

$$\mathcal{I}_0 = \frac{xI_0'(x)}{I_0(x)}, \qquad \mathcal{K}_0 = \frac{yK_0'(y)}{K_0(y)}, \qquad y = k_z a. \tag{3.91}$$

Assuming that when $k_z a$ is large, $m_i a$ is also large, we have

$$\begin{aligned} x &= k_z a \left(1 - \frac{4c_{Az}^2 c_\theta^2}{({c_{ph}}^2 - c_{Az}^2)^2} \frac{1}{(k_z a)^2}\right)^{1/2} \\ &\approx k_z a \left(1 - \frac{2c_{Az}^2 c_\theta^2}{({c_{ph}}^2 - c_{Az}^2)^2} \frac{1}{(k_z a)^2}\right) + O\left(\frac{1}{(k_z a)^3}\right), \end{aligned} \tag{3.92}$$

which is valid for

$$k_z a \gg \frac{\sqrt{2} c_{Az} c_\theta}{|{c_{ph}}^2 - c_{Az}^2|}. \tag{3.93}$$

From (3.85) we have

$$\frac{\mathcal{I}_0}{\mathcal{K}_0} \frac{\rho_e}{\rho_i} ({c_{ph}}^2 - c_{Ae}^2)({c_{ph}}^2 - c_{Az}^2) + \frac{\mathcal{I}_0}{(k_z a)^2} c_\theta^2 ({c_{ph}}^2 - c_{Az}^2) = ({c_{ph}}^2 - c_{Az}^2)^2 - \frac{4c_{Az}^2 c_\theta^2}{(k_z a)^2}. \tag{3.94}$$

Abramowitz and Stegun (1967, p. 378) give

$$\mathcal{I}_0 \approx x \left\{1 - \frac{1}{2x} - \frac{1}{8x^2}\right\}, \tag{3.95}$$

$$\frac{\mathcal{I}_0}{\mathcal{K}_0} \approx -\frac{x}{y} \left\{1 - \frac{1}{2xy}(x+y) + \frac{1}{8x^2y^2}(3x^2 + 2xy - y^2)\right\}, \tag{3.96}$$

$$\frac{\mathcal{I}_0}{(k_z a)^2} \approx \frac{1}{k_z a} - \frac{1}{2}\frac{1}{(k_z a)^2} + O\left(\frac{1}{(k_z a)^3}\right), \tag{3.97}$$

and so

$$\frac{\mathcal{I}_0}{\mathcal{K}_0} \approx -1 + \frac{1}{k_z a} + \frac{2\lambda - 1}{2}\frac{1}{(k_z a)^2} + O\left(\frac{1}{(k_z a)^3}\right), \tag{3.98}$$

where $\lambda = \dfrac{2c_{Az}^2 c_\theta^2}{({c_{ph}}^2 - c_{Az}^2)^2}$.

Substituting in (3.94) and dropping terms $O\left(\frac{1}{(k_z a)^2}\right)$ gives

$$\left[-1 + \frac{1}{k_z a}\right] \frac{\rho_e}{\rho_i} ({c_{ph}}^2 - c_{Ae}^2)({c_{ph}}^2 - c_{Az}^2) + \frac{1}{k_z a} c_\theta^2 ({c_{ph}}^2 - c_{Az}^2) \approx ({c_{ph}}^2 - c_{Az}^2)^2. \tag{3.99}$$

Thus

$$\left[\frac{\rho_e}{\rho_i k_z a} - \frac{\rho_e}{\rho_i} - 1\right] {c_{ph}}^2 \approx -c_{Az}^2 + \frac{\rho_e}{\rho_i k_z a} c_{Ae}^2 - \frac{\rho_e}{\rho_i} c_{Ae}^2 - \frac{c_\theta^2}{k_z a}. \tag{3.100}$$

So

$${c_{ph}}^2 \approx \frac{\rho_i c_{Az}^2 + \rho_e c_{Ae}^2 + \left(\rho_i c_\theta^2 - \rho_e c_{Ae}^2\right)/k_z a}{\rho_i + \rho_e - \dfrac{\rho_e}{k_z a}}, \tag{3.101}$$

which we may write in the form

$${c_{ph}}^2 \approx c_k^2 + \frac{\rho_e \left(c_k^2 - c_{Ae}^2\right) + \rho_i c_\theta^2}{\rho_i + \rho_e} \frac{1}{k_z a}, \tag{3.102}$$

which is valid as $k_z a \to \infty$.

These relations provide useful checks on the numerical for the various modes.

3.6 Stability

Dungey and Loughhead (1954) investigated the stability of the tube and were able to verify Lundquist's (1951) requirement for instability to occur, namely

$$2p < a, \tag{3.103}$$

where $2\pi p$ is the pitch ($= B_i/A$) of the magnetic field. The presence of an external magnetic field — not considered by Dungey and Loughhead — introduces a stabilising effect. This can be seen in Figure 3.17 where we plot the marginal stability curves ($\omega^2 = 0$). In these diagrams the modes found below each curve are stable whilst the modes above are unstable. In order to facilitate a comparison with Dungey and Loughhead's results we have plotted the graphs using the same notation and it is the gradients of the lines that are important for stability concerns.

When $\omega^2 = 0$, the dispersion relation Equation (3.79) becomes

$$\frac{\omega_{Ai}^2 \mathcal{J}_m - 2m \dfrac{A}{\sqrt{\mu_0 \rho_i}} \omega_{Ai}}{4 \dfrac{A^2}{\mu_0 \rho_i} \omega_{Ai}^2 - \omega_{Ai}^4} = \frac{\mathcal{K}_m}{\dfrac{A^2}{\mu_0 \rho_i} \mathcal{K}_m - \dfrac{{k_z}^2 B_e^2}{\mu_0 \rho_i}}, \tag{3.104}$$

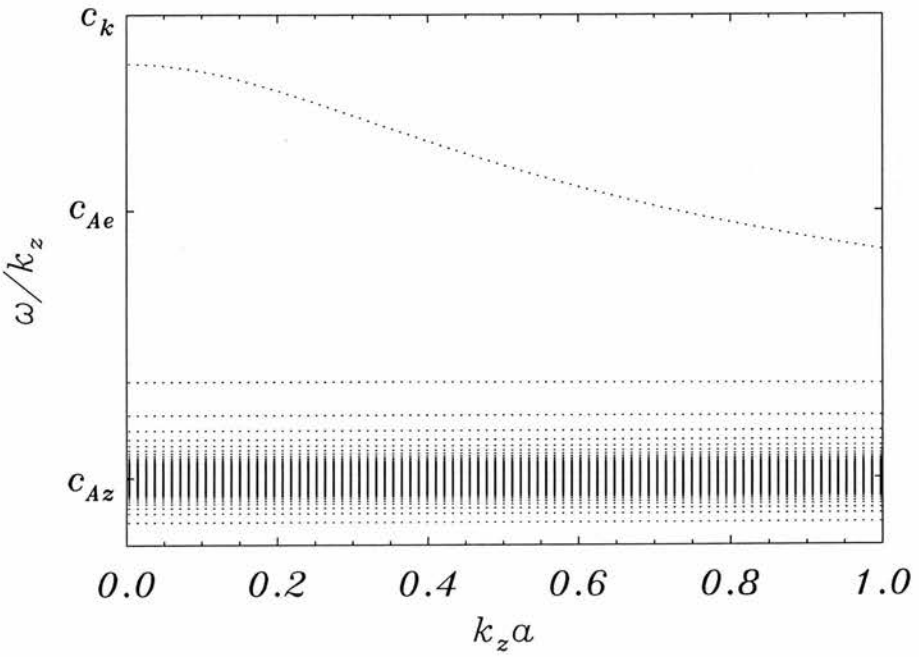

(a) Analytical

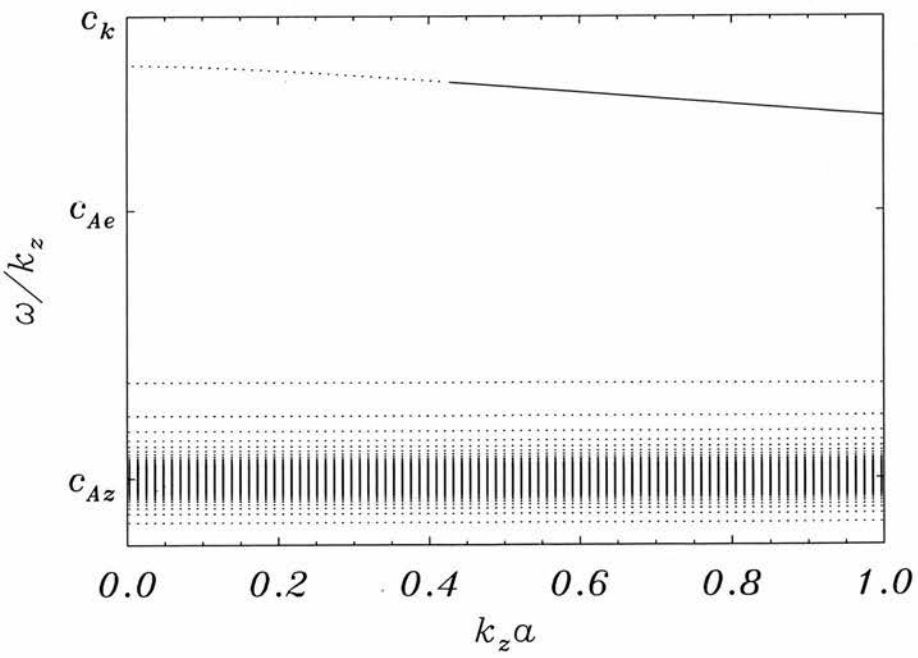

(b) Numerical

Figure 3.16: Phase velocity of the $m = 0$ modes when $B_e/B_i = 0.5$ and $B_\theta/B_z = 10$.

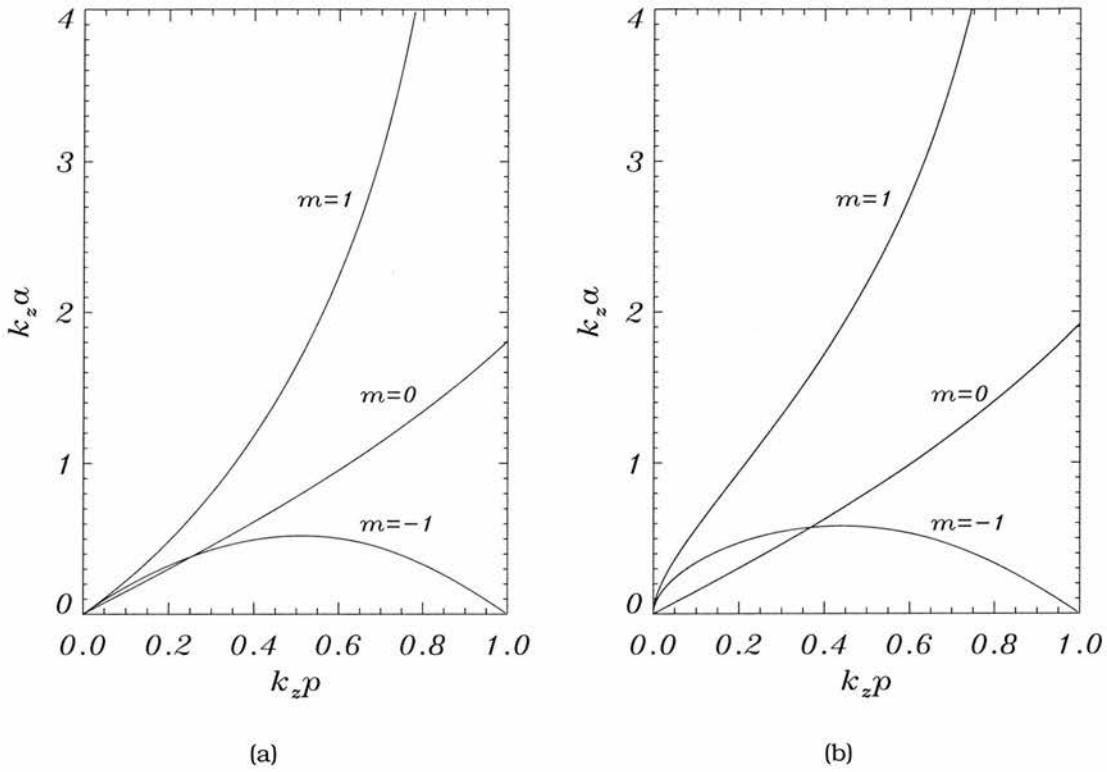

Figure 3.17: Curves of marginal stability ($\omega^2 = 0$), plotting $k_z a$ as a function of dimensionless pitch $k_z p$ for (a) the special case of zero external ($B_e = 0$) field as obtained by Dungey and Loughhead (1954), and (b) the case $B_e = 0.5B$ illustrating the stabilising effect of an external magnetic field. For each of the $m = 0$, $m = -1$ or $m = 1$ curves, the region lying below the curve is a stable zone; the region above is an unstable zone.

where we have written

$$\omega_{Ai} = \frac{A}{\sqrt{\mu_0 \rho_i}} (m + k_z p) \ , \quad (m_i a)^2 = -(n_i a)^2 = (k_z a)^2 \left(1 - \frac{4}{(m + k_z p)^2}\right) .$$

Rearranged, Equation (3.104) gives

$$[(m + k_z p)\, \mathcal{J}_m + 2m] \left[1 - (k_z a)^2 \frac{(B_e/Aa)^2}{\mathcal{K}_m}\right] = 4\,(m + k_z p) - (m + k_z p)^3 \ . \qquad (3.105)$$

Now $-\mathcal{K}_m \geq |m|$ for all m, so we may observe that

$$\alpha \equiv \left(1 - (k_z a)^2 \frac{(B_e/Aa)^2}{\mathcal{K}_m}\right) \geq 1 .$$

Then, Equation (3.105) may be written in the form

$$\frac{2m}{m+k_zp}\alpha = -\left[\alpha\mathcal{J}_m + (m_ia)^2(m+k_zp)^2\right] . \tag{3.106}$$

Suppose that $m_i^2a^2$ is positive. Then $\mathcal{J}_m$, written in terms of the modified Bessel function I_m, may be shown to satisfy $\mathcal{J}_m \geq |m|$ for all m. Then Equation (3.106) gives

$$\frac{2m}{(m+k_zp)} \leq -|m| . \tag{3.107}$$

For $m \geq 1$ this inequality does not hold, and therefore $(m_ia)^2$ must be negative for these mode numbers. For $m = 0$, the marginal dispersion relation (3.104) reduces to the degenerate form

$$\alpha\mathcal{J}_0 = -(m_ia)^2(k_zp)^2 ,$$

which has only the solution $k_zp = \pm 2$, so again $(m_ia)^2$ must be negative. For $m < 0$, inequality (3.107) gives

$$\frac{1}{k_zp - |m|} \geq \frac{1}{2} .$$

But $(m_ia)^2 \geq 0$ gives the contradictory result

$$\frac{1}{k_zp - |m|} \leq \frac{1}{4} .$$

So for the analysis of Equation (3.104) we need only consider $(n_ia)^2 > 0$, i.e.

$$(n_ia)^2 = (k_za)^2\left(\frac{4}{(m+k_zp)^2} - 1\right) > 0 , \tag{3.108}$$

leading to the conditions

$$(m+k_zp)^2 < 4 ,$$

$$0 \leq (m+k_zp) < 2 \quad \text{or} \quad 0 \geq (m+k_zp) > -2 ,$$

$$-k_zp \leq m < 2 - k_zp \quad \text{or} \quad -k_zp \geq m > -2 - k_zp .$$

Since k_zp is always positive, these conditions give $m < 2$ as the requirement for marginal stability to occur.

A computational study of these modes indicates that the most important are $m = \pm 1$. This would appear to be due to the fact that these modes displace the axis of the tube. The $m = 1$ is the most unstable of the two since the helical perturbation formed is in the same sense as the twist. This means that the perturbation acts to increase the twist in the tube and hence makes the tube more unstable. The $m = -1$ mode, on the other hand, acts to unravel the twist. These arguments show that the analysis need only be carried out on the $m = 1$ mode. With $m = 1$, Equation (3.105) reduces to

$$[(1 + k_z p)\,\mathcal{J}_1 + 2]\left[1 - (k_z a)^2 \frac{(B_e/Aa)^2}{\mathcal{K}_1}\right] = 4\,(1 + k_z p) - (1 + k_z p)^3\,,$$

with

$$\mathcal{J}_1 = x\frac{J_0(x)}{J_1(x)} - 1\,, \quad \mathcal{K}_1 = -k_z a \frac{K_0(k_z a)}{K_1(k_z a)} - 1\,,$$

$$x^2 = (k_z a)^2 \left(\frac{4}{(1 + k_z a)^2} - 1\right).$$

For small $k_z a$ and small x,

$$\mathcal{J}_1 \approx 1 - \frac{1}{4}x^2 - \frac{1}{96}x^4 - \frac{1}{1536}x^6 + O\left(x^8\right),$$

$$\frac{1}{\mathcal{K}_1} \approx -\left[1 + (\gamma - \ln 2 + \ln(k_z a))\,(k_z a)^2 + O\left((k_z a)^4\right)\right].$$

Keeping terms up to order 3, we obtain

$$\left[3 + k_z p - \frac{1}{4}(k_z a)^2\,(4(1 - k_z p) - (1 + k_z p))\right]\left[1 + \phi^2 (k_z a)^2\right] = 3 + k_z p - 3(k_z p)^2 - (k_z p)^3\,, \quad (3.109)$$

which can be rewritten in the form

$$(k_z a)^2 = \frac{4}{1 - 4(B_e/Aa)^2}(k_z p)^2 \left(1 + \frac{1}{1 - 4(B_e/Aa)^2} k_z p\right). \quad (3.110)$$

In the absence of an external field, $B_e/Aa = 0$, we obtain

$$k_z a \approx 2k_z p(1 + k_z p)\,. \quad (3.111)$$

When $B_e/Aa \geq 1/2$, Equation (3.110) is no longer valid and we find that the tube

is unconditionally stable for small $k_z a$ and $k_z p$. This can be seen in Figure 3.17(b) where the line for $m = 1$ becomes vertical for small values of $k_z p$.

3.7 Concluding Remarks

The behaviour of waves in a magnetic flux tube has previously been studied in detail only in the absence of twist. In this chapter we have outlined, for the special case of uniform twist, an extensive analytical investigation. Here, for the first time, we have demonstrated analytically that a set of discrete eigenmodes can be identified for the twisted tube. Moreover, these modes have been found to extend throughout the slow continuum, classifying them as quasi-modes within this region. The eigenmodes found exhibit new features not present in the untwisted case. The most striking feature is the introduction of an infinite set of body waves, a feature absent in the straight field case. We have also found that the mode corresponding to that of the slow surface mode in the straight field case changes in nature from that of a surface mode to that of a body mode when twist is introduced. In addition to numerical solutions of the dispersion relation, we have been able to obtain various approximate results valid for large and small dimensionless wavenumber $k_z a$. We also extended the study of Dungey and Loughhead (1954) to show the stabilising effect introduced by the inclusion of a magnetic field outside the flux tube. We found that the condition for the onset of stability changes from $2p < a$ to $2p < a\sqrt{1 - 4(B_e/Aa)^2}$ when a straight magnetic field of strength $B_e \ll Aa$ is introduced in the region external to the flux tube. When $2B_e \geq Aa$ we find that the tube becomes unconditionally stable for small amounts of twist.

In order to obtain a tractable set of equations we have restricted our analysis to that of the incompressible plasma limit. In this extreme the fast waves are eliminated from the system and we also lose the distinction between the Alfvén continuum and the slow continuum. Whilst such simplifications lead to greater simplicity in the final analysis, it is important to note that important information is necessarily lost. It is hoped that this work will serve as a foundation for more sophisticated models in the future.

Chapter 4

Nonlinear Fast Magnetoacoustic Modes of a Magnetic Slab

... they had been selected at birth as those who would witness the answer, but even so they found themselves gasping and squirming like excitid children.

"And you're ready to give it to us?" urged Loonquawl.

"I am."

"Now?"

"Now," said Deep Thought.

They both licked their dry lips.

"Though I don't think," added Deep Thought, "That you're going to like it."

— Douglas Adams, The Hitch Hiker's Guide to the Galaxy

4.1 Introduction

As we have seen throughout this thesis, plasma inhomogeneities have an important effect on magnetohydrodynamic wave propagation. These effects manifest themselves as wave damping, phase mixing, resonant absorption and may lead to ducting of waves by structures such as magnetic flux tubes. We have so far restricted ourselves to the study of small amplitude perturbations in which the leading order perturbation terms are sufficient in describing the nature of

wave propagation. This simplification discards information which sometimes proves essential in describing the true properties of the wave. A modification of the linear behaviour of the wave may come about as a result of large amplitude perturbations or strong dispersion introduced by plasma inhomogeneities in the transverse direction. For example, it has been found that the tendency of wave broadening brought about by dispersive effects may be balanced by a steepening of the wave due to nonlinear terms causing the propagation of solitons (Roberts and Mangeney, 1982, Roberts, 1985, Merzljakov and Ruderman, 1985, Molotovshchikov and Ruderman, 1987, Roberts, 1987). In the Earth's magnetosphere nonlinear terms may be important in explaining long period pulsations (Allan *et al.*, 1991). Nonlinear investigations have also been made examining rapid pulsations in the solar corona (Roberts *et al.*, 1984b, Nakariakov and Oraevsky, 1995), in the generation of waves and shocks through nonlinear wave interactions (Wentzel, 1977, Oraevsky, 1983, Nakariakov and Oraevsky, 1995, Nakariakov *et al.*, 1997) and in examining wave motion in the solar wind (Mann, 1995). Nonlinear effects have also been investigated in the heating of the outer corona by resonant absorption (Ruderman and Goossens, 1993, Ruderman, Hollweg and Goossens, 1997, Ruderman, Goossens and Hollweg, 1997, Ballai and Erdélyi, 1998, Erdélyi and Ballai, 1999). In this chapter we will study the effects of wave interactions brought about by the consideration of weakly nonlinear terms. In this process different wave modes resonate with each other, modifying their behaviour and sometimes leading to the generation of other modes.

4.2 Nonlinear wave equations

The model we consider is for zero plasma-β ideal MHD. This relates the magnetic field $\mathbf{B}$, plasma velocity $\mathbf{U}$ and density ρ through the governing equations:

$$\begin{aligned}
&\rho\frac{\partial \mathbf{U}}{\partial t} + \rho(\mathbf{U}\cdot\nabla)\mathbf{U} = -\frac{\mathbf{B}}{\mu_0}\times(\nabla\times\mathbf{B}),\\
&\frac{\partial \mathbf{B}}{\partial t} = \nabla\times(\mathbf{U}\times\mathbf{B}), \qquad \nabla\cdot\mathbf{B} = 0,\\
&\frac{\partial \rho}{\partial t} + \nabla\cdot(\rho\mathbf{U}) = 0.
\end{aligned} \tag{4.1}$$

We consider equation (4.1) in Cartesian coordinates (x, y, z). We assume there are no variations in the y-direction ($\partial/\partial y = 0$), and we neglect perturbations of B_y

and U_y associated with the Alfvén wave (see the discussion in Nakariakov *et al.*, 1997, for details). In component form, equation (4.1) with $\mathbf{U} = (U_x, 0, U_z)$ and $\mathbf{B} = (B_x, 0, B_z)$ are

$$\rho\left[\frac{\partial U_x}{\partial t} + \left(U_x\frac{\partial U_x}{\partial x} + U_z\frac{\partial U_x}{\partial z}\right)\right] = \frac{B_z}{\mu_0}\left(\frac{\partial B_x}{\partial z} - \frac{\partial B_z}{\partial x}\right), \tag{4.2}$$

$$\rho\left[\frac{\partial U_z}{\partial t} + \left(U_x\frac{\partial U_z}{\partial x} + U_z\frac{\partial U_z}{\partial z}\right)\right] = -\frac{B_x}{\mu_0}\left(\frac{\partial B_x}{\partial z} - \frac{\partial B_z}{\partial x}\right), \tag{4.3}$$

$$\frac{\partial B_x}{\partial t} = -\frac{\partial}{\partial z}\left(U_z B_x - U_x B_z\right), \tag{4.4}$$

$$\frac{\partial B_z}{\partial t} = \frac{\partial}{\partial x}\left(U_z B_x - U_x B_z\right), \tag{4.5}$$

$$\frac{\partial \rho}{\partial t} + \frac{\partial}{\partial x}\left(\rho U_x\right) + \frac{\partial}{\partial z}\left(\rho U_z\right) = 0. \tag{4.6}$$

Consider small but finite amplitude perturbations about the uniform equilibrium magnetic field $B_0\hat{\mathbf{z}}$ and transversally structured plasma density $\rho_0(x)$, expanding quantities in terms of a small parameter ε, taken as a dimensionless measure of amplitude:

$$B_x = \varepsilon b_x, \quad B_z = B_0 + \varepsilon b_z, \tag{4.7}$$

$$U_x = \varepsilon v_x, \quad U_z = \varepsilon v_z, \quad \rho = \rho_0(x) + \varepsilon\tilde{\rho}. \tag{4.8}$$

The tilde will be omitted subsequently. Retaining only quadratic nonlinear terms, equations (4.2)-(4.6) may be written in the form

$$\rho_0(x)\frac{\partial v_x}{\partial t} - \frac{B_0}{\mu_0}\left(\frac{\partial b_x}{\partial z} - \frac{\partial b_z}{\partial x}\right) = \varepsilon N_1, \tag{4.9}$$

$$\rho_0(x)\frac{\partial v_z}{\partial t} = \varepsilon N_2, \tag{4.10}$$

$$\frac{\partial b_x}{\partial t} - B_0\frac{\partial v_x}{\partial z} = \varepsilon N_3, \tag{4.11}$$

$$\frac{\partial b_z}{\partial t} + B_0\frac{\partial v_x}{\partial x} = \varepsilon N_4, \tag{4.12}$$

$$\frac{\partial \rho}{\partial t} + \frac{\partial}{\partial x}\left(\rho_0(x)v_x\right) + \rho_0(x)\frac{\partial v_z}{\partial z} = \varepsilon N_5, \tag{4.13}$$

where we have gathered quadratically nonlinear terms to the right-hand side of the equations. The quantities N_1 to N_5 are as follows:

$$N_1 = \frac{b_z}{\mu_0}\left(\frac{\partial b_x}{\partial z} - \frac{\partial b_z}{\partial x}\right) - \rho\frac{\partial v_x}{\partial t} - \rho_0(x)\left(v_x\frac{\partial v_x}{\partial x} + v_z\frac{\partial v_x}{\partial z}\right), \tag{4.14}$$

$$N_2 = -\frac{b_x}{\mu_0}\left(\frac{\partial b_x}{\partial z} - \frac{\partial b_z}{\partial x}\right) - \rho\frac{\partial v_z}{\partial t} - \rho_0(x)\left(v_x\frac{\partial v_z}{\partial x} + v_z\frac{\partial v_z}{\partial z}\right), \tag{4.15}$$

$$N_3 = -\frac{\partial}{\partial z}\left(v_z b_x - v_x b_z\right), \tag{4.16}$$

$$N_4 = \frac{\partial}{\partial x}\left(v_z b_x - v_x b_z\right), \tag{4.17}$$

$$N_5 = -\frac{\partial}{\partial x}\left(\rho v_x\right) - \frac{\partial}{\partial z}\left(\rho v_z\right). \tag{4.18}$$

Equations (4.9)-(4.13) may be grouped together to give

$$\frac{\partial^2 v_x}{\partial t^2} - c_{\mathrm{A}}^2(x)\nabla^2 v_x = \varepsilon\left[\frac{1}{\rho_0(x)}\frac{\partial N_1}{\partial t} + \frac{B_0}{\mu_0\rho_0(x)}\left(\frac{\partial N_3}{\partial z} - \frac{\partial N_4}{\partial x}\right)\right], \tag{4.19}$$

where $c_{\mathrm{A}} = B_0/\sqrt{\mu_0\rho_0(x)}$ is the Alfvén speed, and $\nabla^2 = \partial^2/\partial x^2 + \partial^2/\partial z^2$.

Other perturbations may be given in terms of v_x and v_z:

$$b_x = B_0 D_t^{-1}\frac{\partial v_x}{\partial z} + O(\varepsilon), \tag{4.20}$$

$$b_z = -B_0 D_t^{-1}\frac{\partial v_x}{\partial x} + O(\varepsilon), \tag{4.21}$$

$$\rho = -D_t^{-1}\left(\frac{\partial}{\partial x}\left(\rho_0(x)v_x\right) + \rho_0(x)\frac{\partial v_z}{\partial z}\right) + O(\varepsilon), \tag{4.22}$$

where D_t^{-1} is the inverse differential operator associated with time t. Expressions (4.20)-(4.22) are used in the nonlinear right-hand side of equation (4.19).

In the linear limit ($\varepsilon \to 0$), when the amplitudes of the perturbations tend to zero, equation (4.19) describes linear fast magnetoacoustic waves perturbing variables v_x, b_x, b_z and ρ; there is no field aligned steady flow v_z (unless v_z is non-zero at infinity), which is consistent with the driving force, $\mathbf{j} \times \mathbf{B}$, for a wave perpendicular to $\mathbf{B}_0$. By contrast, a nonlinear fast magnetoacoustic wave also

perturbs the plasma in the longitudinal direction,

$$v_z = -\varepsilon c_{\mathrm{A}}^2(x) D_t^{-1} \left(D_t^{-1} \frac{\partial v_x}{\partial z} \, D_t^{-1} \nabla^2 v_x \right) + O(\varepsilon^2) \,. \tag{4.23}$$

The amplitude of v_z is proportional to the square of v_x, so its generation is a quadratically nonlinear effect. Since we are interested in the quadratically nonlinear phenomena, terms containing the value v_z can be neglected in expressions (4.14)-(4.18). Note that, in the degenerate case of a plane wave, $\partial/\partial x = 0$, the wave does not perturb b_z and ρ, and the fast wave reduces to a linearly polarised Alfvén wave.

Substituting expressions (4.20)-(4.22) to equation (4.19), we finally arrive at the self-consistent, quadratically nonlinear wave equation describing v_x;

$$\begin{aligned} \frac{\partial^2 v_x}{\partial t^2} - c_{\mathrm{A}}^2(x) \nabla^2 v_x = \varepsilon \Bigg\{ -c_{\mathrm{A}}^2(x) \Bigg[\frac{\partial}{\partial t} \left(D_t^{-1} \frac{\partial v_x}{\partial x} D_t^{-1} \nabla^2 v_x \right) + \\ \nabla^2 \left(v_x D_t^{-1} \frac{\partial v_x}{\partial x} \right) \Bigg] + \frac{\partial}{\partial t} \left(\frac{1}{\rho_0(x)} \frac{\partial v_x}{\partial t} \, D_t^{-1} \frac{\partial}{\partial x} \left(\rho_0(x) v_x \right) - v_x \frac{\partial v_x}{\partial x} \right) \Bigg\} \,. \end{aligned} \tag{4.24}$$

Equation (4.24) describes the weakly nonlinear dynamics of fast magnetoacoustic waves and is equivalent to that derived by Nakariakov *et al.* (1991). Equation (4.24) has to be supplemented by boundary and initial conditions. We consider here the case of rigid wall boundary conditions,

$$v_x(x = -L, z, t) = v_x(x = L, z, t) = 0 \,, \tag{4.25}$$

along with appropriate initial conditions.

4.3 Linear eigenmodes

Our aim is to study the weakly nonlinear resonances produced in a rigid-walled wave guide. Since we wish to investigate higher order corrections to the first-order solution, we must determine the exact linear solution. In the simple case of the rigid-walled wave guide, density is taken to be uniform and does not vary in the transversal direction. This implies that the Alfvén speed is also a constant.

We begin by considering the linear case. Equation (4.24) with $\varepsilon = 0$ describes linear fast magnetoacoustic modes. We take the harmonical dependence on time

t and the longitudinal coordinate z to be

$$v_x(x,z,t) = \Psi(x)\exp(i\omega t - ik_z z)\,, \tag{4.26}$$

where Ψ is a function describing the wave's transversal structure, defined by the boundary conditions. In a zero β plasma, the frequency ω and wave number k_z are connected with each other by the fast wave dispersion relation. This will be derived later in this section. For the harmonical wave, the linear part of equation (4.24) (the left-hand side) along with the boundary conditions (4.25) gives us the eigenvalue problem

$$\frac{\mathrm{d}^2\Psi}{\mathrm{d}x^2} + m^2\Psi = 0\,, \qquad \Psi(-L) = \Psi(L) = 0\,, \tag{4.27}$$

where $m^2 = \omega^2/c_\mathrm{A}^2 - {k_z}^2$ can be considered to be the square of a transversal wave number. Transversal structures of perturbations for other physical values are expressed through Ψ, using (4.20)-(4.22), as

$$b_x = -B_0\frac{k_z}{\omega}\Psi(x)e^{i(\omega t - k_z z)}\,, \quad b_z = i\frac{B_0}{\omega}\frac{\mathrm{d}\Psi}{\mathrm{d}x}e^{i(\omega t - k_z z)}\,, \quad \rho = i\frac{\rho_0}{\omega}\frac{\mathrm{d}\Psi}{\mathrm{d}x}e^{i(\omega t - k_z z)}\,. \tag{4.28}$$

The solution of Equation (4.27) is

$$\Psi = \begin{cases} A\sin(mx) + B\cos(mx)\,, & m^2 > 0\,, \\ Ce^{nx} + De^{-nx}\,, & n^2 = -m^2 > 0\,, \end{cases} \tag{4.29}$$

where A, B, C and D are constants. Application of the boundary conditions $\Psi(-L) = \Psi(L) = 0$ yields

$$\Psi = \begin{cases} A_N\sin(m_N x)\,, & N \quad \text{even}\,, \\ A_N\cos(m_N x)\,, & N \quad \text{odd}\,, \end{cases} \tag{4.30}$$

where m_N is given by the relation $m = m_N = N\pi/2L$, with N as an integer. Written out, the dispersion relation is

$$\omega^2 = c_\mathrm{A}^2\left({k_z}^2 + \left(\frac{N\pi}{2L}\right)^2\right)\,. \tag{4.31}$$

This is illustrated in Figure 4.1. Sausage modes are represented using a solid line and kink modes with a dotted line.

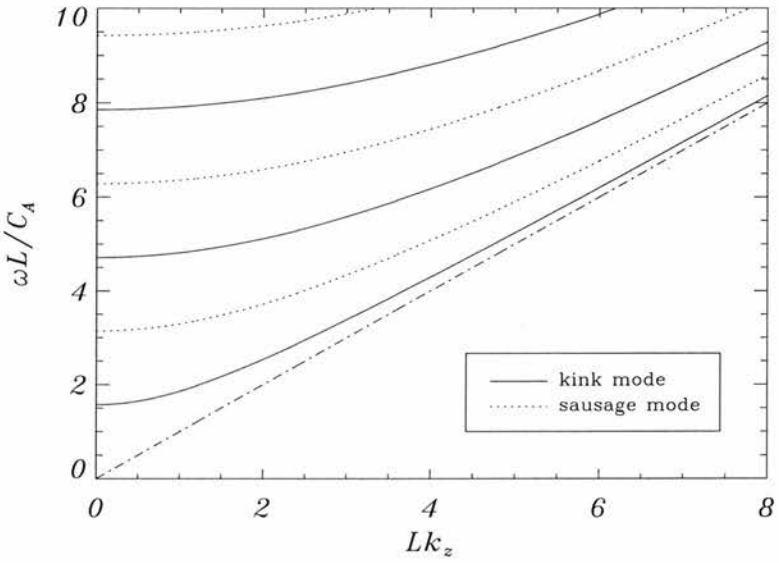

Figure 4.1: The dispersion curves of (4.31), with $N \in \mathbb{N}$. The solutions $\Psi(x)$ are oscillatory, giving body modes. Sausage modes correspond to N being even; kink modes are for odd values of N. The diagonal dot-dashed line corresponds to $N = 0$ and is not a mode.

4.4 Weakly nonlinear resonances

We now turn to a consideration of the effects introduced by the non-linear resonant interactions between different wave modes. We will consider the more general case in which density may vary in the transversal direction and later simplify this to consider the specific case of the rigid-walled wave guide in which density is uniform.

In section 4.2 we derived equation (4.24) for weakly nonlinear waves using the zero β plasma approximation

$$\nabla^2 v_x - \frac{1}{c_{\mathrm{A}}^2(x)}\frac{\partial^2 v_x}{\partial t^2} = \varepsilon\left\{\frac{\partial}{\partial t}\left[\int \frac{\partial v_x}{\partial x}\mathrm{d}t \int \nabla^2 v_x \mathrm{d}t - \frac{1}{\rho_0(x)c_{\mathrm{A}}^2(x)}\frac{\partial v_x}{\partial t}\int \frac{\partial \rho_0(x) v_x}{\partial x}\mathrm{d}t + \frac{v_x}{c_{\mathrm{A}}^2(x)}\frac{\partial v_x}{\partial x}\right] + \nabla^2\left(v_x \int \frac{\partial v_x}{\partial x}\mathrm{d}t\right)\right\}. \quad (4.32)$$

The solution to this equation may be sought in the following general form

$$v_x = \sum_{\alpha=1}^{\infty} \Psi_\alpha(x) A_\alpha(\varepsilon z, \varepsilon t) e^{i(\omega_\alpha t - k_{z\alpha} z)} + \varepsilon Q_\alpha(x, \varepsilon z, \varepsilon t) e^{i(\omega_\alpha t - k_{z\alpha} z)} + C.C., \quad (4.33)$$

where α is the mode number, $\Psi_\alpha(x)$ describes the transverse structure of the

mode of amplitude $A_\alpha(\varepsilon z, \varepsilon t)$, Q_α is a small nonlinear correction, ω_α and $k_{z\alpha}$ are the frequency and longitudinal wavenumbers of the mode, and $C.C.$ denotes the complex conjugate.

We now consider modes with the following resonance:

$$\omega_a + \omega_b = \omega_c\,, \quad k_{zl}(\omega_a) + k_{zm}(\omega_b) = k_{zn}(\omega_c)\,, \tag{4.34}$$

where l, m and n denote mode numbers and the frequencies ω_a, ω_b and ω_c satisfy the linear eigenmode problem.

If we substitute (4.33) into (4.32) and group terms of order ε, we obtain an equation in the following form

$$\begin{aligned}\{\ldots\}e^{\theta_a} + \{\ldots\}e^{\theta_b} + \{\ldots\}e^{\theta_c} + \{\ldots\}e^{-\theta_a} + \{\ldots\}e^{-\theta_b} + \{\ldots\}e^{-\theta_c} \\ = \{\ldots\}e^{\theta_a+\theta_a} + \{\ldots\}e^{\theta_a+\theta_b} + \{\ldots\}e^{\theta_a+\theta_c} + \{\ldots\}e^{\theta_a-\theta_a} + \{\ldots\}e^{\theta_a-\theta_b} + \\ \{\ldots\}e^{\theta_a-\theta_c} + \{\ldots\}e^{-\theta_a-\theta_a} + \{\ldots\}e^{-\theta_a-\theta_b} + \ldots\,,\end{aligned} \tag{4.35}$$

where we have used the shorthand $e^{i(\omega_\alpha t - k_{z\alpha} z)} = e^{\theta_\alpha}$. We are only interested in the *form* of the equation and hence the terms that would appear within the curly braces in the above equation have been omitted here for the sake of brevity.

Some of the terms on the right-hand side of (4.35) may be re-written using the resonance condition (4.34), i.e. $e^{\theta_a+\theta_b} = e^{\theta_c}$, $e^{\theta_c-\theta_b} = e^{\theta_a}$, etc. Assuming that we can equate terms that oscillate in phase with each other (i.e. to be resonant) we can reduce the above to a set of equations of the form:

$$\{L.H.S.\}\,e^{\theta_a} = \{R.H.S.\}\,e^{\theta_a}\,, \quad \{L.H.S.\}\,e^{\theta_b} = \{R.H.S.\}\,e^{\theta_b}\,, \quad \text{etc.} \tag{4.36}$$

The function on the right-hand side of each of the equations (4.36) may be represented as $F(U)G(U)$. It is clear that to obtain a resonance with $\{\ldots\}\,e^{\theta_a}$, for example, we need only consider the terms $\Psi_c A_c e^{\theta_c}$ and $\Psi_b^* A_b^* e^{-\theta_b}$, i.e.

$$F(\Psi_c A_c)G(\Psi_b^* A_b^*)e^{\theta_c-\theta_b} = F(\Psi_c A_c)G(\Psi_b^* A_b^*)e^{\theta_a}\,, \tag{4.37}$$

$$F(\Psi_b^* A_b^*)G(\Psi_c A_c)e^{-\theta_b+\theta_c} = F(\Psi_b^* A_b^*)G(\Psi_c A_c)e^{\theta_a}\,. \tag{4.38}$$

So our equation will be

$$\begin{aligned}
&\nabla^2\left(\Psi_a A_a+\varepsilon Q_a\right)-\frac{1}{c_{\mathrm{A}}^2(x)}\frac{\partial^2}{\partial t^2}\left(\Psi_a A_a+\varepsilon Q_a\right)\\
&\qquad=\varepsilon\left\{\frac{\partial}{\partial t}\left[\int A_c\frac{\partial\Psi_c}{\partial x}\mathrm{dt}\int\nabla^2(\Psi_b^* A_b^*)\mathrm{dt}\right.\right.\\
&\qquad\quad+\int A_b^*\frac{\partial\Psi_b^*}{\partial x}\mathrm{dt}\int\nabla^2(\Psi_c A_c)\mathrm{dt}\\
&\qquad\quad-\frac{1}{\rho_0(x)c_{\mathrm{A}}^2(x)}\frac{\partial(\Psi_c A_c)}{\partial t}\int A_b^*\frac{\partial}{\partial x}(\rho_0(x)\Psi_b^*)\mathrm{dt}\\
&\qquad\quad-\frac{1}{\rho_0(x)c_{\mathrm{A}}^2(x)}\frac{\partial(\Psi_b^* A_b^*)}{\partial t}\int A_c\frac{\partial}{\partial x}(\rho_0(x)\Psi_c)\mathrm{dt}\\
&\qquad\quad\left.+\frac{\Psi_c A_c A_b^*}{c_{\mathrm{A}}^2(x)}\frac{\partial\Psi_b^*}{\partial x}+\frac{\Psi_b^* A_b^* A_c}{c_{\mathrm{A}}^2(x)}\frac{\partial\Psi_c}{\partial x}\right]\\
&\qquad\quad\left.+\nabla^2\left[\Psi_c A_c\int A_b^*\frac{\partial\Psi_b^*}{\partial x}\mathrm{dt}+\Psi_b^* A_b^*\int A_c\frac{\partial\Psi_c}{\partial x}\mathrm{dt}\right]\right\}.
\end{aligned}\tag{4.39}$$

To lowest order, ε^0, we recover the linear equation

$$\Psi_a''+\left(\frac{\omega_a^2}{c_{\mathrm{A}}^2(x)}-k_{z_a}^2\right)\Psi_a=0\,,\tag{4.40}$$

where a dash denotes the derivative with respect to x. This equation, when supplemented with boundary conditions (for example, the requirement that the function Ψ tend to zero at an infinite distance from a slab boundary), represents an eigenproblem, the solutions of which are eigenfunctions. Collecting terms of order ε, we obtain

$$Q_a''+\left(\frac{\omega_a^2}{c_{\mathrm{A}}^2(x)}-k_{z_a}^2\right)Q_a=F_a(A_a,A_b^*,A_c,\dots)\,,\tag{4.41}$$

where F_a is given by

$$\begin{aligned}
F_a=&\frac{2i\omega_a}{c_{\mathrm{A}}^2(x)}\Psi_a\frac{\partial A_a}{\partial t}+2ik_{z_a}\Psi_a\frac{\partial A_a}{\partial z}+A_cA_b^*\left\{i\left(\omega_c-\omega_b\right)\left[\frac{\Psi_c'}{i\omega_c}\frac{(\Psi_b^{*\prime\prime}-k_{z_b}^2\Psi_b^*)}{-i\omega_b}\right.\right.\\
&+\frac{\Psi_b^{*\prime}}{-i\omega_b}\frac{(\Psi_c''-k_{z_c}^2\Psi_c)}{i\omega_c}-\frac{i\omega_c\Psi_c}{\rho_0(x)c_{\mathrm{A}}^2(x)}\frac{(\rho_0(x)\Psi_b^*)'}{-i\omega_b}\\
&\left.-\frac{-i\omega_b\Psi_b^*}{\rho_0(x)c_{\mathrm{A}}^2(x)}\frac{(\rho_0(x)\Psi_c)'}{i\omega_c}+\frac{\Psi_c\Psi_b^{*\prime}}{c_{\mathrm{A}}^2(x)}+\frac{\Psi_b^*\Psi_c'}{c_{\mathrm{A}}^2(x)}\right]+\left(\frac{\Psi_c\Psi_b^{*\prime}}{-i\omega_b}+\frac{\Psi_b^*\Psi_c'}{i\omega_c}\right)''\\
&\left.-\left(k_{z_c}^2-2k_{z_c}k_{z_b}+k_{z_b}^2\right)\left(\frac{\Psi_c\Psi_b^{*\prime}}{-i\omega_b}+\frac{\Psi_b^*\Psi_c'}{i\omega_c}\right)\right\}
\end{aligned}$$

$$
\begin{aligned}
&= 2i\omega_a \left[\frac{\Psi_a}{c_{\mathrm{A}}^2(x)} \frac{\partial A_a}{\partial t} + \frac{k_{za}}{\omega_a} \Psi_a \frac{\partial A_a}{\partial z} \right] + iA_c A_b^* \left\{ \frac{\omega_a}{\omega_b \omega_c} \Psi_c' \left(\Psi_b^{*\prime\prime} - k_{z_b}^2 \Psi_b^* \right) \right. \\
&+ \frac{\omega_a}{\omega_b \omega_c} \Psi_b^{*\prime} \left(\Psi_c'' - k_{z_c}^2 \Psi_c \right) + \frac{\omega_a \omega_c}{\omega_b} \frac{\Psi_c (\rho_0(x) \Psi_b^*)'}{\rho_0(x) c_{\mathrm{A}}^2(x)} + \frac{\omega_a \omega_b}{\omega_c} \frac{\Psi_b^* (\rho_0(x) \Psi_c)'}{\rho_0(x) c_{\mathrm{A}}^2(x)} \\
&+ \frac{\omega_a}{c_{\mathrm{A}}^2(x)} \left(\Psi_c \Psi_b^{*\prime} + \Psi_b^* \Psi_c' \right) + \frac{(\Psi_c \Psi_b^{*\prime})''}{\omega_b} - \frac{(\Psi_b^* \Psi_c')''}{\omega_c} \\
&\left. + k_{z_a}^2 \left(\frac{\Psi_b \Psi_c^{*\prime}}{\omega_c} - \frac{\Psi_c^* \Psi_b'}{\omega_b} \right) \right\} .
\end{aligned}
$$

The condition for Q_a to be non-secular is the orthogonality of the right-hand side of equation (4.41), to the eigenfunction solution of the eigenproblem (4.40),

$$
\int \Psi_a F_a \mathrm{dx} = 0 . \tag{4.42}
$$

This yields an equation for the amplitude of the mode A_a,

$$
\begin{aligned}
&\int \frac{\Psi_a^2}{c_{\mathrm{A}}^2(x)} \mathrm{dx} \frac{\partial A_a}{\partial t} + \frac{k_{za}}{\omega_a} \int \Psi_a^2 \mathrm{dx} \frac{\partial A_a}{\partial z} \\
&\qquad = \frac{A_c A_b^*}{2\omega_a} \left\{ \frac{\omega_a}{\omega_b \omega_c} \left[k_{z_b}^2 \int \Psi_a \Psi_b^* \Psi_c' \mathrm{dx} + k_{z_c}^2 \int \Psi_a \Psi_b^{*\prime} \Psi_c \mathrm{dx} \right. \right. \\
&\qquad\quad \left. - \int \Psi_a \left(\Psi_c' \Psi_b^{*\prime\prime} + \Psi_b^{*\prime} \Psi_c'' \right) \mathrm{dx} \right] + k_{z_a}^2 \left[\frac{1}{\omega_b} \int \Psi_a \Psi_b^{*\prime} \Psi_c \mathrm{dx} \right. \\
&\qquad\quad \left. - \frac{1}{\omega_c} \int \Psi_a \Psi_b^* \Psi_c' \mathrm{dx} \right] + \frac{1}{\omega_c} \int \Psi_a (\Psi_b^* \Psi_c')'' \mathrm{dx} \\
&\qquad\quad - \frac{1}{\omega_b} \int \Psi_a (\Psi_b^{*\prime} \Psi_c)'' \mathrm{dx} - \omega_a \left[\frac{\omega_c}{\omega_b} \int \frac{\Psi_a \Psi_c (\rho_0(x) \Psi_b^*)'}{\rho_0(x) c_{\mathrm{A}}^2(x)} \mathrm{dx} \right. \\
&\qquad\quad \left. \left. + \frac{\omega_b}{\omega_c} \int \frac{\Psi_a \Psi_b^* (\rho_0(x) \Psi_c)'}{\rho_0(x) c_{\mathrm{A}}^2(x)} \mathrm{dx} + \int \frac{\Psi_a \left(\Psi_c \Psi_b^{*\prime} + \Psi_b^* \Psi_c' \right)}{c_{\mathrm{A}}^2(x)} \mathrm{dx} \right] \right\} .
\end{aligned} \tag{4.43}
$$

We consider solutions with purely real transversal structure $\Psi(x)$, so $\Psi_b^* = \Psi_b$.

An equation for A_b may be obtained simply by exchanging the indices a and b in equations (4.42) and (4.43).

To obtain an equation for A_c we must look for the following terms on the right-hand side of equation (4.35):

$$
F(\Psi_a A_a) G(\Psi_b A_b) e^{\theta_a + \theta_b} , \quad F(\Psi_b A_b) G(\Psi_a A_a) e^{\theta_b + \theta_a} . \tag{4.44}
$$

Then our governing equation for Q_c (to order ε) is

$$
Q_c'' + \left(\frac{\omega_c^2}{c_{\mathrm{A}}^2(x)} - k_{z_c}^2 \right) Q_c = F_c(A_a, A_b, A_c, \dots) , \tag{4.45}
$$

with F_c given by

$$\begin{aligned} F_c = 2i\omega_c \left[\frac{\Psi_c}{c_{\mathrm{A}}^2(x)} \frac{\partial A_c}{\partial t} + \frac{k_{zc}}{\omega_c} \Psi_c \frac{\partial A_c}{\partial z} \right] - iA_a A_b \left\{ \omega_c \left[\frac{\Psi_a'}{\omega_a} \frac{\left(\Psi_b'' - k_{zb}^2 \Psi_b\right)}{\omega_b} \right.\right. \\ + \frac{\Psi_b'}{\omega_b} \frac{\left(\Psi_a'' - k_{za}^2 \Psi_a\right)}{\omega_a} + \frac{\omega_a \Psi_a}{\rho_0(x) c_{\mathrm{A}}^2(x)} \frac{(\rho_0(x)\Psi_b)'}{\omega_b} + \frac{\omega_b \Psi_b}{\rho_0(x) c_{\mathrm{A}}^2(x)} \frac{(\rho_0(x)\Psi_a)'}{\omega_a} \\ \left. - \frac{\Psi_a \Psi_b'}{c_{\mathrm{A}}^2(x)} - \frac{\Psi_a' \Psi_b}{c_{\mathrm{A}}^2(x)} \right] + \left(\frac{\Psi_a \Psi_b'}{\omega_b} + \frac{\Psi_a' \Psi_b}{\omega_a} \right)'' - k_{zc}^2 \left(\frac{\Psi_a \Psi_b'}{\omega_b} + \frac{\Psi_a' \Psi_b}{\omega_a} \right) \Bigg\} . \end{aligned} \tag{4.46}$$

The orthogonality condition then yields

$$\begin{aligned} \int \frac{\Psi_c^2}{c_{\mathrm{A}}^2(x)} \mathrm{d}x \frac{\partial A_c}{\partial t} + \frac{k_{zc}}{\omega_c} \int \Psi_c^2 \mathrm{d}x \frac{\partial A_c}{\partial z} \\ = \frac{A_a A_b}{2\omega_c} \left\{ \frac{\omega_c}{\omega_a \omega_b} \left[-k_{za}^2 \int \Psi_a \Psi_b' \Psi_c \mathrm{d}x - k_{zb}^2 \int \Psi_a' \Psi_b \Psi_c \mathrm{d}x \right.\right. \\ + \int \Psi_c \left(\Psi_a' \Psi_b'' + \Psi_b' \Psi_a'' \right) \mathrm{d}x \Big] - k_{zc}^2 \left[\frac{1}{\omega_a} \int \Psi_a \Psi_b' \Psi_c \mathrm{d}x \right. \\ \left. + \frac{1}{\omega_b} \int \Psi_a' \Psi_b \Psi_c \mathrm{d}x \right] + \frac{1}{\omega_a} \int \Psi_c (\Psi_a' \Psi_b)'' \mathrm{d}x \\ + \frac{1}{\omega_b} \int \Psi_c (\Psi_a \Psi_b')'' \mathrm{d}x + \omega_c \left[\frac{\omega_a}{\omega_b} \int \frac{\Psi_a \Psi_c (\rho_0(x)\Psi_b)'}{\rho_0(x) c_{\mathrm{A}}^2(x)} \mathrm{d}x \right. \\ \left. \left. + \frac{\omega_b}{\omega_a} \int \frac{\Psi_b \Psi_c (\rho_0(x)\Psi_a)'}{\rho_0(x) c_{\mathrm{A}}^2(x)} \mathrm{d}x + \int \frac{\Psi_c \left(\Psi_a' \Psi_b + \Psi_a \Psi_b' \right)}{c_{\mathrm{A}}^2(x)} \mathrm{d}x \right] \right\} . \end{aligned} \tag{4.47}$$

There is a degenerate case when resonant conditions for equation (4.34) are fulfilled by the two eigenmodes, ω_1 and ω_2. In this case equation (4.34) reduces to the resonance condition

$$k_{z2} = 2k_{z1} , \quad \omega_2 = 2\omega_1 + \Delta , \tag{4.48}$$

where Δ is some small mismatch parameter for modes where the resonance is not exact. We look for solutions of equation (4.47) in the form

$$\begin{aligned} v = \Psi_1 \left(A_1 e^{i(\omega_1 t - k_{z1} z)} + A_1^* e^{-i(\omega_1 t - k_{z1} z)} \right) \\ + \Psi_2 \left(A_2 e^{i(\omega_2 t - k_{z2} z)} + A_2^* e^{-i(\omega_2 t - k_{z2} z)} \right) + \varepsilon Q . \end{aligned} \tag{4.49}$$

For terms in the form $\{\ldots\} e^{i(\omega_1 t - k_{z1} z)}$ on the left-hand side we get a resonance on the right-hand side due to terms of the forms:

$$F(\Psi_1 A_1^*) G(\Psi_2 A_2) e^{i(\omega_2 - \omega_1)t - i(k_{z2} - k_{z1})z} = F(\Psi_1 A_1^*) G(\Psi_2 A_2) e^{i(\omega_1 t - k_{z1} z)} e^{i\Delta t} , \tag{4.50}$$

$$F(\Psi_2 A_2) G(\Psi_1 A_1^*) e^{i(\omega_2 - \omega_1)t - i(k_{z2} - k_{z1})z} = F(\Psi_2 A_2) G(\Psi_1 A_1^*) e^{i(\omega_1 t - k_{z1} z)} e^{i\Delta t} . \tag{4.51}$$

Then we obtain

$$Q_1'' + \left(\frac{\omega_1^2}{c_{\rm A}^2(x)} - k_{z1}^2\right) Q_1 = F_1(A_1, A_1^*, A_2, \dots)\,, \tag{4.52}$$

with F_1 given by

$$\begin{aligned} F_1 = {} & 2i\omega_1 \left[\frac{\Psi_1}{c_{\rm A}^2(x)}\frac{\partial A_1}{\partial t} + \frac{k_{z1}}{\omega_1}\Psi_1\frac{\partial A_1}{\partial z}\right] \\ & - ie^{i\Delta t}A_2A_1^*\left\{-(\omega_1+\Delta)\left[\frac{\Psi_1'}{\omega_1}\frac{(\Psi_2''-k_{z2}^2\Psi_2)}{\omega_2} + \frac{\Psi_2'}{\omega_2}\frac{(\Psi_1''-k_{z1}^2\Psi_1)}{\omega_1}\right.\right. \\ & + \frac{\omega_1\Psi_1}{\rho_0(x)c_{\rm A}^2(x)}\frac{(\rho_0(x)\Psi_2)'}{\omega_2} + \frac{\omega_2\Psi_2}{\rho_0(x)c_{\rm A}^2(x)}\frac{(\rho_0(x)\Psi_1)'}{\omega_1} \\ & \left.\left.\frac{\Psi_1\Psi_2' + \Psi_1'\Psi_2}{c_{\rm A}^2(x)}\right] + \left(\frac{\Psi_1\Psi_2'}{\omega_2} - \frac{\Psi_1'\Psi_2}{\omega_1}\right)'' - k_{z1}^2\left(\frac{\Psi_1\Psi_2'}{\omega_2} - \frac{\Psi_1'\Psi_2}{\omega_1}\right)\right\}. \end{aligned} \tag{4.53}$$

The orthogonality condition then gives

$$\begin{aligned} & \int \frac{\Psi_1^2}{c_{\rm A}^2(x)}{\rm d}x\,\frac{\partial A_1}{\partial t} + \frac{k_{z1}}{\omega_1}\int \Psi_1^2{\rm d}x\,\frac{\partial A_1}{\partial z} \\ & \qquad = A_1^*A_2\frac{e^{i\Delta t}}{2\omega_2}\left\{\frac{\omega_1+\Delta}{\omega_1\omega_2}\left[k_{z1}^2\int \Psi_1^2\Psi_2'{\rm d}x\right.\right. \\ & \qquad\quad + k_{z2}^2\int \Psi_1\Psi_2\Psi_1'{\rm d}x - \int \Psi_1(\Psi_1'\Psi_2'' + \Psi_1''\Psi_2'){\rm d}x\Big] \\ & \qquad\quad + k_{z1}^2\left[\frac{1}{\omega_1}\int \Psi_1\Psi_2\Psi_1'{\rm d}x - \frac{1}{\omega_2}\int \Psi_1^2\Psi_2'{\rm d}x\right] \\ & \qquad\quad - \frac{1}{\omega_1}\int \Psi_1(\Psi_1'\Psi_2)''{\rm d}x + \frac{1}{\omega_2}\int \Psi_1(\Psi_2'\Psi_1)''{\rm d}x \\ & \qquad\quad - (\omega_1+\Delta)\left[\frac{\omega_1}{\omega_2}\int \frac{\Psi_1^2(\rho_0(x)\Psi_2)'}{\rho_0(x)c_{\rm A}^2(x)}{\rm d}x\right. \\ & \qquad\quad \left.\left. + \frac{\omega_2}{\omega_1}\int \frac{\Psi_1\Psi_2(\rho_0(x)\Psi_1)'}{\rho_0(x)c_{\rm A}^2(x)}{\rm d}x + \int \frac{\Psi_1^2\Psi_2' + \Psi_1\Psi_2\Psi_1'}{c_{\rm A}^2(x)}{\rm d}x\right]\right\}. \end{aligned} \tag{4.54}$$

For A_2 we need terms on the right-hand side in the form

$$F(\Psi_1A_1)G(\Psi_1A_1)e^{i(2\omega_1t-2k_{z1}z)} = F(\Psi_1A_1)G(\Psi_1A_1)e^{i(\omega_2t-k_{z2}z)}e^{-i\Delta t}\,. \tag{4.55}$$

This gives

$$
\begin{aligned}
F_2 = 2i\omega_2 & \left[\frac{\Psi_2}{c_{\mathrm{A}}^2(x)}\frac{\partial A_2}{\partial t} + \frac{k_{z1}}{\omega_2}\Psi_2\frac{\partial A_2}{\partial z}\right] \\
& - ie^{-i\Delta t}A_1^2\left\{-(\omega_2-\Delta)\left[\frac{\Psi_1'}{i\omega_1}\frac{(\Psi_1''-k_{z1}^2\Psi_1)}{i\omega_1}\right.\right. \\
& \left.\left. - \frac{i\omega_1\Psi_1}{\rho_0(x)c_{\mathrm{A}}^2(x)}\frac{(\rho_0(x)\Psi_1)'}{i\omega_1} + \frac{\Psi_1\Psi_1'}{c_{\mathrm{A}}^2(x)}\right] + \left(\frac{\Psi_1\Psi_1'}{\omega_1}\right)'' - k_{z2}^2\left(\frac{\Psi_1\Psi_1'}{\omega_1}\right)\right\},
\end{aligned}
\tag{4.56}
$$

and we obtain an equation for A_2,

$$
\begin{aligned}
\int \frac{\Psi_2^2}{c_{\mathrm{A}}^2(x)}\mathrm{d}x\,\frac{\partial A_2}{\partial t} + \frac{k_{z2}}{\omega_2}\int \Psi_2^2\mathrm{d}x\,\frac{\partial A_2}{\partial z} & \\
= A_1^2\frac{e^{-i\Delta t}}{2\omega_2}\left\{\frac{\omega_2-\Delta}{\omega_1^2}\left[-k_{z1}^2\int \Psi_1\Psi_2\Psi_1'\mathrm{d}x\right.\right. & \\
\left. + \int \Psi_1'\Psi_1''\Psi_2\mathrm{d}x\right] - \frac{k_{z2}^2}{\omega_1}\int \Psi_1\Psi_1'\Psi_2\mathrm{d}x & \\
+ \frac{1}{\omega_1}\int \Psi_2(\Psi_1'\Psi_1)''\mathrm{d}x - (\omega_2-\Delta)\left[\int \frac{\Psi_2\Psi_1\Psi_1'}{c_{\mathrm{A}}^2(x)}\mathrm{d}x\right. & \\
\left.\left. - \int \frac{\Psi_2\Psi_1(\rho_0(x)\Psi_1)'}{\rho_0(x)c_{\mathrm{A}}^2(x)}\mathrm{d}x\right]\right\}. &
\end{aligned}
\tag{4.57}
$$

This equation along with equation (4.54) represents the reduced set of magnetohydrodynamic equations for a zero β plasma describing weakly nonlinear resonant interactions between two wave modes. They may be written in the simplified form

$$
\frac{\partial A_1}{\partial t} + v_{g1}\frac{\partial A_1}{\partial z} = \sigma_1 A_2 A_1^*, \tag{4.58}
$$

$$
\frac{\partial A_2}{\partial t} + v_{g2}\frac{\partial A_2}{\partial z} = \sigma_2 A_1^2. \tag{4.59}
$$

These two equations describe the evolution of two resonantly interacting wave modes. The group velocities, v_{g1} and v_{g2}, and the parameters, σ_1 and σ_2 are independent of t and z, so only the slowly varying wave amplitudes, A_1 and A_2, evolve. The two terms on the right-hand sides represent coupling between the equations. For the case when A_1 is zero, both right-hand sides will also be zero and the two equations become decoupled. In this situation, the evolution of the second wave amplitude, A_2, has no effect on the first, A_1. On the other hand, if A_1 is non-zero and the second wave is initially absent from the system then it will be generated through the term on the right-hand side of equation (4.59). When A_2 grows sufficiently large, it will then have a back reaction on A_1 through

the term on the right-hand side of equation (4.58).

In the equations (4.58)-(4.59) presented above we have introduced the two group velocities, v_{g1} and v_{g2}, and the two coefficients σ_1 and σ_2. These are defined as follows

$$v_{g1} = \frac{k_{z1}}{\omega_1} c_A^2 , \qquad v_{g2} = \frac{k_{z2}}{\omega_2} c_A^2 , \tag{4.60}$$

$$\begin{aligned} \sigma_1 = \frac{c_A^2 e^{i\Delta t}}{2\omega_2 I_{10}} \Bigg\{ & \frac{(\omega_1 + \Delta)}{\omega_1 \omega_2} \left[k_{z1}^2 I_{11} + k_{z2}^2 I_{12} - I_{13} \right] + k_{z1}^2 \left[\frac{I_{12}}{\omega_1} - \frac{I_{11}}{\omega_2} \right] + \frac{I_{14}}{\omega_2} \\ & - \frac{I_{15}}{\omega_1} - \frac{(\omega_1 + \Delta)}{c_A^2} \left[\frac{\omega_1}{\omega_2} I_{11} + \frac{\omega_2}{\omega_1} I_{12} + I_{11} + I_{12} \right] \Bigg\} , \end{aligned} \tag{4.61}$$

$$\sigma_2 = \frac{c_A^2 e^{-i\Delta t}}{2\omega_1 I_{20}} \left\{ \frac{2}{\omega_1} \left[-k_{z1}^2 I_{21} + I_{22} \right] - \frac{4 k_{z1}^2}{\omega_1} I_{21} + \frac{I_{23}}{\omega_1} \right\} . \tag{4.62}$$

The various integrals terms are given by:

$$I_{10} = \int_0^{2L} \Psi_1^2 \mathrm{d}x , \qquad I_{11} = \int_0^{2L} \Psi_1^2 \Psi_2' \mathrm{d}x , \tag{4.63}$$

$$I_{12} = \int_0^{2L} \Psi_1 \Psi_2 \Psi_1' \mathrm{d}x , \qquad I_{13} = \int_0^{2L} \Psi_1 (\Psi_1' \Psi_2'' + \Psi_1'' \Psi_2') \mathrm{d}x , \tag{4.64}$$

$$I_{14} = \int_0^{2L} \Psi_1 (\Psi_1 \Psi_2')'' \mathrm{d}x , \qquad I_{15} = \int_0^{2L} \Psi_1 (\Psi_1' \Psi_2)'' \mathrm{d}x , \tag{4.65}$$

$$I_{20} = \int_0^{2L} \Psi_2^2 \mathrm{d}x , \qquad I_{21} = \int_0^{2L} \Psi_1 \Psi_2 \Psi_1' \mathrm{d}x , \tag{4.66}$$

$$I_{22} = \int_0^{2L} \Psi_2 \Psi_1' \Psi_1'' \mathrm{d}x , \qquad I_{23} = \int_0^{2L} \Psi_2 (\Psi_1' \Psi_1)'' \mathrm{d}x . \tag{4.67}$$

These integral terms are introduced by the application of the orthogonality condition (4.42).

4.4.1 Expression for group velocity

We give here a proof of the equation

$$v_g = \frac{\frac{k_z}{\omega}\int \Psi^2 \mathrm{dx}}{\int \frac{\Psi^2}{c_\mathrm{A}^2}\mathrm{dx}}, \tag{4.68}$$

where v_g is the group velocity, over a general domain x_1 to x_2 (where $x_2 > x_1$). The proof is in two stages. First we prove that ω^2 is stable to small variations in Ψ and then differentiate it with respect to k_z. We start with the governing equation for Ψ, taking the leading order terms from equation (4.32)

$$H[\Psi] = \frac{\omega^2}{c_\mathrm{A}^2}\Psi, \tag{4.69}$$

where the operator $H = ({k_z}^2 - \frac{\partial^2}{\partial x^2})$. If we pre-multiply by Ψ and integrate over the domain, we can rearrange to get

$$\omega^2 = \frac{\int_{x_1}^{x_2} \Psi H[\Psi]\mathrm{dx}}{\int_{x_1}^{x_2} \frac{\Psi^2}{c_\mathrm{A}^2}\mathrm{dx}}. \tag{4.70}$$

The task now is to show that this is a stationary expression for ω^2 with respect to small variations in $\Psi(x)$. Suppose a small variation in Ψ, from Ψ to $\Psi + \delta\Psi$, yields a corresponding change in ω^2, from ω^2 to $\omega^2 + \delta\omega^2$.

We may write:

$$\begin{aligned}
\delta\omega^2 &\approx \frac{\int_{x_1}^{x_2}(\Psi+\delta\Psi)H[\Psi+\delta\Psi]\mathrm{dx}}{\int_{x_1}^{x_2}\frac{(\Psi^2+2\Psi\delta\Psi)}{c_\mathrm{A}^2}\mathrm{dx}} - \frac{\int_{x_1}^{x_2}\Psi H[\Psi]\mathrm{dx}}{\int_{x_1}^{x_2}\frac{\Psi^2}{c_\mathrm{A}^2}\mathrm{dx}} \\
&= \frac{\int_{x_1}^{x_2}(\Psi H[\Psi]+\delta\Psi H[\Psi]+\Psi H[\delta\Psi]+\delta\Psi H[\delta\Psi])\mathrm{dx}}{\int_{x_1}^{x_2}\frac{\Psi^2}{c_\mathrm{A}^2}\mathrm{dx}\left[1+\frac{2\int_{x_1}^{x_2}\Psi\delta\Psi\mathrm{dx}}{\int_{x_1}^{x_2}\frac{\Psi^2}{c_\mathrm{A}^2}\mathrm{dx}}\right]} \\
&\quad - \frac{\int_{x_1}^{x_2}\Psi H[\Psi]\mathrm{dx}+\frac{2\int_{x_1}^{x_2}\Psi H[\Psi]\mathrm{dx}}{\int_{x_1}^{x_2}\frac{\Psi^2}{c_\mathrm{A}^2}\mathrm{dx}}\int_{x_1}^{x_2}\Psi\delta\Psi\mathrm{dx}}{\int_{x_1}^{x_2}\frac{\Psi^2}{c_\mathrm{A}^2}\mathrm{dx}\left[1+\frac{2\int_{x_1}^{x_2}\Psi\delta\Psi\mathrm{dx}}{\int_{x_1}^{x_2}\frac{\Psi^2}{c_\mathrm{A}^2}\mathrm{dx}}\right]} \\
&\approx \frac{\int_{x_1}^{x_2}(\delta\Psi H[\Psi]+\Psi H[\delta\Psi])\mathrm{dx}-2\omega^2\int_{x_1}^{x_2}\Psi\delta\Psi\mathrm{dx}}{\int_{x_1}^{x_2}\frac{\Psi^2}{c_\mathrm{A}^2}\mathrm{dx}}.
\end{aligned} \tag{4.71}$$

Next we require that H is self-adjoint. This will be true provided Ψ is chosen such that both Ψ and $\partial\Psi/\partial x$ vanish at the boundaries $x = x_1, x_2$ as shown by

$$\begin{aligned}
&\int_{x_1}^{x_2}(\Psi_1 H[\Psi_2]-\Psi_2 H[\Psi_1])\,\mathrm{dx} \\
&\qquad = \int_{x_1}^{x_2}({k_z}^2\Psi_1\Psi_2-\Psi_1\Psi_2''-{k_z}^2\Psi_1\Psi_2+\Psi_1''\Psi_2)\mathrm{dx} \\
&\qquad = \left[-\Psi_1\Psi_2'\right]_{x_2}^{x_1}+\int_{x_1}^{x_2}\Psi_1'\Psi_2'\mathrm{dx}+\left[-\Psi_1'\Psi_2\right]_{x_2}^{x_1}-\int_{x_1}^{x_2}\Psi_1'\Psi_2'\mathrm{dx} \\
&\qquad = 0\,.
\end{aligned} \tag{4.72}$$

Hence $\Psi_1 H[\Psi_2] = \Psi_2 H[\Psi_1]$, and thus we obtain

$$\delta\omega^2 \approx \frac{2\int_{x_1}^{x_2}\delta\Psi(H[\Psi]-\omega^2\Psi)\mathrm{dx}}{\int_{x_1}^{x_2}\frac{\Psi^2}{c_\mathrm{A}^2}\mathrm{dx}}. \tag{4.73}$$

Now, since (4.70) is stationary for small variations in $\Psi(x)$, we may differentiate it with respect to k_z whilst keeping $\Psi(x)$ fixed

$$\frac{\mathrm{d}\omega^2}{\mathrm{d}k_z} = \frac{\mathrm{d}}{\mathrm{d}k_z}\left[\frac{\int_{x_1}^{x_2}({k_z}^2\Psi^2 - \Psi\Psi'')\mathrm{dx}}{\int_{x_1}^{x_2}\frac{\Psi^2}{c_\mathrm{A}^2}\mathrm{dx}}\right]. \tag{4.74}$$

Thus,

$$2\omega\frac{\mathrm{d}\omega}{\mathrm{d}k_z} = 2k_z\frac{\int_{x_1}^{x_2}\Psi^2\mathrm{dx}}{\int_{x_1}^{x_2}\frac{\Psi^2}{c_\mathrm{A}^2}\mathrm{dx}}, \tag{4.75}$$

yielding

$$v_g = \frac{\frac{k_z}{\omega}\int\Psi^2\mathrm{dx}}{\int\frac{\Psi^2}{c_\mathrm{A}^2}\mathrm{dx}}. \tag{4.76}$$

which concludes the proof.

The general result (4.76) can easily be confirmed for the rigid-wall wave guide using the dispersion relation (4.31). We have

$$\frac{\omega^2}{c_\mathrm{A}^2} - {k_z}^2 = \frac{N^2\pi^2}{4L^2}. \tag{4.77}$$

Thus,

$$\omega^2 = {k_z}^2c_\mathrm{A}^2 + \left(\frac{N\pi c_\mathrm{A}}{2L}\right)^2, \tag{4.78}$$

and so

$$2\omega\frac{\partial\omega}{\partial k_z} = 2k_zc_\mathrm{A}^2, \tag{4.79}$$

$$\frac{\partial\omega}{\partial k_z} = \frac{k_z}{\omega}c_\mathrm{A}^2. \tag{4.80}$$

4.5 Rigid-walled waveguide.

Now consider waves in a rigid-walled waveguide ($v_x = 0$ at the boundary). The density is constant throughout the region and there is a uniform magnetic field in the z-direction. The Alfvén speed c_A and the density ρ_0 are no longer functions of x inside the waveguide. To linear order, equation (4.32) reduces to an equation in terms of $\Psi(x)$ alone, giving the transverse structure of the waves

$$\Psi_\alpha'' + \left(\frac{\omega_\alpha^2}{c_A^2} - {k_{z\alpha}}^2\right)\Psi_\alpha = 0\,. \tag{4.81}$$

This is supplemented by the boundary conditions $\Psi_\alpha(-L) = \Psi_\alpha(L) = 0$. The solutions of (4.81) with these boundary conditions are:

$$\begin{aligned} &\Psi_N = \sin(m_0 x)\,, \quad m_0 L = N\pi && \text{for sausage modes}\,, \\ &\Psi_N = \cos(m_0 x)\,, \quad m_0 L = \frac{\pi}{2}(2N+1) && \text{for kink modes}\,, \end{aligned} \tag{4.82}$$

where

$$m_0 = \left(\frac{\omega^2}{c_A^2} - {k_z}^2\right)^{1/2}\,. \tag{4.83}$$

It is convenient to move the slab boundaries to $x = 0, 2L$. Then

$$\Psi_N = \sin(m_0 x)\,, \quad m_0 L = \frac{N\pi}{2}\,, \tag{4.84}$$

with sausage modes when N is even and kink modes when N is odd.

Using the methods outlined previously, we can now use these equations for the transverse structure of the waves to investigate the nonlinear resonant interaction of wave modes using the equations (4.58)-(4.59) relating the wave amplitudes for the case when $k_{z2} = 2k_{z1}$ and $\omega_2 = 2\omega_1 + \Delta$. In the specific case of the rigid-walled waveguide, it will be shown that $\Delta = 0$ and the wave modes are exactly resonant.

4.5.1 Two wave resonances

We now investigate the relationship between the size of the resonant frequency correction term, Δ, and the mode numbers using the following relationships:

$$k_{z2} = 2k_{z1}\,, \quad \omega_2 = 2\omega_1 + \Delta\,, \tag{4.85}$$

combined with the dispersion relation

$$\omega_\alpha = \left\{ (k_{z\alpha} c_A)^2 + \left(\frac{N_\alpha \pi c_A}{2L} \right)^2 \right\}^{1/2} , \tag{4.86}$$

where N_α is the mode number of ω_α, $k_{z\alpha}$. Specifically,

$$\begin{aligned} \omega_2 &= \left\{ (k_{z2} c_A)^2 + \left(\frac{N_2 \pi c_A}{2L} \right)^2 \right\}^{1/2} \\ &= \left\{ (2k_{z1} c_A)^2 + \left(4 + \frac{N_2^2}{N_1^2} - 4 \right) \left(\frac{N_1 \pi c_A}{2L} \right)^2 \right\}^{1/2} \\ &= \left\{ (2\omega_1)^2 - (4N_1^2 - N_2^2) \left(\frac{\pi c_A}{2L} \right)^2 \right\}^{1/2} \\ &= 2\omega_1 \left\{ 1 - (4N_1^2 - N_2^2) \left(\frac{\pi c_A}{4L\omega_1} \right)^2 \right\}^{1/2} , \end{aligned} \tag{4.87}$$

when $N_2 = 2N_1$, $\Delta = 0$ implying that $\omega_2 = 2\omega_1$.

When $\omega_1 \gg \pi c_A / 4L$,

$$\omega_2 \approx 2\omega_1 - (4N_1^2 - N_2^2) \frac{\pi^2 c_A^2}{8L^2} . \tag{4.88}$$

Now we evaluate the coefficients. When $N_2 \neq 2N_1$ equations (4.61) and (4.62) show that $\sigma_1 = \sigma_2 = 0$ and equations (4.58) and (4.59) reduce to

$$\frac{\partial A_1}{\partial t} + \frac{k_{z1}}{\omega_1} c_A^2 \frac{\partial A_1}{\partial z} = 0 , \tag{4.89}$$

$$\frac{\partial A_2}{\partial t} + \frac{k_{z2}}{\omega_2} c_A^2 \frac{\partial A_2}{\partial z} = 0 . \tag{4.90}$$

Hence, the equations relating the amplitudes of the two wave modes are decoupled and no resonant excitation of either wave mode occurs. When $N_2 = 2N_1$, on the other hand, we find that $\Delta = 0$ and there is an exact resonance between the two wave modes. For the parameters governing the coupling between the two equations (4.58)-(4.59) which describe the evolution of the wave amplitudes, we

obtain

$$\begin{aligned}\sigma_1 &= \frac{c_A^2}{4\omega_1^2 L}\left(k_{z1}^2\frac{3\pi}{4}N_1 + \frac{3\pi^3}{16L^2}N_1^3\right)\\ &= \frac{c_A^2}{64\omega_1^2 L^3}\left(12\pi N_1 k_{z1}^2 L^2 + 3\pi^3 N_1^3\right)\\ &= \frac{3\pi N_1}{64L}\left(\frac{c_A}{\omega_1 L}\right)^2\left[4k_{z1}^2L^2 + \pi^2 N_1^2\right],\end{aligned} \tag{4.91}$$

and

$$\begin{aligned}\sigma_2 &= \frac{-c_A^2}{16\omega_1^2 L^3}\left(12\pi N_1 k_{z1}^2 L^2 + 3\pi^3 N_1^3\right)\\ &= \frac{3\pi N_1}{64L}\left(\frac{c_A}{\omega_1 L}\right)^2\left[4k_{z1}^2L^2 + \pi^2 N_1^2\right].\end{aligned} \tag{4.92}$$

But

$$\left(\frac{\omega_1 L}{c_A}\right)^2 = (k_{z1}L)^2 + \left(\frac{\pi N_1}{2}\right)^2, \tag{4.93}$$

and so we obtain the simple expressions

$$\sigma_1 = \frac{3\pi}{16L}N_1, \quad \sigma_2 = \frac{-3\pi}{4L}N_1. \tag{4.94}$$

These two parameters determine the way in which the amplitudes of two resonant wave modes are coupled, the rate at which the amplitudes will change and the spatial scales over which this will occur.

4.6 Numerical investigation

Using the results from the previous section we can make some predictions on the behaviour of wave modes when resonant excitation of wave modes occurs.

To carry out this numerical investigation, a Lagrangian scheme is used (see Craig and Sneyd, 1986, 1990, Longbottom *et al.*, 1998, Arber *et al.*, 1999). This method is ideally suited to the problem at hand since it is exactly ideal unlike other schemes which always introduce spurious, numerically generated viscosity. The Lagrangian method ensures that the frozen in flux theorem is always

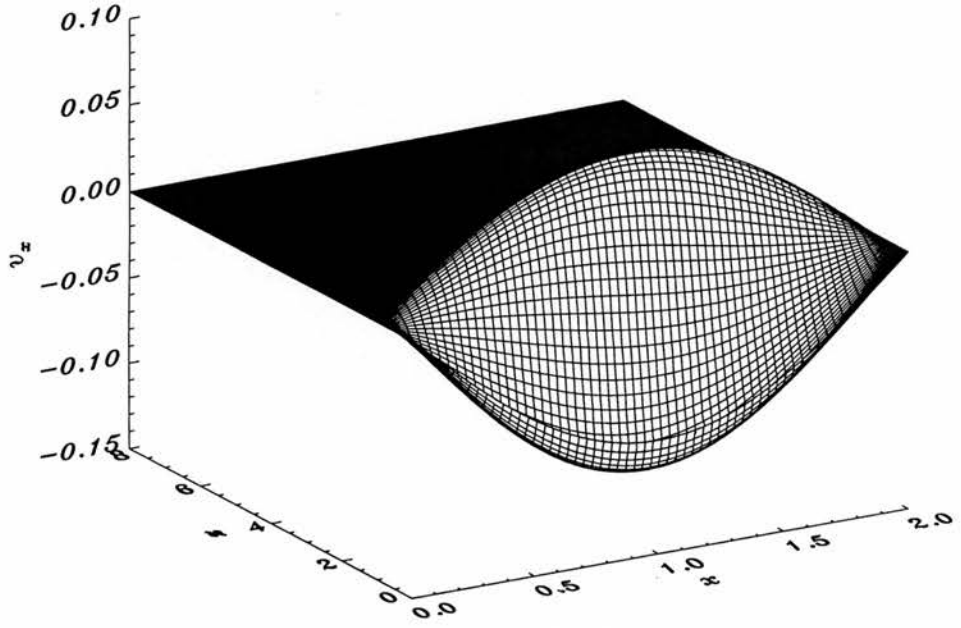

Figure 4.2: Surface plot of the numerical simulation of a driven fast magnetoacoustic wave mode. The wave is driven by velocity perturbations at the lower boundary ($z = 0$). The z-coordinate is normalised with respect to the width of the slab. Nonlinear effects are already apparent in the asymmetry of the wave.

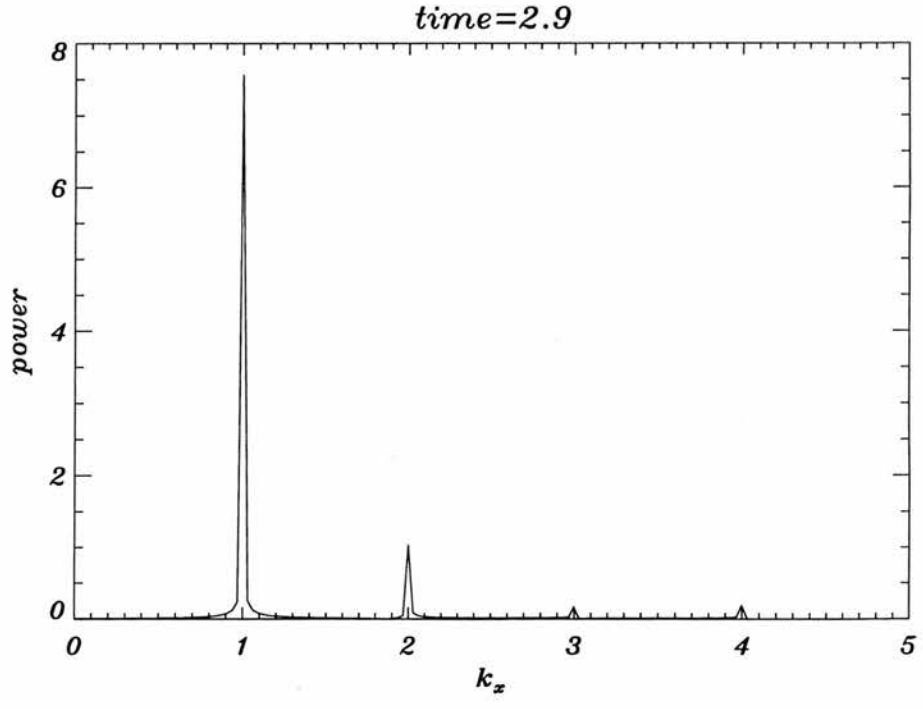

Figure 4.3: Power spectra for the propagating wave after two Alfvén times. Only the fundamental mode is driven, higher harmonics are the result of resonant excitation.

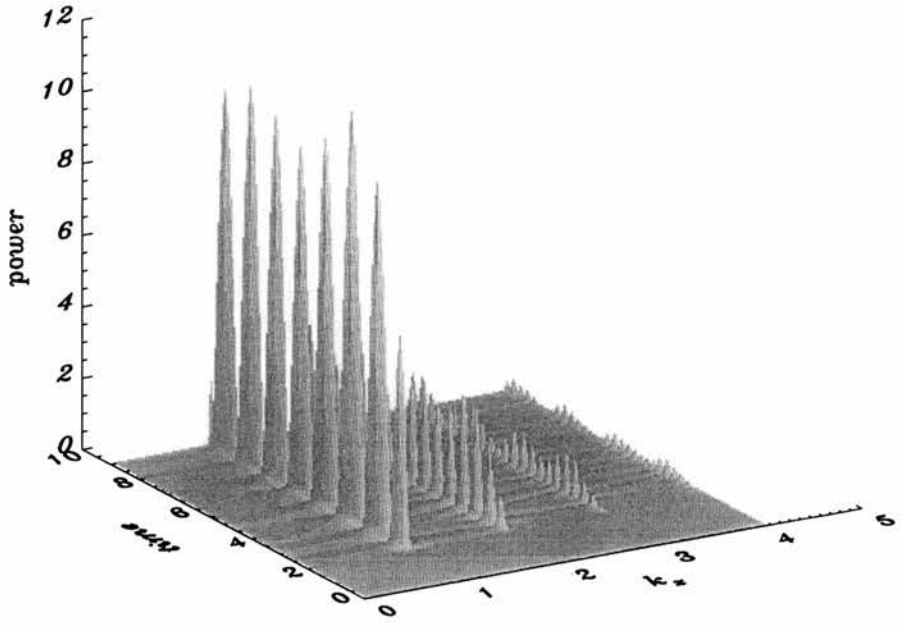

Figure 4.4: Evolution of the power spectra for the driven fast wave as a function of time. The largest set of peaks represent those of the fundamental mode, the other sets are higher harmonics.

satisfied due to the fact that the numerical grid moves with the fluid and the magnetic field moves with the grid. It also ensures that entropy is always conserved to machine precision. Analytical expressions are used for the gradients of all the fundamental plasma parameters. This reduces errors introduced by the process of calculating them numerically and effectively increases the resolution of the scheme. Position and velocity are the only parameters used in the evolution of the scheme. This eases the specification of the rigid-walled boundary conditions since the position and velocity of the boundaries can be specified and do not need to be calculated using symmetry conditions. It also greatly simplifies the specification of the wave driving condition at the lower boundary.

The fundamental wave mode is generated by driving v_x at one end of the computational domain with a frequency given by the linearly derived dispersion relation, equation (4.31). The wave is driven from the lower boundary and as it propagates up in the z-direction, its amplitude profile along the line $z = 2$ is recorded over time. This is done in order to eliminate any spurious numerical effects introduced by being too close to the boundary and to allow the wave time to establish itself as a normal mode of the system. Figure 4.2 shows the amplitude of v_x throughout the computational domain at time $t = 0.7$ where time has been normalised with respect to the time taken for an Alfvén wave to traverse

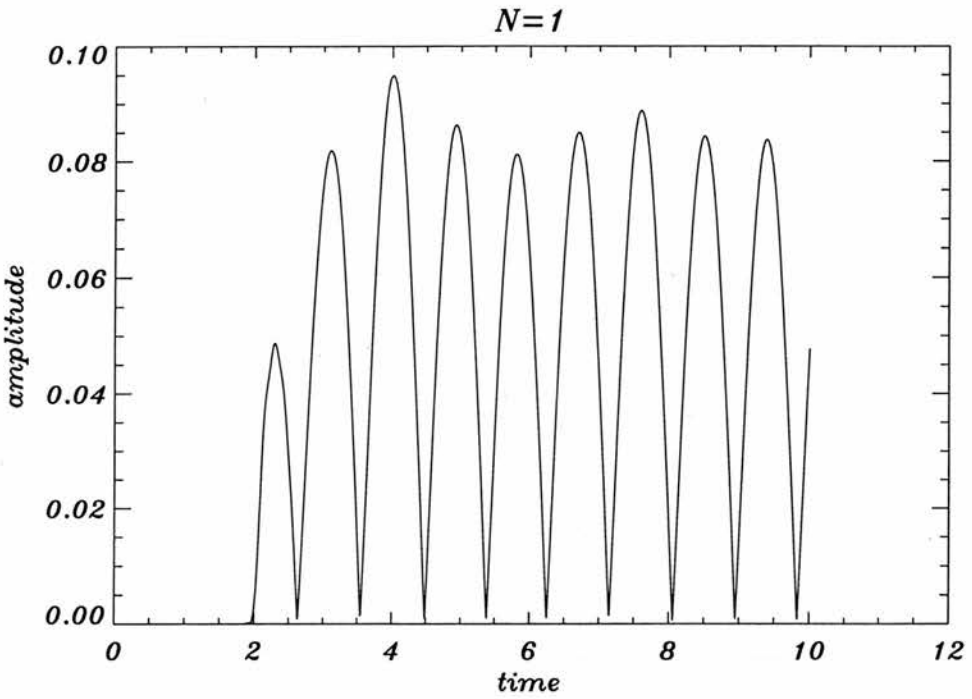

Figure 4.5: Evolution of the fundamental mode amplitude over time. The amplitude of the mode is modulated over a timescale of approximately three times that of the Alfvén period.

the width of the slab. The asymmetry in the wave is due to the fact that by this time the wave no longer consists of just the fundamental mode but also contains resonantly generated harmonics.

The presence of wave modes and their relative amplitudes can be determined by performing a Fourier transform on one of these curves. Figure 4.3 illustrates the power spectra obtained from a Fourier transform of the wave profile at time $t = 2.5$. Note that only the fundamental mode is driven in the numerical simulation so the harmonics shown for $k_z = 2, 3$ and 4 are all generated as a result of nonlinear resonant interactions. This Fourier transformation can be performed on each of the profiles recorded to build up a picture of the way in which the relative amplitudes of the different wave harmonics change over time. This is illustrated in Figure 4.4 in which a series of power spectra, such as that shown in Figure 4.3, are plotted for $t = 0 - 9$.

We can now take cuts along the time axis for given values of k_z to see how the amplitude of each wave harmonic evolves over time. Figure 4.5 illustrates the case for the fundamental mode ($N = 1$). In this figure we can clearly see that the wave has a slowly varying modulation of about three times the period

of the Alfvén wave. This may be connected with the modulational instability investigated by Nakariakov *et al.* (1997).

For a rigid walled waveguide in a zero β plasma we have the following differential equations relating the amplitudes of two resonant wave modes

$$\frac{\partial A_1}{\partial t} + v_{g1}\frac{\partial A_1}{\partial z} = \frac{3\pi}{16L} N_1 A_2 A_1^*, \tag{4.95}$$

$$\frac{\partial A_2}{\partial t} + v_{g2}\frac{\partial A_2}{\partial z} = \frac{-3\pi}{4L} N_1 A_1^2, \tag{4.96}$$

where the mode numbers of the two resonant modes satisfies the condition that $N_2 = 2N_1$. If A_1 is initially zero then the right-hand side of equation (4.96) is also zero and there is no mechanism for coupling the two equations. This means that driving a higher harmonic will not resonantly generate a lower harmonic in this weakly nonlinear formulation. However, if we make the simplifying assertion that A_2 is initially uniform in z then we can write down a simple expression for the initial growth rate of a resonantly generated wave

$$A_2 = -\frac{3\pi}{4L} N_1 A_1^2 t\,. \tag{4.97}$$

Using the method outlined above, this expression may be verified using the numerical scheme. In Figure 4.6 we show the development of the first harmonic to the fast wave in a rigid walled waveguide. This wave mode is absent from the initial wave so the diagram illustrates the onset of a resonantly excited harmonic. We have over-plotted the analytically predicted initial growth rate derived above. This prediction, which appears as a solid diagonal line on the figure, appears to be a good approximation to the initial state of evolution as observed from the numerically generated results.

4.7 Solution of the boundary value problem

In this section, we show that an analytical expression is possible for the boundary value problem of a driven fast wave in a rigid walled waveguide. This can be used to verify the results given by numerical methods when the wave amplitude is small.

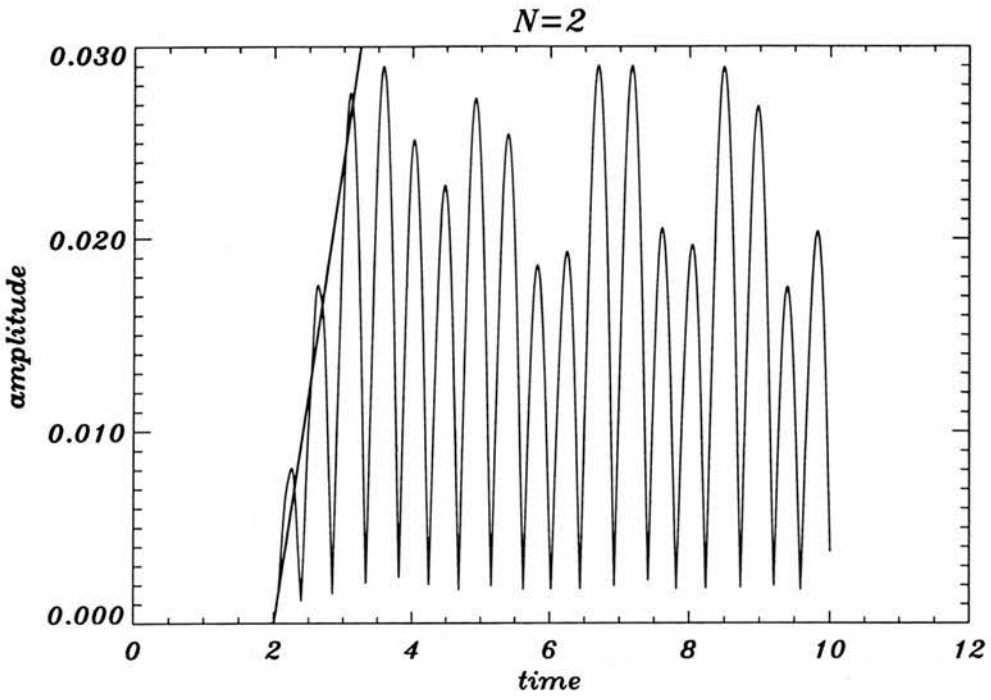

Figure 4.6: Evolution of the first harmonic mode amplitude over time. The solid line shows the analytically predicted initial growth rate.

We wish to solve the equation

$$\frac{\partial^2 v_x}{\partial t^2} - c_{\mathrm{A}}^2 \left(\frac{\partial^2 v_x}{\partial x^2} + \frac{\partial^2 v_x}{\partial z^2} \right) = 0 \,, \tag{4.98}$$

subject to the boundary conditions

$$v_x(-L, z, t) = v_x(L, z, t) = 0 \quad \text{and} \quad v_x(x, z = 0, t) = V_0 X(x) T(t) \,, \tag{4.99}$$

supplemented by the imposed physical conditions that v_x remains finite as $z \to \infty$ and that all waves travel away from the source at $z = 0$. We start by assuming that the solution is separable and then we Fourier transpose in time to obtain

$$v_x = G(\omega) X(x) Z(z) \,, \tag{4.100}$$

where

$$G(\omega) = \frac{1}{\sqrt{2\pi}} \int_{-\infty}^{\infty} T(t) e^{-i\omega t} dt \,. \tag{4.101}$$

Substituting the separable expression (4.100) into the wave equation (4.98) and

rearranging we get the following expression in terms of X and Z,

$$\frac{1}{X}\frac{\mathrm{d}^2X}{\mathrm{d}x^2} + \frac{\omega^2}{c_\mathrm{A}^2} = -\frac{1}{Z}\frac{\mathrm{d}^2Z}{\mathrm{d}z^2}\,. \tag{4.102}$$

Now the left-hand side of this equation is dependent on x alone and similarly the right-hand side on z alone, so each must be equal to some constant κ^2. Thus we obtain the two ordinary differential equations

$$\frac{\mathrm{d}^2X}{\mathrm{d}x^2} + \left(\frac{\omega^2}{c_\mathrm{A}^2} - \kappa^2\right) X = 0\,, \tag{4.103}$$

$$\frac{\mathrm{d}^2Z}{\mathrm{d}z^2} + \kappa^2 Z = 0\,. \tag{4.104}$$

The first of these ordinary differential equations we have already solved and we can immediately write down the solution, given the boundary conditions in equation (4.99):

$$X(x) = A_N \left\{\sin\left(N\frac{\pi}{2}\right)\sin(m_N x) + \sin\left((2N+1)\frac{\pi}{2}\right)\cos(m_N x)\right\}\,, \tag{4.105}$$

where $m_N = (\omega^2/C_A^2 - \kappa^2)^{1/2}$ is supplemented by the condition $m_N = N\pi/2L$.

The general solution to equation (4.104) may be written

$$Z(z) = \begin{cases} Ae^{\kappa z} + Be^{-\kappa z}\,, & \kappa^2 > 0\,, \\ Ce^{i\gamma z} + De^{-i\gamma z}\,, & \gamma^2 = -\kappa^2 > 0\,, \end{cases} \tag{4.106}$$

where we take κ and γ to be the principle square root of κ^2 and γ^2 respectively. The evanescent wave condition implies that $A = 0$ for non-trivial X and G. The outgoing wave condition implies that $C = 0$. We may now write

$$Z(z) = \begin{cases} e^{-\kappa z}\,, & \kappa^2 > 0\,, \\ e^{-i\gamma z}\,, & \gamma^2 = -\kappa^2 > 0\,, \end{cases} \tag{4.107}$$

where the arbitrary constants have been absorbed into those for X. Using the relationship between κ and m_N we may now write the general solution to (4.98) as follows

$$v_x(x,z,t) = \frac{1}{\sqrt{2\pi}}\sum_{N=0}^{\infty}\left\{\int_{-\infty}^{-\frac{N\pi}{2d}C_A} G(\omega)X(x)e^{i\omega t - \kappa z}d\omega +\right.$$

$$\int_{\frac{N\pi}{2d}C_A}^{\infty} G(\omega)X(x)e^{i\omega t-\kappa z}d\omega + \int_{-\frac{N\pi}{2d}C_A}^{\frac{N\pi}{2d}C_A} G(\omega)X(x)e^{i\omega t-i\gamma z}d\omega \Bigg\} . \quad (4.108)$$

Notice that $G(-\omega) = [G(\omega)]^*$. With a little algebra, we may rearrange (4.108) into the form

$$v_x(x,z,t) = \sqrt{\frac{2}{\pi}} \sum_{N=1}^{\infty} \mathrm{Re} \Bigg\{ \int_{\frac{N\pi}{2d}C_A}^{\infty} G(\omega)X(x)e^{i\omega t-\kappa z}d\omega + \int_0^{\frac{N\pi}{2d}C_A} G(\omega)X(x)e^{i\omega t-i\gamma z}d\omega \Bigg\} . \quad (4.109)$$

All that remains now is to specify our driver, i.e.

$$v_x(x,0,t) = V_0\mathcal{X}(x)T(t) , \quad (4.110)$$

where

$$\mathcal{X}(x) = \sum_{N=1}^{\infty} X(x) . \quad (4.111)$$

For the time dependent part we take

$$T(t) = H(t)\sin(\omega_d t) , \quad (4.112)$$

where $H(t)$ is the Heaviside function. Formally, this can be written as

$$T(t) = \lim_{t_0\to 0} \left\{ \frac{1}{2}[1+\tanh(t/t_0)]\sin(\omega_d t) \right\} . \quad (4.113)$$

The Fourier transform yields (after some algebra)

$$G(\omega) = \frac{1}{2\sqrt{2\pi}} \lim_{t_0\to 0} \Bigg\{ \int_{-\infty}^{\infty} \sin(\omega_d t)dt + \int_0^{\infty} \tanh(t/t_0)[\sin((\omega_d+\omega)t) + \sin((\omega_d-\omega)t)]dt \Bigg\} . \quad (4.114)$$

Now, according Gradshteyn and Ryzhik (1980, p. 504),

$$\int_0^{\infty} \tanh(at)\sin(bt)dt = \frac{\pi}{2a}\frac{1}{\sinh\left(\frac{\pi b}{2a}\right)} . \quad (4.115)$$

And with this information our transform can be written

$$G(\omega) = \frac{1}{2\sqrt{2\pi}} \lim_{t_0 \to 0} \left\{ \frac{i}{2}[\delta(\omega + \omega_d) - \delta(\omega - \omega_d)] + \right.$$
$$\left. \frac{\pi t_0}{2} \frac{t_0}{\sinh\left(\frac{\pi}{2}(\omega_d + \omega)\right)} + \frac{\pi t_0}{2} \frac{t_0}{\sinh\left(\frac{\pi}{2}(\omega_d - \omega)\right)} \right\} . \quad (4.116)$$

Evaluating the limit gives

$$G(\omega) = \frac{1}{\sqrt{2\pi}} \left\{ i[\delta(\omega + \omega_d) - \delta(\omega - \omega_d)] + \frac{4\omega_d}{\omega_d^2 - \omega^2} \right\} . \quad (4.117)$$

To summarise, we have used a method of Fourier transformation to establish an analytical solution, equation (4.109) together with equation (4.117), to the boundary value problem specified by equations (4.98)-(4.99) and the time dependent component of the driver function equation (4.112).

4.8 Conclusion

In this chapter we have outlined a technique for analysing the weakly nonlinear resonant interactions between the wave modes of a transversely structured zero β plasma. We then turned our attention to the specific case of a rigid-walled waveguide. From this we were able to draw conclusions about resonantly generated wave modes in the nonlinear regime and made a prediction of the initial growth rate for such a wave. We outlined a method for the numerical investigation of the weakly nonlinear resonances between wave modes and employed this method in the verification of our previously derived growth rate prediction. Finally, we presented an analytical solution to the boundary value problem of the rigid-walled waveguide for a zero β plasma in the linear regime.

Chapter 5

Conclusion

"We have to have something that sounds *good," said Benjy.*

"Something that sounds *good?" exclaimed Arthur. "An Ultimate Question that* sounds *good? From a couple of mice?"*

The mice bristled.

"Well, I mean, yes *idealism,* yes *the dignity of pure research,* yes *the pursuit of truth in all its forms, but there comes a point I'm afraid where you begin to suspect that if there's any* real *truth, it's that the entire multi-dimensional infinity of the Universe is almost certainly being run by a bunch of maniacs. And if it comes to a choice between spending yet another ten million years finding that out, and on the other hand just taking the money and running, then I for one could do with the exercise," said Frankie.*

— Douglas Adams, The Hitch Hiker's Guide to the Galaxy

5.1 Summary

Chapter 3

The behaviour of waves in a magnetic flux tube has previously been studied in detail only in the absence of twist. In this chapter we have outlined, for the special case of uniform twist, an extensive analytical investigation. We have derived a fully analytical dispersion relation in terms of generalised Bessel functions and performed a detailed study of the results to be gained from this representation.

We find that waves in a twisted tube exhibit new features not present in the untwisted case. The most striking feature is the introduction of an infinite set of body waves, a feature absent in the straight field case. It is possible that this could provide a unique signature in observable wave frequencies. The width of this band of wave modes is found to be dependent on the amount of twist within the tube and could provide a useful means by which twist could be measured indirectly. In addition to numerical solutions of the dispersion relation, we have been able to obtain various approximate results valid for large and small dimensionless wavenumber $k_z a$. These are particularly useful when considering the closely packed band of wave modes since these are difficult to compute numerically. It also provides verification to the validity of the numerically calculated dispersion diagrams.

Chapter 4

In this chapter we outline a method for the investigation of the resonant interaction between waves that is introduced when the linear regime is extended to take into account the first order non-linear effects. We have outlined a technique by which a useful mathematical analysis may be undertaken and have been able to derive a pair of equations describing the relationship between two resonant wave modes. We have applied these equations to the simple uniform slab model and have been able to make predictions about the growth rates of resonantly generated waves based on their frequencies. We also investigated the fully non-linear behaviour of this model using an ideal Lagrangian numerical code. We were able to establish a good agreement between the mathematically predicted results and those generated by the numerical simulations. By making this comparison between the purely analytical approach and the computationally generated solutions we are able to establish both the strengths and weaknesses of the analytical technique and identify the conditions under which they may be used effectively.

Chapter 5

In chapter 5 we have investigated the effect of steady field-aligned flows in transversally structured plasma configurations. A generalised dispersion relation was derived for sheared magnetic field models in Cartesian geometries. We then applied this to the magnetic interface model and noted that the effect

of compressibility could produce a significant change in the solutions obtained, demonstrating the need for further investigation. This work forms a basis on which a thorough investigation could be undertaken outlining important features introduced into these models by the inclusion of steady flow.

5.2 Further work

Chapter 3

As has already been noted, it has been necessary to impose certain restrictions on our twisted tube model in order for an analytical treatment to be made. The most severe limitation of this model is that it only considers the behaviour of waves in the incompressible plasma limit. In this extreme the fast waves are eliminated from the system and we also lose the distinction between the Alfvén continuum and the slow continuum. The relaxation of this requirement introduces a huge amount of mathematical complexity into the equations to be solved and there seems to be no obvious method by which a further analytical investigation may be made. However, the two first order ordinary differential equations can be integrated numerically with boundary conditions being imposed using shooting methods. It would be useful to undertake a numerical investigation of the transition from infinite to finite compressibility to determine the most important new features that must be taken into account. It would also be useful to repeat the investigation into the effects introduced as twist is increased, this time when the plasma is incompressible.

Another limitation of this model is the need for a uniform magnetic field profile. One unfortunate problem imposed by this restriction is that it becomes necessary to have a discontinuous field profile at the edge of the tube. Another result of this profile is that the Alfvén frequency is constant throughout the tube and the Alfvén resonant surface is removed. As in the incompressible assumption outlined above, the relaxation of this restriction brings with it severe mathematical complication. In this case analytical treatment may still be undertaken by making use of series expansion methods. An investigation could also be performed numerically in the same manner as explained above.

Chapter 4

This chapter introduced a method by which an analytical investigation of non-linear resonant interactions between wave modes may be undertaken. Some initial results were obtained but a full investigation was not undertaken. There is the potential for many other non-linear phenomena to be examined using this method and useful results may arise from a more detailed investigation. Another area which demands further study is to vary the parameters of the slab geometry. The model was chosen for its flexibility since it is able to describe two analytically solvable field profiles (the discontinuous uniform slab and the Epstein field profiles) and the whole range of profiles that lie between these two limits. In the current study we have only considered the uniform slab limit and the Epstein profile will certainly yield some interesting results. It should also be noticed that the uniform field profile exhibits a minimum in the group velocity whilst the Epstein profile does not. The non-linear behaviour should be different on either side of this minimum and so this certainly warrants further study.

"The first ten million years were the worst," said Marvin, "and the second ten million, they were the worst too. The third ten million I didn't enjoy at all. After that I went into a bit of a decline."

— Douglas Adams, The Restaurant at the End of the Universe

Appendix

A.1 Pressure Tensors

$$\Pi_{zz} = -\eta_0 W_{zz} \tag{A.1}$$

$$\Pi_{xx} = -\frac{1}{2}\eta_0 \left(W_{xx} + W_{yy}\right) - \frac{1}{2}\eta_1 \left(W_{xx} - W_{yy}\right) - \eta_3 W_{xy} \tag{A.2}$$

$$\Pi_{yy} = -\frac{1}{2}\eta_0 \left(W_{xx} + W_{yy}\right) - \frac{1}{2}\eta_1 \left(W_{yy} - W_{xx}\right) + \eta_3 W_{xy} \tag{A.3}$$

$$\Pi_{xy} = \Pi_{yx} = -\eta_1 W_{xy} + \frac{1}{2}\eta_3 \left(W_{xx} - W_{yy}\right) \tag{A.4}$$

$$\Pi_{xz} = \Pi_{zx} = -\eta_2 W_{xz} - \eta_4 W_{yz} \tag{A.5}$$

$$\Pi_{yz} = \Pi_{zy} = -\eta_2 W_{yz} + \eta_4 W_{xz} \tag{A.6}$$

Bibliography

Abramowitz, M. and Stegun, I. A.: 1967, *Handbook of Mathematical Functions*, Dover, New York.

Alfvén, H.: 1942, *Ark. f. Mat., Astr. o. Fysik* **92B**, No. 2.

Allan, W., Poulter, E. M. and Manuel, J. R.: 1991, *J. Geophys. Res.* **96**, 11461.

Allan, W. and Wright, A. N.: 1998, *J. Geophys. Res.* **103**, 2359–2368.

Appert, K., Gruber, R. and Vaclavik, J.: 1974, *Phys. Fluids* **17**, 1471.

Arber, T. D., Longbottom, A. W. and van der Linden, R. A. M.: 1999, *Astrophys. J.* **517**, 990–1001.

Ballai, I. and Erdélyi, R.: 1998, *Solar Phys.* **180**, 65–79.

Bennett, K., Roberts, B. and Narain, U.: 1999, *Solar Phys.* **185**, 41–59.

Bogdan, T. J.: 1984, *Astrophys. J.* **282**, 769–775.

Boyd, T. J. M. and Sanderson, J. J.: 1969, *Plasma Dynamics*, Nelson, London.

Braginskii, S. I.: 1965, *in* M. A. Leontovich (ed.), *Reviews of Plasma Physics*, Consultants Bureau, New York.

Bray, R. J., Cram, L. E., Durrant, C. J. and Loughhead, R. E.: 1991, *Plasma Loops in the Solar Corona*, Cambridge University Press, Cambridge.

Brown, D. S., Parnell, C. E., Deluca, E. E., Golub, L. and McMullen, R. A.: 2001, in press .

Cally, P. S.: 1986, *Solar Phys.* **103**, 277–298.

Cowling, T. G.: 1976, *Magnetohydrodynamics*, Adam Hilger, Bristol.

Craig, I. J. D. and Sneyd, A. D.: 1986, *Astrophys. J.* **311**, 451–459.

Craig, I. J. D. and Sneyd, A. D.: 1990, *Astrophys. J.* **357**, 653–661.

Dungey, J. W. and Loughhead, R. E.: 1954, *Austr. J. Phys.* **7**, 5.

Eddy, J. A.: 1976, *Science* **192**, 1189.

Edwin, P. M. and Roberts, B.: 1982, *Solar Phys.* **76**, 239–259.

Edwin, P. M. and Roberts, B.: 1983, *Solar Phys.* **88**, 179–191.

Erdélyi, R. and Ballai, I.: 1999, *Solar Phys.* **186**, 67–97.

Goedbloed, J. P.: 1971a, *Physica* **53**, 412.

Goedbloed, J. P.: 1971b, *Physica* **53**, 501.

Goedbloed, J. P.: 1971c, *Physica* **53**, 535.

Goedbloed, J. P.: 1975, *Phys. Fluids* **18**, 1258–1268.

Goedbloed, J. P.: 1983, *Lecture Notes on Ideal Magnetohydrodynamics*, thirteenth edn, Rijnhuizen Rep.

Goedbloed, J. P. and Hagenbeuk, H. J. L.: 1972, *Phys. Fluids* **15**, 1090.

Goossens, M.: 1991, *in* E. R. Priest and A. W. Hood (eds), *Advances in Solar System Magnetohydrodynamics*, Cambridge University Press, Cambridge, p. 135.

Goossens, M., Ruderman, M. S. and Hollweg, J. V.: 1995, *Solar Phys.* **145**, 19.

Gradshteyn, I. S. and Ryzhik, I. M.: 1980, *Table of Integrals, Series and Products*, fourth edn, Academic Press, New York.

Hain, K. and Lüst, R.: 1958, *Z. Naturforsch* **13a**, 936.

Kruskal, M. and Schwarzschild, M.: 1954, *Proc. Roy. Soc. Lond.* **A233**, 348.

Longbottom, A. W., Rickard, G. J., Craig, I. J. D. and Sneyd, A. D.: 1998, *Astrophys. J.* **500**, 471.

Lundquist, S.: 1951, *Phys. Rev.* **83**, 307.

Mann, G.: 1995, *J. Plasma Phys.* **53**, 109.

Maunder, E. W.: 1922, *Br. Astron. Ass. J.* **32**, 140.

Merzljakov, E. G. and Ruderman, M. S.: 1985, *Solar Phys.* **95**, 51.

Molotovshchikov, A. L. and Ruderman, M. S.: 1987, *Solar Phys.* **109**, 247.

Nakariakov, V. M. and Oraevsky, V. N.: 1995, *Solar Phys.* **160**, 289–302.

Nakariakov, V. M., Petrukhin, N. S. and Fainshtein, S. M.: 1991, *Sov. Astron. Lett.* **17**, 423–424.

Nakariakov, V. M., Roberts, B. and Petrukin, N. S.: 1997, *J. Plasma Phys.* **58**, 315–327.

Oraevsky, V. N.: 1983, *in* A. A. Galeev and R. Sudan (eds), *Foundations of plasma physics*, Nuaka, Moscow.

Parker, E. N.: 1964, *Astrophys. J.* **139**, 690.

Parker, E. N.: 1974a, *Solar Phys.* **37**, 127.

Parker, E. N.: 1974b, *Astrophys. J.* **191**, 245.

Parker, E. N.: 1979, *Cosmical Magnetic Fields*, Oxford University Press, England.

Phillips, K. J. H.: 1992, *Guide to the Sun*, Cambridge University Press, Great Britain.

Priest, E. R.: 1982, *Solar Magnetohydrodynamics*, D. Reidel, Dordrecht.

Roberts, B.: 1981a, *Solar Phys.* **69**, 27–38.

Roberts, B.: 1981b, *Solar Phys.* **69**, 39–56.

Roberts, B.: 1985, *Physics of Fluids* **28**, 3280–3286.

Roberts, B.: 1987, *Astrophys. J.* **318**, 590.

Roberts, B., Edwin, P. M. and Benz, A. O.: 1984a, *Astrophys. J.* **279**, 857–865.

Roberts, B., Edwin, P. M. and Benz, A. O.: 1984b, *Astrophys. J.* **279**, 857–865.

Roberts, B. and Mangeney, A.: 1982, *Monthly Notices Roy. Astron. Soc.* **198**, 7P–11P.

Roberts, P. H.: 1967, *An Introduction to Magnetohydrodynamics*, Longmans, London.

Ruderman, M. S. and Goossens, M.: 1993, *Solar Phys.* **143**, 69–88.

Ruderman, M. S., Goossens, M. and Hollweg, J. V.: 1997, *Phys. Plasmas* **4**, 91.

Ruderman, M. S., Hollweg, J. V. and Goossens, M.: 1997, *Phys. Plasmas* **4**, 75.

Smith, J. M., Roberts, B. and Oliver, R.: 1997, *Astron. Astrophys.* **327**, 377.

Spörer, G.: 1874, *Publ. Astron. Gesellsc.* **13**, 1.

Spruit, H. C.: 1982, *Solar Phys.* **75**, 3.

Sturrock, P. A.: 1994, *Plasma Physics*, Cambridge University Press, Cambridge.

Tarbell, T. D. and Hurlburt, N. E.: 1998, *Nature* **394**, 152.

Uberoi, C. and Somasunddaram, K.: 1979, *J. Plasma Phys.* **22**, 747.

Wentzel, D. G.: 1977, *Solar Phys.* **52**, 163–177.

Wentzel, D. G.: 1979, *Astrophys. J.* **227**, 319.

Wentzel, D. G.: 1989, *The Restless Sun*, Smithsonian, Washington, D. C.

Wesson, J.: 1997, *Tokamaks*, Clarendon Press, Oxford.

Wright, A. N.: 1994, *J. Geophys. Res.* **99**, 159–167.